

Dynamic Characteristics of a Full-sized Five-story Steel Structure and a 2/5 Scale Model

by

K.C. Chang, G.C. Yao, G.C. Lee, D.S. Hao and Y.C. Yeh

Technical Report NCEER-91-0011

July 2, 1991

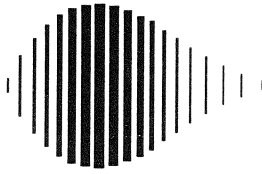
This research was conducted at the University at Buffalo, State University of New York and Beijing Polytechnic University and was supported in whole or in part by the National Science Foundation under grant number ECE 86-07591.

NOTICE

This report was prepared by the University at Buffalo, State University of New York and Beijing Polytechnic University as a result of research sponsored by the National Center for Earthquake Engineering Research (NCEER) through a grant from the National Science Foundation, and other sponsors. Neither NCEER, associates of NCEER, its sponsors, the University at Buffalo, State University of New York and Beijing Polytechnic University nor any person acting on their behalf:

- a. makes any warranty, express or implied, with respect to the use of any information, apparatus, method, or process disclosed in this report or that such use may not infringe upon privately owned rights; or
- b. assumes any liabilities of whatsoever kind with respect to the use of, or the damage resulting from the use of, any information, apparatus, method, or process disclosed in this report.

Any opinions, findings, and conclusions or recommendations expressed in this publication are those of the author(s) and do not necessarily reflect the views of NCEER, the National Science Foundation, or other sponsors.



Dynamic Characteristics of a Full-Size Five-Story Steel Structure and a 2/5 Scale Model

by

K.C. Chang¹, G.C. Yao², G.C. Lee³, D.S. Hao⁴ and Y.C. Yeh⁵

July 2, 1991

Technical Report NCEER-91-0011

NCEER Project Number 90-1004

NSF Master Contract Number ECE 86-07591

- 1 Professor, Department of Civil Engineering, National Taiwan University, Taipei, Taiwan; former Research Associate Professor, Department of Civil Engineering, State University of New York at Buffalo
- 2 Associate Professor, Department of Civil Engineering, National Chen-Kong University, Tainan, Taiwan; former Graduate Research Assistant, Department of Civil Engineering, State University of New York at Buffalo
- 3 Professor and Dean of Engineering, Department of Civil Engineering, State University of New York at Buffalo
- 4 Associate Professor, Department of Civil Engineering, Beijing Polytechnic University, Beijing, China
- 5 Professor, Department of Civil Engineering, Beijing Polytechnic University, Beijing, China

NATIONAL CENTER FOR EARTHQUAKE ENGINEERING RESEARCH
State University of New York at Buffalo
Red Jacket Quadrangle, Buffalo, NY 14261

PREFACE

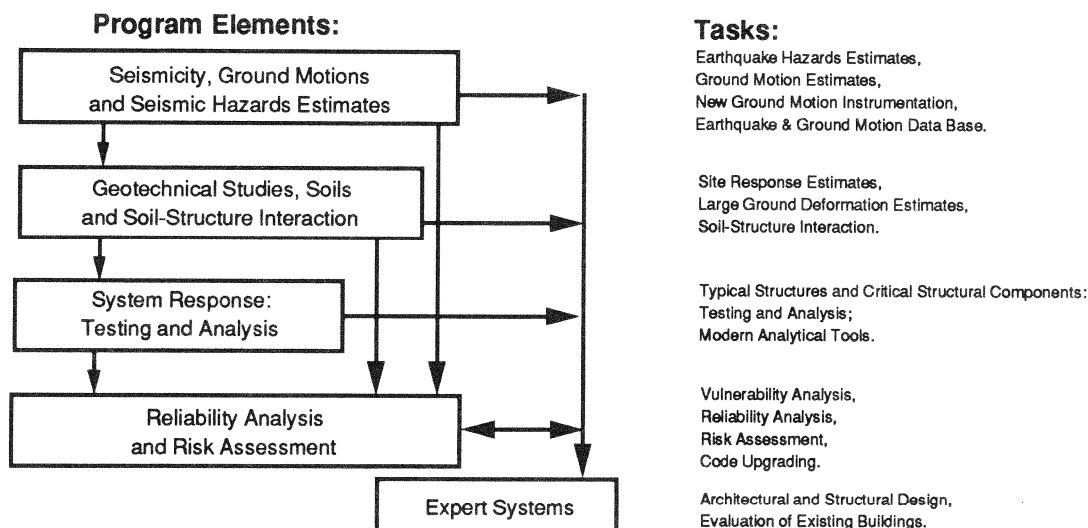
The National Center for Earthquake Engineering Research (NCEER) is devoted to the expansion and dissemination of knowledge about earthquakes, the improvement of earthquake-resistant design, and the implementation of seismic hazard mitigation procedures to minimize loss of lives and property. The emphasis is on structures and lifelines that are found in zones of moderate to high seismicity throughout the United States.

NCEER's research is being carried out in an integrated and coordinated manner following a structured program. The current research program comprises four main areas:

- Existing and New Structures
- Secondary and Protective Systems
- Lifeline Systems
- Disaster Research and Planning

This technical report pertains to Program 1, Existing and New Structures, and more specifically to system response investigations.

The long term goal of research in Existing and New Structures is to develop seismic hazard mitigation procedures through rational probabilistic risk assessment for damage or collapse of structures, mainly existing buildings, in regions of moderate to high seismicity. The work relies on improved definitions of seismicity and site response, experimental and analytical evaluations of systems response, and more accurate assessment of risk factors. This technology will be incorporated in expert systems tools and improved code formats for existing and new structures. Methods of retrofit will also be developed. When this work is completed, it should be possible to characterize and quantify societal impact of seismic risk in various geographical regions and large municipalities. Toward this goal, the program has been divided into five components, as shown in the figure below:



System response investigations constitute one of the important areas of research in Existing and New Structures. Current research activities include the following:

1. Testing and analysis of lightly reinforced concrete structures, and other structural components common in the eastern United States such as semi-rigid connections and flexible diaphragms.
2. Development of modern, dynamic analysis tools.
3. Investigation of innovative computing techniques that include the use of interactive computer graphics, advanced engineering workstations and supercomputing.

The ultimate goal of projects in this area is to provide an estimate of the seismic hazard of existing buildings which were not designed for earthquakes and to provide information on typical weak structural systems, such as lightly reinforced concrete elements and steel frames with semi-rigid connections. An additional goal of these projects is the development of modern analytical tools for the nonlinear dynamic analysis of complex structures.

This report compares the dynamic characteristics of a five-story steel frame structure with a laboratory model. Various system identification tests were performed on both structures to identify basic structural properties. The tests showed good agreement between the prototype structure and the laboratory model.

ABSTRACT

In this report, the dynamic characteristics of a full-size five-story steel prototype structure and a 2/5 scale laboratory model are compared and correlated. The prototype structure was built in Beijing, China and the laboratory model was built in the seismic laboratory at the University at Buffalo. The design and manufacture of both the prototype structure and the model are described. The test program was carried out by performing experimental system identification tests on both the prototype structure and the laboratory model. The basic structural properties of both structures were identified, and it is shown that the model structure can suitably simulate the dynamic behavior of the prototype.

TABLE OF CONTENTS

SECTION	TITLE	PAGE
1	INTRODUCTION	1-1
2	PROTOTYPE DESIGN AND MANUFACTURE	2-1
2.1	Introduction	2-1
2.2	Structural System	2-1
2.3	Member Sizes and Materials	2-4
2.4	Foundation Soil	2-4
2.5	Design Code	2-9
2.6	Design Loading	2-10
2.7	Construction	2-12
2.7.1	Foundation Plates	2-12
2.7.2	Five-Story Steel Frame	2-12
2.7.3	Cast-in-situ Concrete Floor	2-12
2.7.4	Bracing	2-15
3	MODEL DESIGN AND MANUFACTURE	3-1
3.1	Determination of Model Scale	3-1
3.2	Similitude Requirement	3-1
3.3	Model Component Design	3-1
3.4	Model Manufacturing	3-13
3.4.1	Coupon Test	3-15
3.4.2	Residual Stress Test	3-15
4	PROTOTYPE EXPERIMENT	4-1
4.1	Test Program	4-1
4.2	Test Results	4-1
4.2.1	Prototype Structure Without Concrete Slabs	4-1
4.2.2	Prototype Structure With Concrete Slabs	4-13
4.2.3	Dynamic Tests of Structures With Different Bracing Systems	4-20
4.3	Summary	4-20
5	MODEL TESTS	5-1
5.1	Introduction	5-1
5.2	Test Program and Instrumentation	5-1
5.3	Data Analysis	5-6
5.4	Test Results and Discussion	5-6
5.4.1	Frequency	5-12
5.4.2	Mode Shape	5-15
5.4.3	Damping	5-15
5.5	Summary	5-18

TABLE OF CONTENTS (Continued)

SECTION	TITLE	PAGE
6	SUMMARY AND CONCLUSION	6-1
7	REFERENCES	7-1

LIST OF ILLUSTRATIONS

FIGURE	TITLE	PAGE
2-1	Location of Prototype on West Campus of BPU	2-2
2-2	Connection of Column and Foundation	2-3
2-3	Prototype with Different Bracing Systems	2-3
2-4	Typical Connection of Beam-Column	2-5
2-5	Connection of Column and Foundation	2-6
2-6	Section of Prototype Member	2-7
2-7	Prototype Foundation	2-13
2-8	Picture of Prototype Building	2-14
3-1	Model Dimension	3-4
3-2	Model Member Cross Section	3-5
3-3	Model Beam-Column Connection	3-6
3-4	Model Foundation	3-7
3-5	E Bracing Detail	3-10
3-6	V Bracing Detail	3-11
3-7	X Bracing Detail	3-12
3-8	Model Beam-Column Connection Missing Plate	3-14
3-9	Model Material Property	3-16
3-10	Residual Stress Test	3-17
3-11	Residual Stress Distribution	3-19
4-1	Vibration Generator on the Foundation of Prototype	4-2
4-2	Force Vibration Displacement Response (without floor plate)	4-5
4-3	Transfer Function from Ambient Vibration at X-X Direction (without floor plate)	4-7
4-4	Transfer Function from Ambient Vibration at Y-Y Direction (without floor plate)	4-8
4-5	Mode Shape Comparison	4-9
4-6	Test Setup of Free Vibration	4-11
4-7	Time History of Free Vibration	4-11
4-8	Block Diagram of Impact Vibration Tests	4-12
4-9	First Three Bending and First Two Torsional Modes of Prototype (without floor plate)	4-14
4-10	Force Vibration Test - Frequency Response Curve (1st Mode) (with floor plate)	4-17
4-11	Transfer Function from Ambient Vibration Test in Y-Y Direction (with floor plate)	4-21
4-12	Mode Shape Comparison	4-22

LIST OF ILLUSTRATIONS, (Continued)

FIGURE	TITLE	PAGE
5-1	Spectrum of Input White Noise	5-2
5-2	Instrumentation of Model Test	5-3
5-3	Free Decay Vibration	5-5
5-4	Higher Mode Free Vibration	5-7
5-5	Transfer Function of "F"	5-8
5-6	Transfer Function of "E"	5-9
5-7	Transfer Function of "V"	5-10
5-8	Transfer Function of "X"	5-11
5-9	Comparison of Model and Prototype	5-16
5-10	Comparison of Models and Prototype	5-17
5-11	Higher Mode Free Vibration	5-19

LIST OF TABLES

TABLE	TITLE	PAGE
2-I	Prototype Material Properties	2-8
2-II	Prototype Loading Condition	2-8
2-III	Prototype Design Loads	2-11
2-IV	Loading During Tests	2-11
2-V	Loads at First Stage Testing	2-11
3-I	Modeling Laws for Artificial Mass Simulation	3-2
3-II	Model Member Properties	3-8
3-III	Weight Comparison of Prototype and Model	3-13
4-I	Prototype Mode Shape from Forced Vibration (without floor plate) . . .	4-4
4-II	Translational Modes from Forced Vibration	4-4
4-III	Translational Modes from Ambient Vibration	4-6
4-IV	Mode Shape from Ambient Vibration (without floor plate)	4-6
4-V	Results from Impact Test	4-15
4-VI	Torsional Modes	4-15
4-VII	Comparison of Analytical and Experimental Results	4-15
4-VIII	Results from Vibration Generator on the Foundation Under the Prototype	4-18
4-IX	Prototype Mode Shape from Forced Vibration (with floor plate)	4-18
4-X	Natural Frequency Comparison	4-19
4-XI	Results from Vibration Generator on Another Foundation (with floor plate)	4-19
4-XII	Natural Frequency Comparison	4-19
4-XIII	Results from Ambient Vibration	4-23
4-XIV	Mode Shapes from Ambient Vibration	4-23
4-XV	Comparison of Analytical and Experimental Results	4-24
4-XVI	Mode Shapes of Braced Frames	4-25
5-I	Frequency Comparison of Model Test Result	5-13
5-II	Mode Shape Comparison of Model and Prototype	5-13
5-III	Damping Comparison of Model and Prototype	5-18

SECTION 1 INTRODUCTION

In 1986, a cooperative research project between the National Center for Earthquake Engineering Research at the State University of New York at Buffalo (UB) and the Beijing Polytechnic University (BPU) in Beijing, China, was established. The project concerned the dynamic behavior of a five-story steel structure. More specifically, the project was aimed at providing a better understanding of the behavior of steel structures and soil-structure interaction under dynamic and seismic loading conditions. Measured data from an actual full-scale structure and from its laboratory model were obtained to enhance the state-of-the-art knowledge in structural dynamics and to develop new methodologies in seismic design and retrofit, and damage monitoring and diagnosis.

In the first stage of this joint research, BPU designed and constructed a prototype single bay five-story steel structure with cast-in-situ floor slabs, while UB designed and constructed a model steel structure. Dynamic loading on the prototype structure was accomplished by using synchronous vibrators, and on the model structure by a shaking table.

The major objectives of this joint research project were as follows:

- Correlation study on the dynamic characteristics between the prototype and the model structure with various bracing systems.
- Study the effect of soil-structure interaction, foundation rigidity and buried depth on the prototype structure.
- Study the effect of energy absorption devices on the seismic behavior of braced frames.
- Develop a structural diagnosis system for damage assessment.

In this report, only the results of the correlation on the dynamic characteristics between the prototype and the model structure are presented and discussed.

SECTION 2 PROTOTYPE DESIGN AND MANUFACTURE

2.1 Introduction

According to an agreement between NCEER and Beijing Polytechnic University (BPU) on **Cooperative Research for Dynamic Testing and Analysis**, a 5-story steel frame structure was constructed on the west campus of BPU at the end of 1987. It was intended that the full-scale prototype structure be tested to obtain its dynamic characteristics and to compare its behavior with a scaled model. The prototype structure was designed by BPU as an office building. It was considered an experimental building which could be used to perform a series of tests. The prototype structure was located on the west field campus of BPU, which is considered a good testing site since there are no large buildings, and a source of strong vibration exists. The location of the prototype is shown in Figure 2-1.

2.2 Structural System

The prototype structure is a five-story steel frame, consisting of two frames parallel in two directions (X and Y). The center to center distance of columns is 10.8 ft. (3.3 meters). The first floor height is 8.91 ft. (2.715 meters). Floor height is 9.84 ft. (3.0 meters) from the second floor up. The columns extend 0.71 ft. (0.215 meters) out above the center line of the roof beam. The prototype's total height is 48.9 ft. (14.915 meters). The foundation plate is cast-in place reinforced concrete. The walls are filler walls. The progress of the construction of the prototype is based on different stages of the test described below:

1. The thickness of the foundation plate is 7.87 inches (20 cm) in the initial stage as shown in Figure 2-2. It will be changed to 15.7 inches (40 cm) in later stages.
2. In the Y-Y direction (weak axis of column) of the prototype, the structure is strengthened by adding different bracing systems. Three bracing types are used: X-bracing, V-bracing and eccentric-bracing, as shown in Figure 2-3.

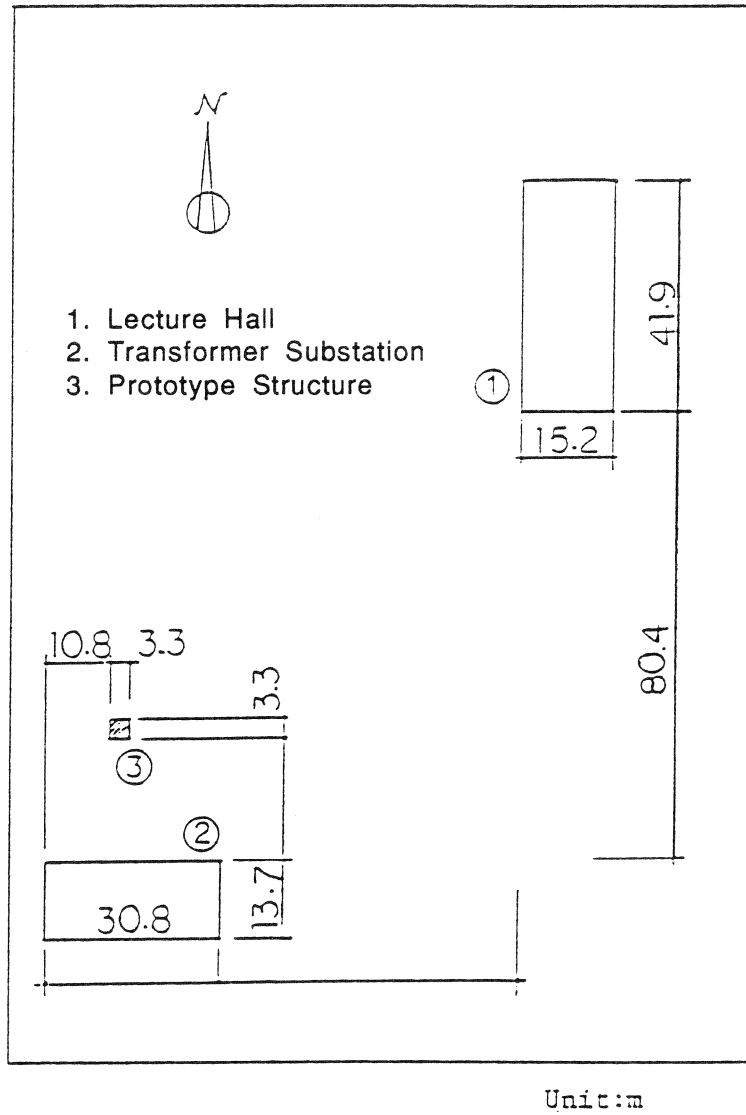


FIGURE 2-1 Location of Prototype on West Campus of BPU

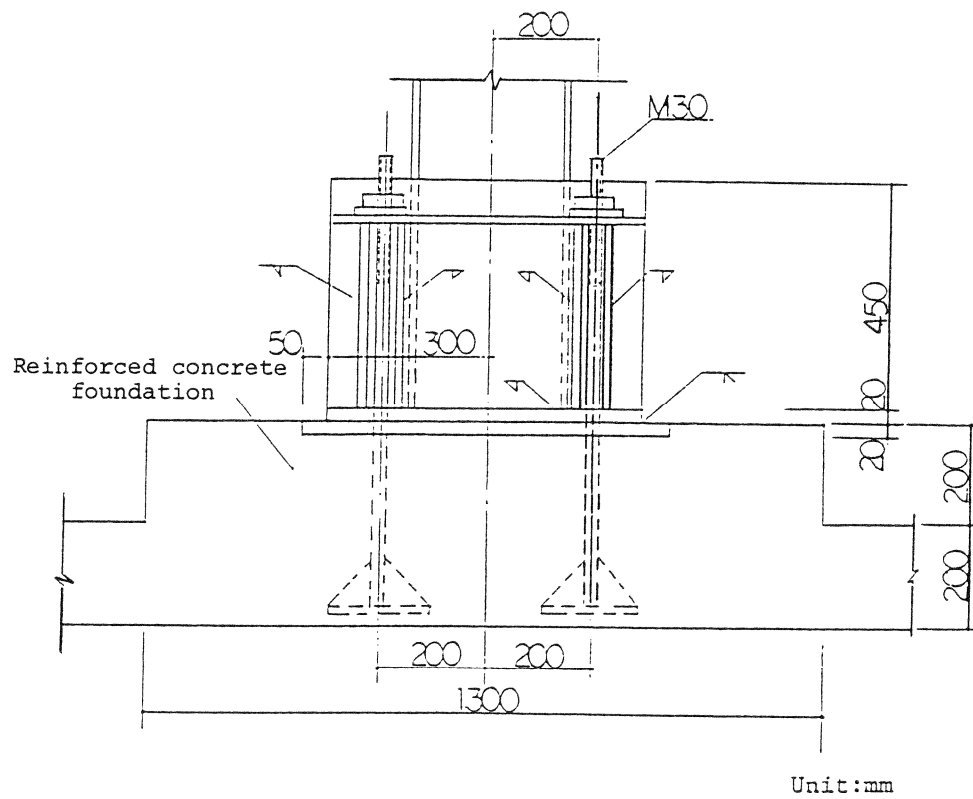


FIGURE 2-2 Connection of Column and Foundation

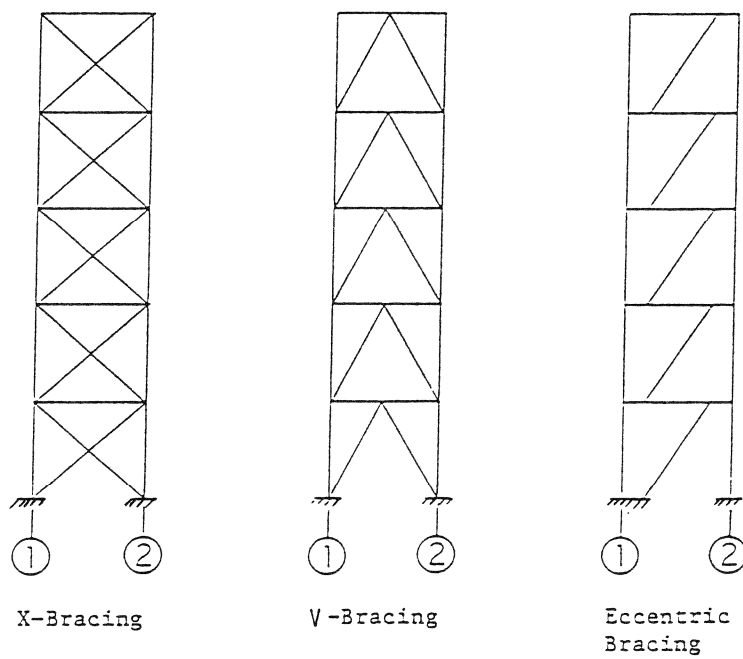


FIGURE 2-3 Prototype with Different Bracing Systems

3. For the last testing stage, the first floor will be changed to a box shape foundation to allow structural dynamic characteristics at different embedded foundation depths to be observed. The bottom of the foundation plate is 9.84 ft. (3.00 meters) below ground.
4. All of the beam-column joints are rigidly connected, as shown in Figure 2-4.
5. The column wing plates are welded to foundation bolts, as shown in Figure 2-5.

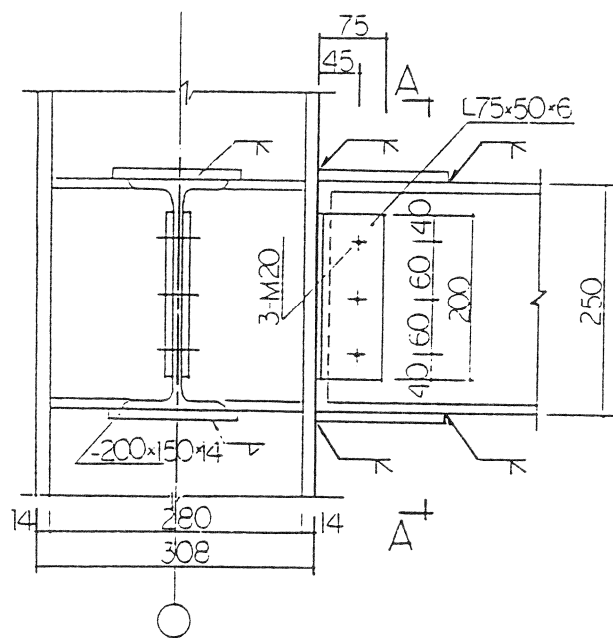
2.3 Member Sizes and Materials

The material properties of the prototype structure are shown in Table 2-I. The structural member properties are described as follows:

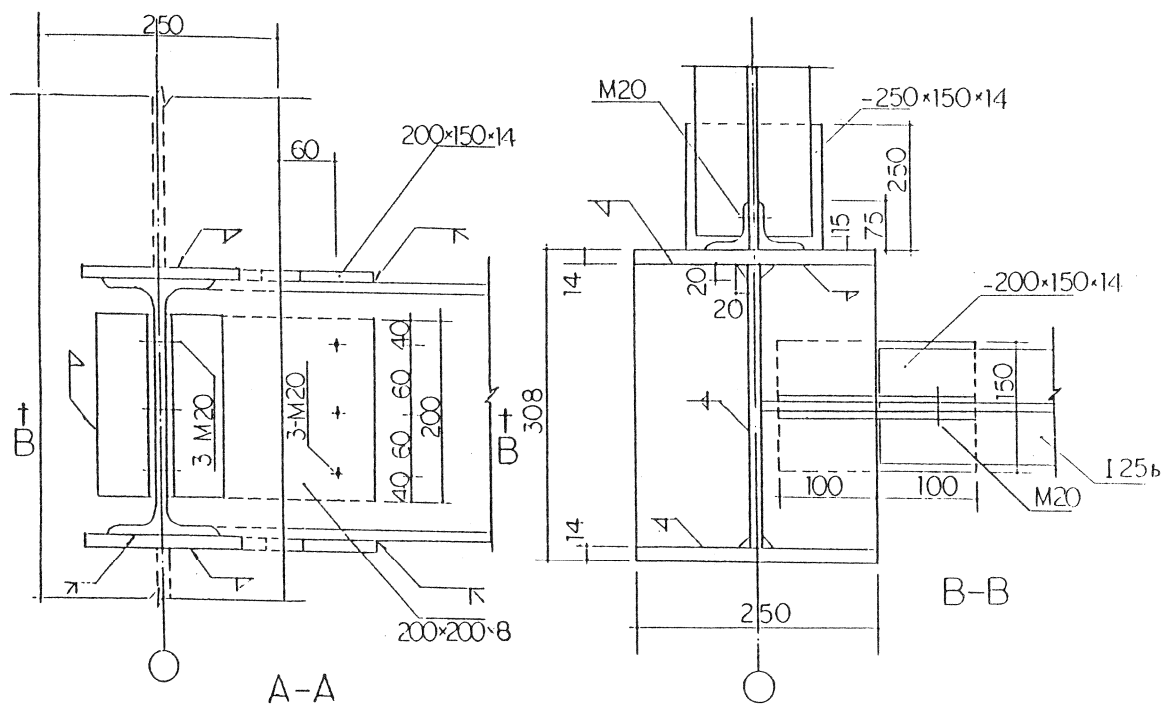
1. Columns were manufactured by welding a piece of web metal to two flanges. The cross section is H-308 x 250 x 10 x 14 (mm). The web of column is A3 steel (Chinese product) and the flange of column is SS41 steel (Japanese product). The elastic material properties are the same.
2. The beams are hot-rolled I25b-shaped A3 steel.
3. All the bracings are double angles with equal legs (L63 x 63 x 6 A3 steel). The section and size of the members are shown in Figure 2-6.

2.4 Foundation Soil

Two 30 m. deep sampling boreholes were drilled to obtain a clear understanding of the stratum in the field, and to determine the physical and mechanical characteristics and dynamic parameters of soils in the laboratory. One borehole is located east of the prototype steel structure, the other is located between the two reinforced concrete foundation plates. The soil specimens were tested with dynamic triaxial apparatus to determine their shearing strain, γ , shear modulus, G , and relation curve of γ versus soil damping factor, β . These experimental results will be used as the basis for analyzing the dynamic interaction between soil, foundation and superstructure. The shear wave velocities of the field soils were determined by crosshole method in situ.

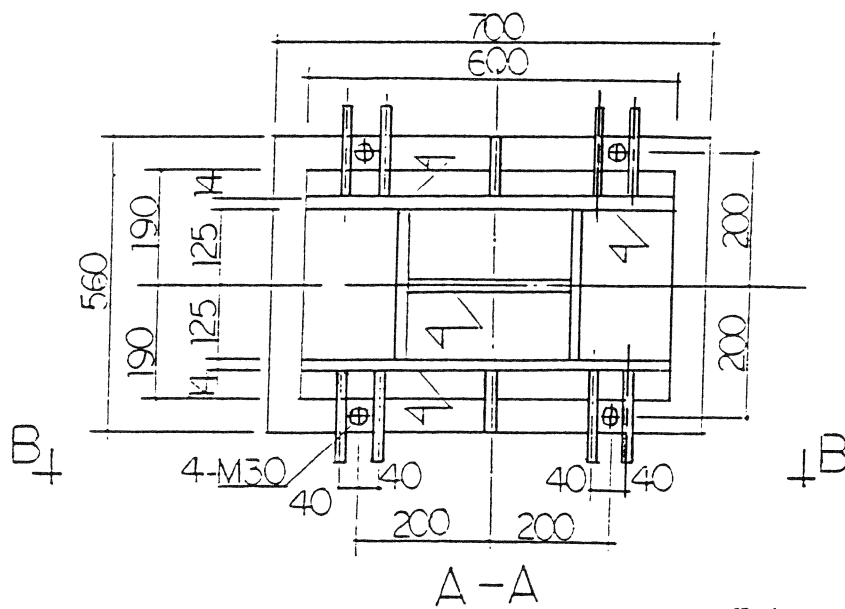
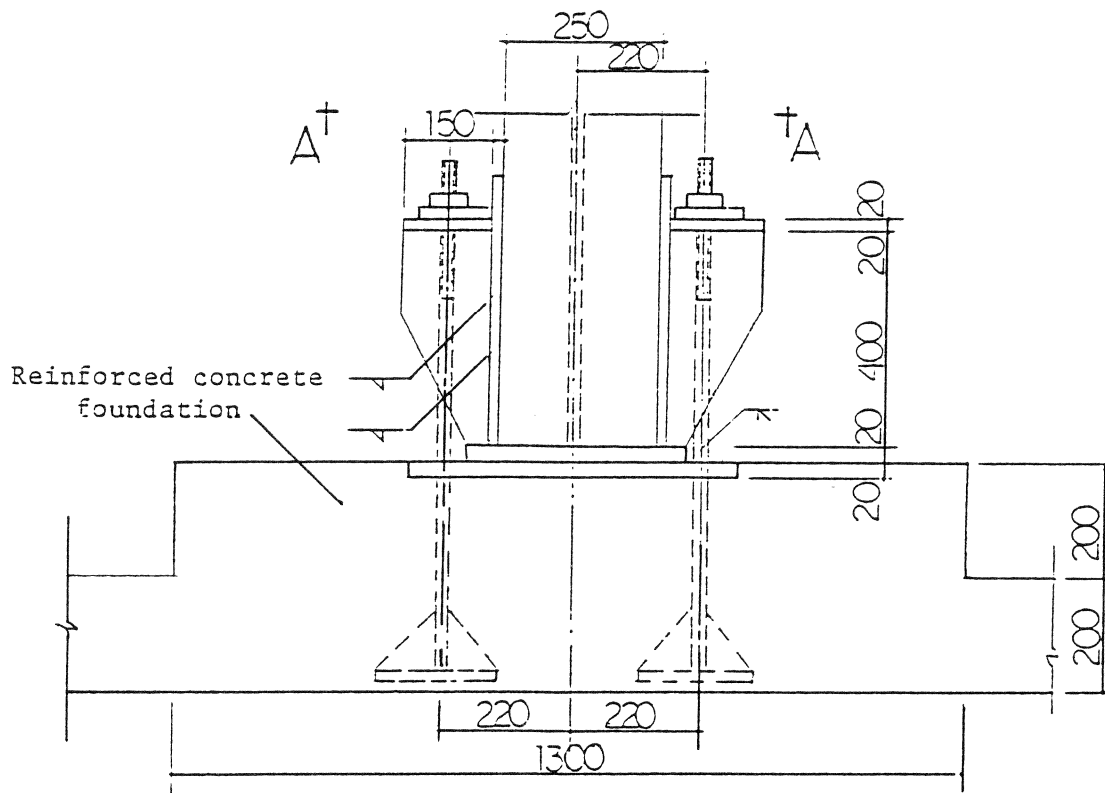


Unit:mm



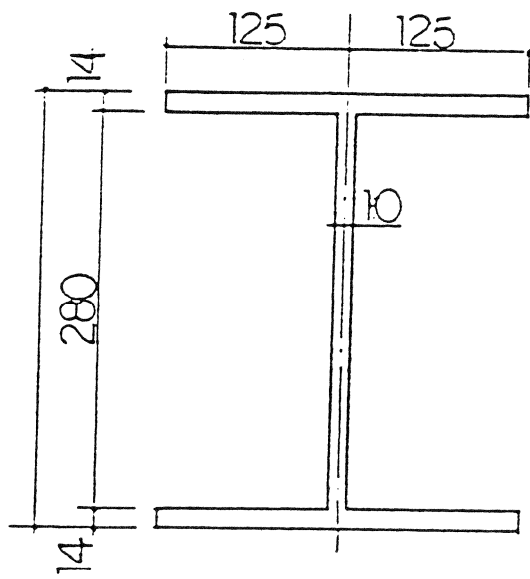
Unit:mm

FIGURE 2-4 Typical Connection of Beam-Column

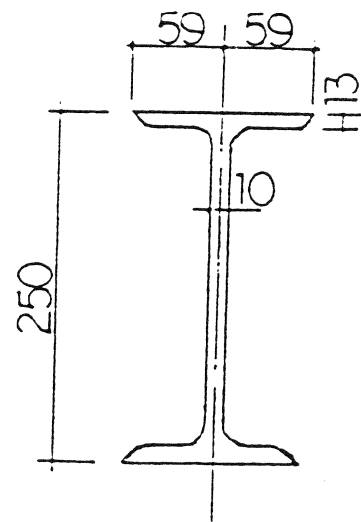


Unit:mm

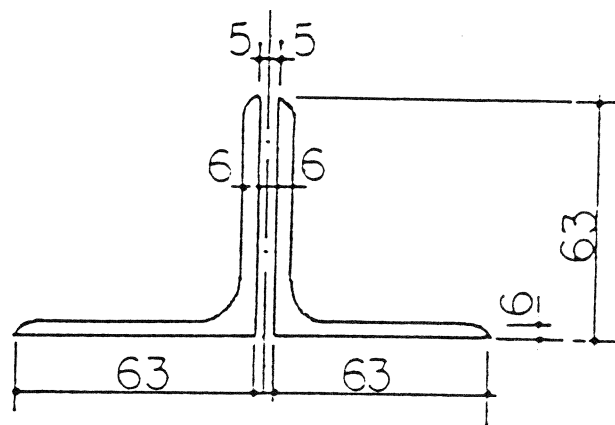
FIGURE 2-5 Connection of Column and Foundation



Column



Beam



Bracing

Unit:mm

FIGURE 2-6 Section of Prototype Member

TABLE 2-I Prototype Material Properties

Structure Member				Nominal stress (kg/mm ²)		Sample mean stress (kg/mm ²)	
		Type	Size	Yield	Tensile	Yield	Tensile
Column	Web	A3	-10	≥24	38~47	27.64	42.37
	Flange	SS41	-14	≥24	-	27.55	42.62
Beam		A3	I25b	≥24	38~47	33.25	48.06
Bracing		A3	L63x6	≥24	38~47	29.49	41.43

A3: Chinese product

SS41: Japanese product

TABLE 2-II Prototype Loading Condition

	Weight (kg/m ²)	Floor				
		Roof	5th	4th	3rd	2nd
Insulating layer of air entrainment	335	x				
70mm floor finishes	136		x	x		x
110mm floor finishes	205				x	
80mm concrete floor	200	x	x	x	x	x
ceiling No. 6	20	x	x			
ceiling No. 6b	30			x	x	x
Total		555	356	366	435	366

Floor	Roof	5th	4th	3rd	2nd
Live load weight (kg/m ²)	50	250	400	250	400

Five soil-pressure cells were carefully buried in the soil, and are located at the midpoints of the four sides and at the center of the foundation plate (raft), just touching its bottom. They are used to measure the static and dynamic soil pressures which act from beneath the foundation before and during vibration tests.

In addition, two circular test shafts of 10 m. deep and 1.2 m. diameter were dug, one at a distance of 7.5 m. to the east of the prototype structure, the other 7.5 m. to the north. Accelerometers were placed along the side wall from top to bottom of the shafts at several positions where the stratum changes. The soil acceleration response was measured simultaneously when the displacement responses of every floor of the prototype structure with V type bracing system were measured, while the foundation plate under the prototype structure and its nearby plate were excited by the vibrator in turn.

The soil layers under the foundation, counted from beneath its bottom downward, are: 2.8 m. light/heavy loam, 1.2 m. silty sand, 2.55 m. light loam, 4.15 m. fine sand, 7.8 m. light loam, 5.1 m. medium sand, 2.7 m. gravel, and a layer of loam over 2.2. m. thick.

The experimental results will be detailed in a future report.

2.5 Design Code

The prototype structure was designed by Chinese design codes as follows:

1. Loading Code for Industrial and Civil Architecture Structure (TJ 9-74).
2. Earthquake Resistant Design Code for Industrial and Civil Architecture (TJ 11-78)
3. Foundation Design Code for Industry and Architecture (TJ 7-74).
4. Design Code of Reinforced Concrete Structure (TJ 10-74).

In addition, the rigid beam-column joint satisfies the calculation and design method in an engineering community accepted reference book, **Design of Welded Structures** [1].

2.6 Design Loading

The dead and live loads on every floor of the prototype structure are shown in Table 2-II. The wall weight is not included. Table 2-III shows the prototype design loads. In actual design, the wall weight is included in dead load. But in the test plan, the wall weight is considered only half in order to satisfy the test. Loading during tests is shown in Table 2-IV. The testing load for the first stage is shown in Table 2-V. Earthquake loading is based on **The Earthquake Resistant Design Code of Industrial and Civil Architecture** (TJ 11-78). The total base shear Q_0 (total lateral force) is:

$$Q_0 = C \alpha_1 W \quad (2.1)$$

Where Q_0 is total base shear, and C is a structural influence coefficient which varies according to structural type. For steel structures, C equals 0.25. W is the total inertia weight. α_1 is an earthquake influence coefficient. It depends on the fundamental period of the structure. For a multi-story frame, α_1 equals 0.45. The lateral force distributed to every floor, P_i , depends on the floor height, as in the following equation:

$$P_i = \frac{W_i H_i}{\sum_{k=1}^n W_k H_k} \dot{Q}_0 \quad (2.2)$$

Where W_i is the weight at the i th floor, W_k is the weight at the k th floor, H_k is height of the k th story, and H_i is height of the i th story.

TABLE 2-III Prototype Design Loads

Floor	Floor Weight (ton)			
	Dead	Live	Wall	Total
Roof	6.04	0.55	-	6.59
5th	3.88	2.72	10.93	17.53
4th	3.98	4.36	10.93	19.27
3rd	4.74	2.72	11.02	18.48
2nd	3.98	4.36	10.93	19.27

TABLE 2-IV Loading During Tests

Floor	Floor weight (ton)			
	Dead	Live	Wall	Total
roof	6.04	0.55	-	6.59
5th	3.88	2.72	5.95	12.55
4th	3.98	4.36	5.95	14.28
3rd	4.74	2.72	6.00	13.48
2nd	3.98	4.36	5.95	14.28

TABLE 2-V Loads at First Stage Testing

Floor	Floor Weight (ton)	
	Prototype with floor plate	Prototype with floor plate and bracing
roof	2.18	2.70
5th	2.18	2.18
4th	2.18	2.18
3rd	2.18	2.18
2nd	2.18	2.18

2.7 Construction

In order to meet the requirements of tests, the construction stages of the prototype included the following elements: foundation plates, five-story steel frame, cast-in-situ concrete plate and bracing. Each of these stages are described in the following subsections.

2.7.1 Foundation Plates

Two identical foundation plates were constructed in September 1987. The plate is 17.4 x 17.4 ft. (5.3 x 5.3 meters) with a thickness of 7.87 inches (0.20 meters). The distance of center line of the two foundations is 28.3 ft. (8.63 meters), as shown in Figure 2-7. Two foundation plates were constructed because: (1) the five-story structure is constructed on one plate, and no structure is on the second plate so the influence of structure-foundation interaction can be compared; and (2) two vibration generators can be located on both foundation plates to observe the effect of wave propagation between the two foundation plates.

2.7.2 Five-Story Steel Frame

After the five-story steel frame was shop welded in the factory, it was transported to the test field and erected on a foundation plate (Figure 2-8). The dynamic testing of the pure frame without the floor plate was finished in the spring of 1988.

2.7.3 Cast-in-situ Concrete Floor

A cast-in-situ concrete floor was applied on every floor with a plate thickness of 3.15 inches (8 cm). The dynamic tests were successfully finished in the fall of 1988.

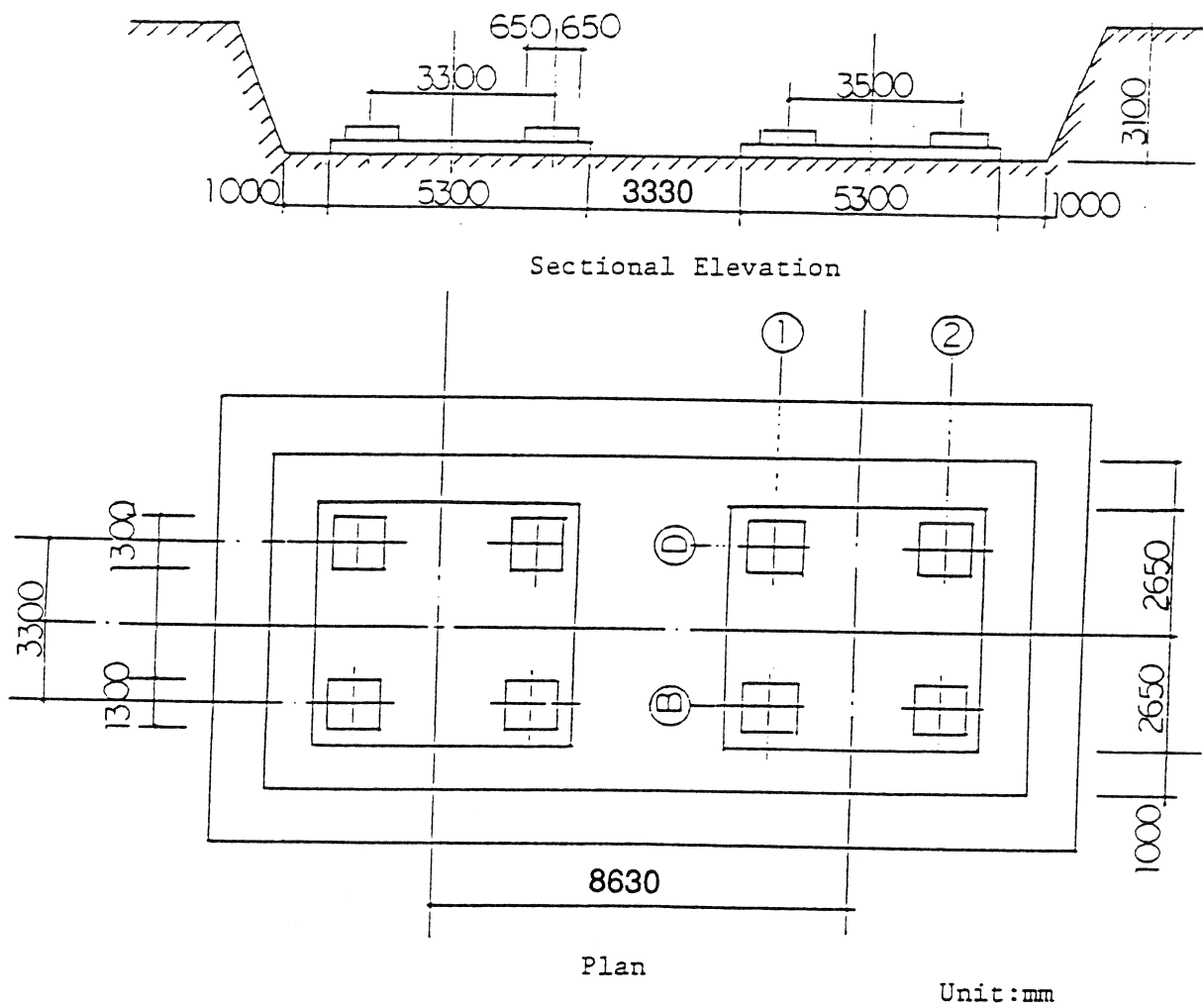


FIGURE 2-7 Prototype Foundation

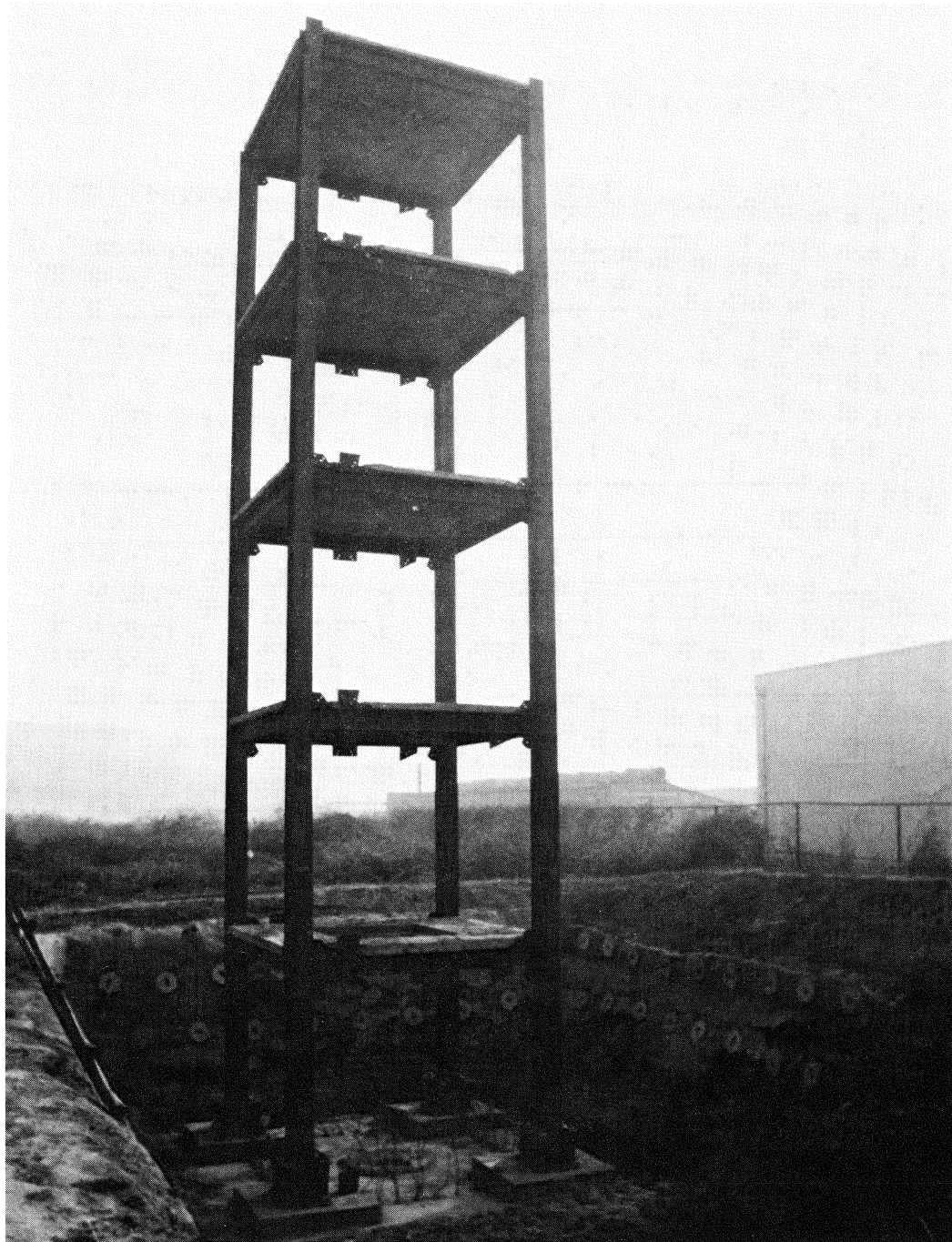


FIGURE 2-8 Picture of Prototype Building

2.7.4 Bracing

The prototype, with floor plate, was strengthened by adding a different bracing system in the fall of 1988. Three types of bracing were used: eccentric, V and X bracing. In the following text, "E," "V," and "X" will be used to represent these three types of bracing systems, respectively. "F" will be used to represent the structure without bracing in the Y-Y direction.

SECTION 3

MODEL DESIGN AND MANUFACTURE

3.1 Determination of Model Scale

It is well known that model testing is inherently inaccurate due to the scale of the models. The smaller the scale, the larger the errors. Therefore, large models provide more reliable test results.

The controlling factor which decided the model size was height. The overhead crane in the laboratory has a ceiling clearance of 24 feet. The prototype structure is approximately 49 ft. in the vertical direction. The foundation block, which connects the model to shaking table, is 2 ft., 8 inches. Therefore, a model scale of 0.4 was chosen which allows the model height to be 19 ft., 8 inches. It was determined that with this scaling factor, the model to be built would provide satisfactory results.

3.2 Similitude Requirement

In conforming to the similitude laws, several assumptions were made, and consequently, the scaling law was established based upon these assumptions. For example, it was assumed that the gravity constant and the building material (mass density and Young's Modulus), were the same for both the prototype and the model. In addition, a lumped mass system [2], typical for dynamic tests, was used. To satisfy the requirement of a lumped mass system, artificial mass was added to the structure. This was done by adding steel plates and lead blocks at all floor levels on the model. In Table 3-I, the similitude scaling laws for artificial mass simulation tests are listed.

3.3 Model Component Design

The similitude requirements described above were followed when the model structure was designed. Descriptions and discussions of the model design are presented below.

TABLE 3-I Modeling Laws for Artificial Mass Simulation

Scaling Parameters*		Scale
Length	$\underline{l_r}$	1:2.5
Time	t_r	$l_r^{1/2}$
Frequency	ω_r	$l_r^{-1/2}$
Velocity	v_r	$l_r^{1/2}$
Gravitational acceleration	$\underline{g_r}$	1:1
Acceleration	a_r	1
Structure mass	M_r	$E_r l_r^2$
Strain	ϵ_r	1
Stress	σ_r	E_r
Modulus of elasticity	$\underline{E_r}$	1:1
Displacement	δ_r	l_r
Force	F_r	$E_r l_r^2$
Energy	$(EN)_r$	$E_r l_r^3$

*Underlined scale ratios are chosen by the investigator.

Overall Dimension and Cross Section: The height and width of every floor are shown in Figure 3-1. It is noted that the first floor has a smaller floor height (43 inches) than the rest of the floors (47 inches), however, the member layout is identical.

In the model structure, all columns are of one size and all beams have the same dimension. The cross sections of columns, beams, and bracing members are shown in Figure 3-2. In order to satisfy both the similitude laws and the availability of materials, the dimensions of the sections were designed so that the cross sectional areas, moments of inertia, and elastic and plastic section moduli, conformed to the scaling laws as closely as possible. However, the width and thickness of the flange and web are distorted slightly from the exact value, due to the commercial availability of metal sheets.

Since the scaled beam and column sections were not standard stock sizes, they were made by welding two flange strips to a web plate. Their geometrical properties are listed in Table 3-II.

Connections: Beam to column connections in the prototype were designed to transfer moments. To serve this purpose, flanges and webs of the beams are welded and bolted, respectively, to the columns. Backup stiffeners [3] are used on the column as would be done in standard design practice. Details of the prototype were carefully followed in the model except for the weld size. Due to manufacturing difficulties, the smallest weld size used in the model structure is 0.125 inches. Figure 3-3 shows the connection details.

Foundation: Figure 3-4 shows the model foundation. The prototype has a reinforced concrete footing, which is unnecessary to model. Therefore, the column base plates are fully welded to a connector plate (41 x 27 x 1 inch) and bolted onto the foundation block via nine 1-1/8 inch bolts. It is designed so that a rigid foundation can be assumed.

Bracings: There were three types of bracings incorporated into the structure. They are the eccentric, V, and X type bracings. Bracings are installed in the weak axis of the column to increase the structure's lateral stiffness. Figures 3-5 to 3-7 show the typical bracing connection

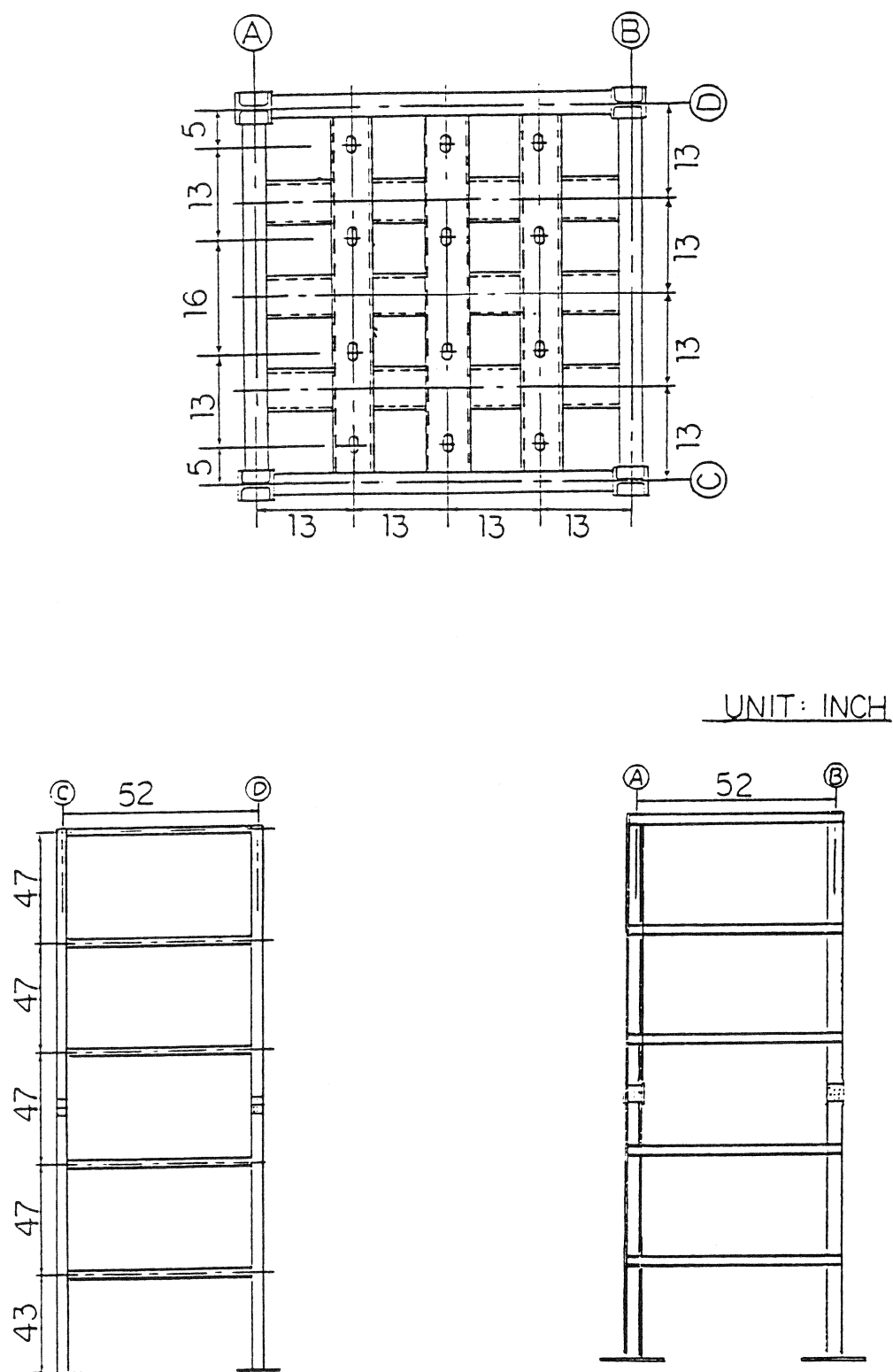
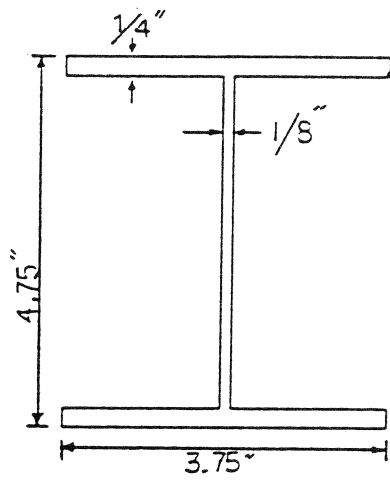
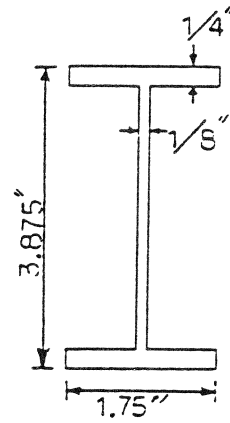


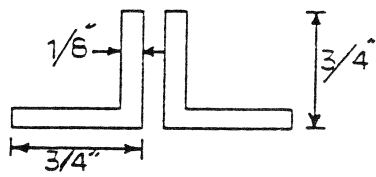
FIGURE 3-1 Model Dimension



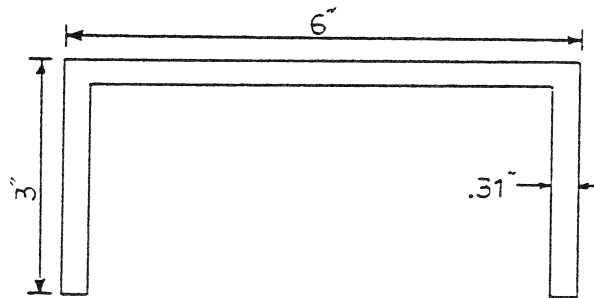
COLUMN



BEAM



BRACING



FLOOR

FIGURE 3-2 Model Member Cross Section

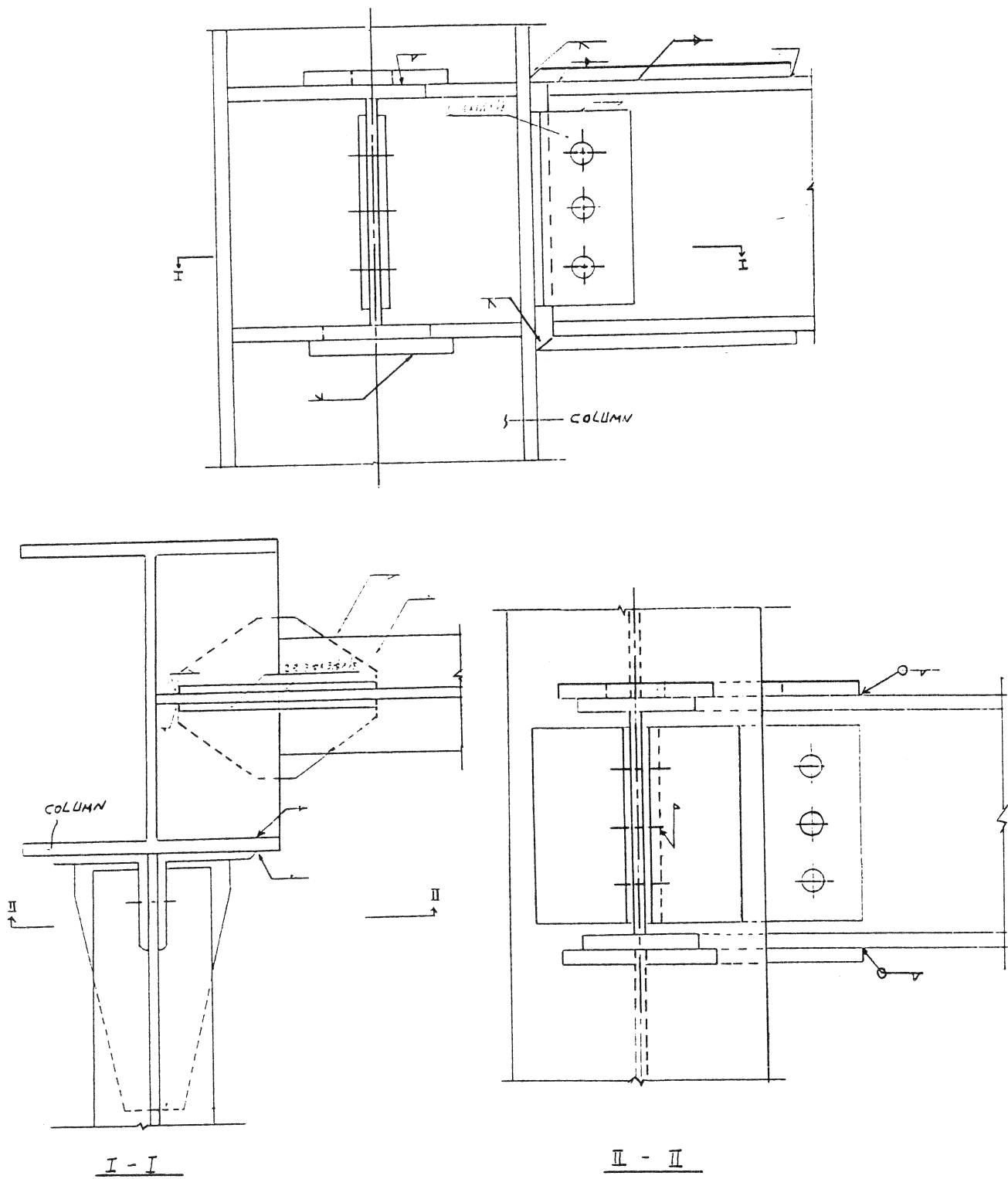


FIGURE 3-3 Model Beam-Column Connection

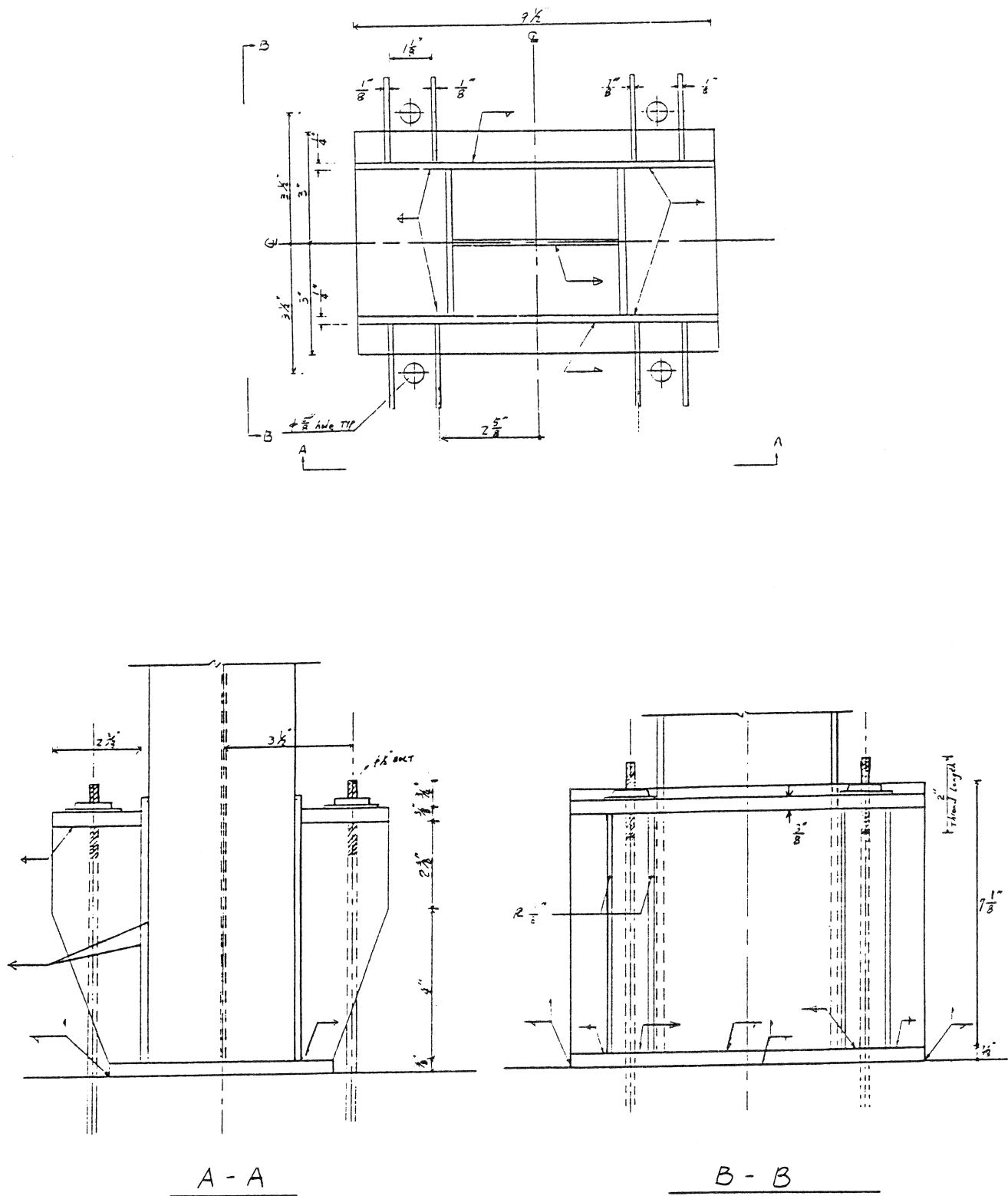
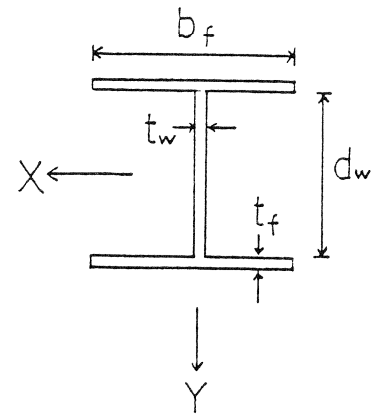


FIGURE 3-4 Model Foundation

TABLE 3-II Model Member Properties

COLUMN	PROTOTYPE	THEORETICAL	ACTUAL
b_f	9.84	3.94	3.75
t_f	0.55	0.22	0.25
d_w	11.02	4.41	4.25
t_w	0.39	0.16	0.125
Area	15.19	2.43	2.41
I_x	407.5	10.43	10.30
S_x	67.2	4.3	4.34
Z_x	74.72	4.78	4.35
I_y	87.65	2.24	2.20
S_y	17.81	1.14	1.17
Z_y	27.1	1.73	1.76
$b_f / (2t_f)$	8.93	8.93	7.50
d_w/t_w	27.97	27.97	34.0



BEAM	PROTOTYPE	THEORETICAL	ACTUAL
b_f	4.65	1.86	1.75
t_f	.51	0.20	0.25
d_w	8.82	3.53	3.38
t_w	0.39	0.16	0.125
Area	8.29	1.33	1.30
I_x	126.95	3.25	3.28
S_x	25.79	1.65	1.69
Z_x	30.07	1.92	1.94
$b_f / (2t_f)$	4.54	4.54	3.50
d_w/t_w	22.38	22.38	27.0

BRACING	PROTOTYPE	THEORETICAL	ACTUAL
Area	2.148	0.344	0.344

and their dimensions. A bracing member was made of two angles (Figure 3-2) combined by bracing stiffeners along the length at the intermediate points. The ends of the bracing are bolted into a gusset plate, which is welded to the center of beam flange and column web. The bolted bracing ends are removable, so that different bracing systems can be tested.

Weight: Since the artificial mass simulation method requires model weight be proportional to the square of the model scale [2], there must be extra weight, other than the member self weight, added to the structure. This was satisfied by bolting down steel plates to the floors. Steel plates were purchased at different sizes so that combinations of them would meet the requirements of the different loading cases. In addition, lead bricks, each weighing 25 pounds, were placed on the top of the steel plates to fine tune the weight simulation.

Based on the weight of the prototype and the scaling laws, the weight of the model structure can be determined. The weight of the prototype is shown in Table 3-III, which is the combination of the 3.15 inch (80 mm) thick concrete slabs and structural members. In addition, there was an eccentric vibrator on the roof of the prototype. It accounts for 1.157 kip (0.526 ton) and is included in the first column of Table 3-III. The theoretical and actual weight of the model is also shown in Table 3-III.

Floor: The prototype building has reinforced concrete slabs which are not used in the model structure. They are not used because:

1. The model slab would be very thin (1.25 inches) if the correct modeling law is to be followed. This is difficult and expensive to construct, considering the reinforcement material manufacturing and detailing.
2. The model will be used in a multi-purpose research program which involves many operations on the floor. Using a brittle material for the floor cannot guarantee the uniformity of the structural properties.

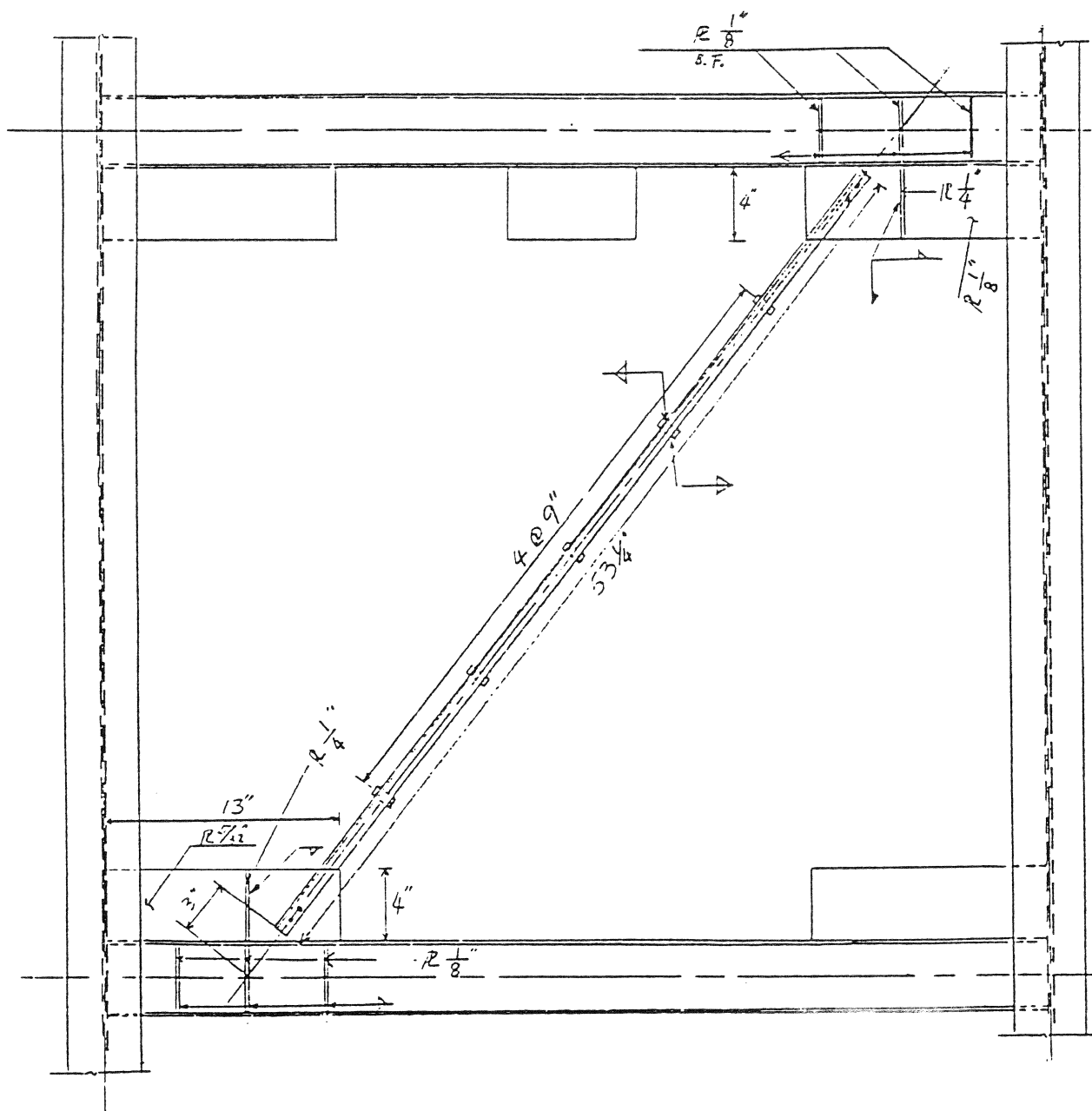


FIGURE 3-5 E Bracing Detail

3-11

TABLE 3-III Weight Comparison of Prototype and Model

FLOOR	PROTOTYPE WT.	THEORETICAL MODEL WT.	ACTUAL MODEL WT.
ROOF	8.188	1.310	1.313
5	8.039	1.286	1.269
4	8.039	1.286	1.269
3	8.039	1.286	1.269
2	8.039	1.286	1.269

Unit: Kip

As a result of the above considerations, the floor was made of MC 6 x 12 channel sections. The channels are pin connected to the peripheral beams to avoid introducing any torsion to the latter. On the channel webs, slots are opened so that spacers between weight plates and channels could be connected to the floors. The spacers work to prevent weight plates' rigidity from attaching to the structural stiffness of the beams [4].

Inconsistency: Although much effort has been put into the model design and construction, inconsistency was found after completion of the model construction. It was found that backup stiffeners, located behind the gusset plates in each floor for the X bracing on the column (Figure 3-8), were not included in the model. The effect of this inconsistency will be discussed in Section 5.

3.4 Model Manufacturing

After design drawings of the model were completed, the model was built by WSF, a local company known for manufacturing high-quality welded structures.

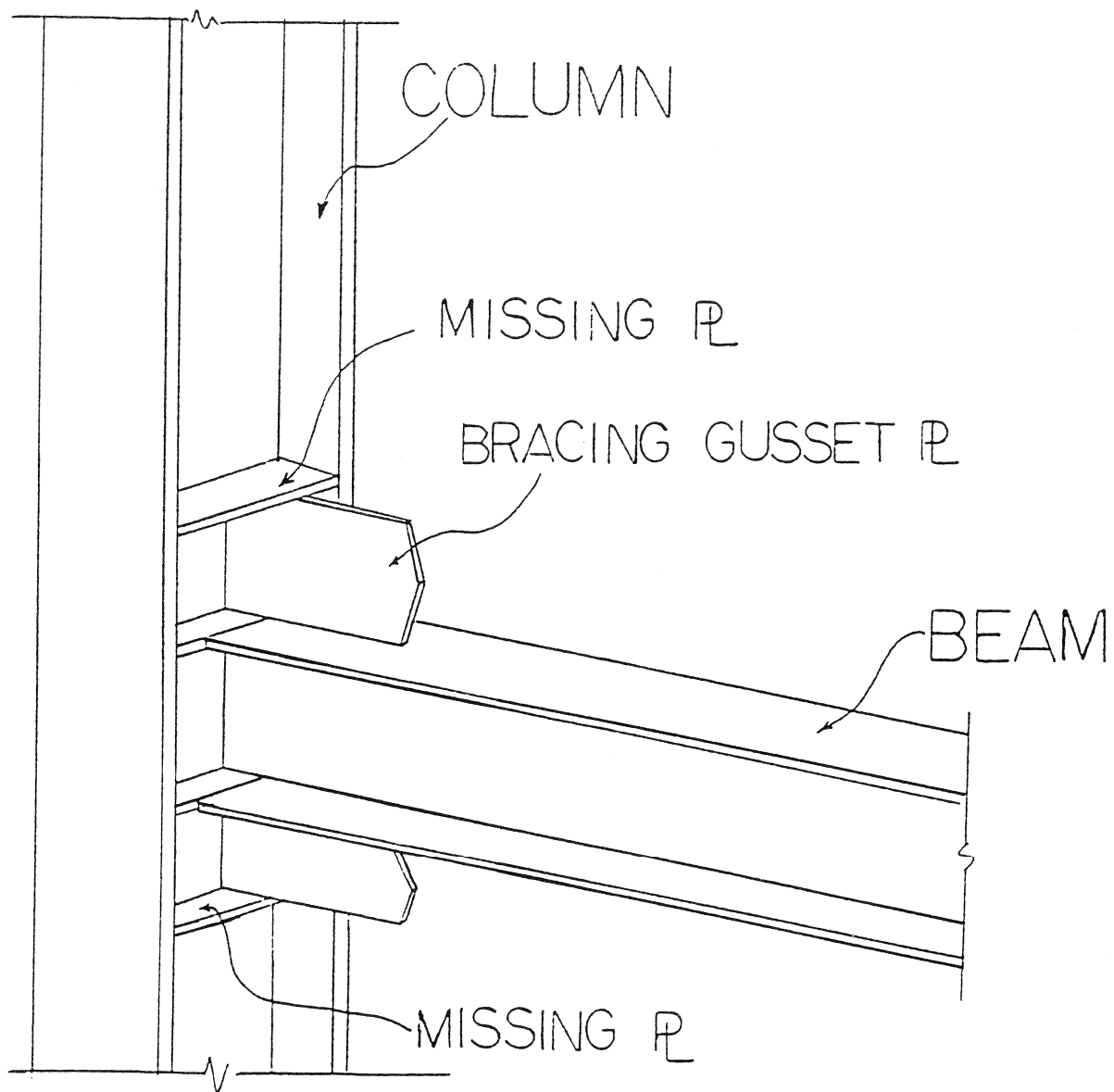


FIGURE 3-8 Model Beam-Column Connection Missing Plate

3.4.1 Coupon Test

One of the most important assumptions in the similitude laws used in this project are that material for the model is the same as that of the prototype. As one of the major objectives of the research program is to evaluate the reliability of scaled-down models in predicting the behavior of full-scale structures, the stress-strain curve of the model material should exhibit a similar relationship as that of the full-scaled structure. Figure 3-9 illustrates the coupon tests of the model specimen. Two different coupon sizes, 1/4 and 1/8-inch thick, cut from a sample column's flange and web, were tested. A total of eight coupons, four from the flange and four from the web, were tested under uniaxial monotonic tensile loading to determine the basic material properties. The conclusions of the tests were as follows:

1. Flange samples have yielding stress around 50 ksi and strain hardening starts at around 2% strain.
2. Web samples have yielding stress around 39 ksi and strain hardening starts at around 1.3% strain.
3. The averaged Young's Modulus is 29000 ksi.

3.4.2 Residual Stress Test

The influence of residual stress to the column strength has been extensively discussed in many publications [5]. Since the model structure was made of welded sections, its residual stress distribution was thus worth investigating. Results of the residual stress test are presented in this section.

The column sections were manufactured with 1/8-inch TIG welding [6], connecting a web plate to two flange plates. The sequence of welding along the member length were numbered from 1 to 4 as shown in Figure 3-10a. During and after the welding, metal plates were placed against the flange to conduct heat generated from welding away from the model. Also, the flange tips were clamped to avoid cambering owing to the thermal effect.

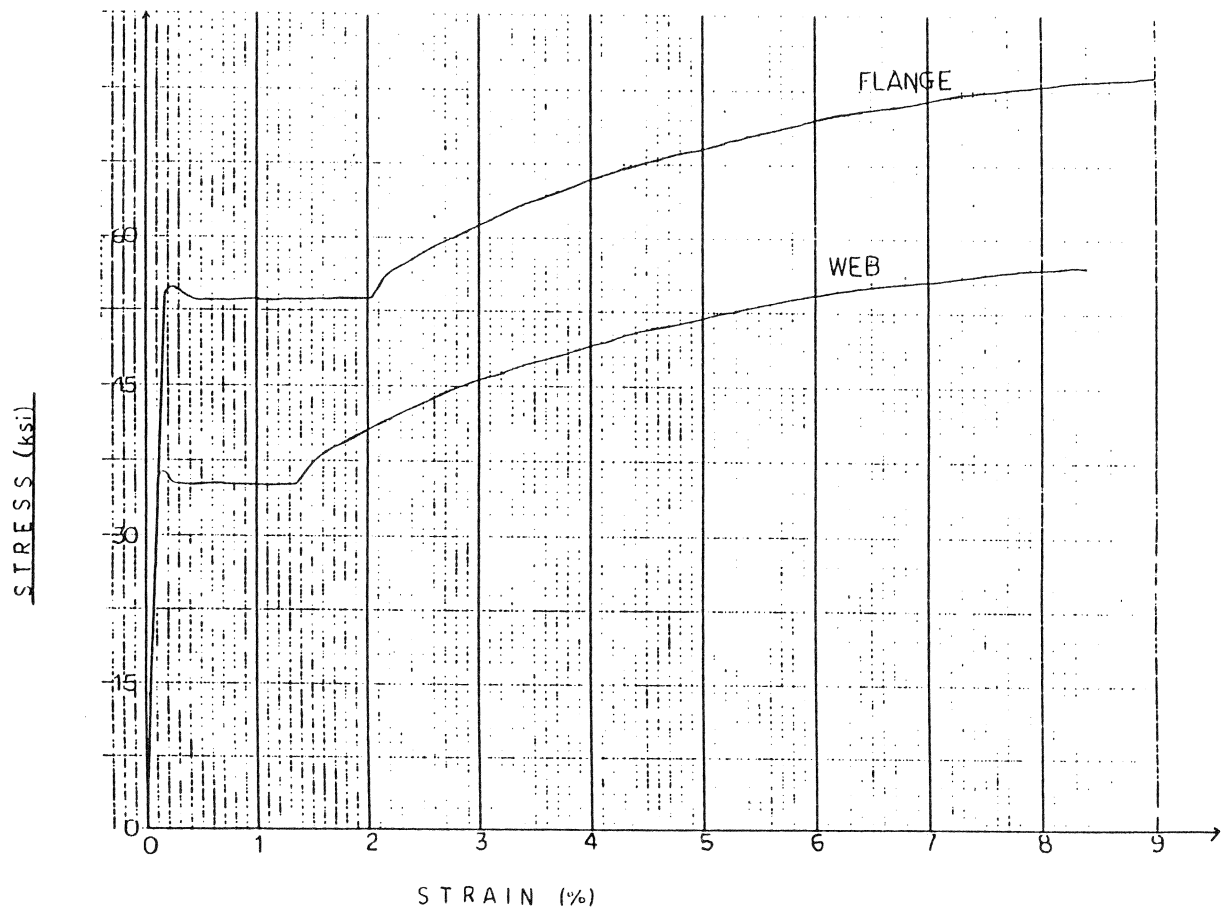
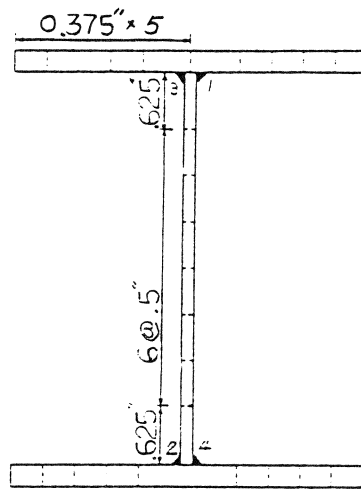
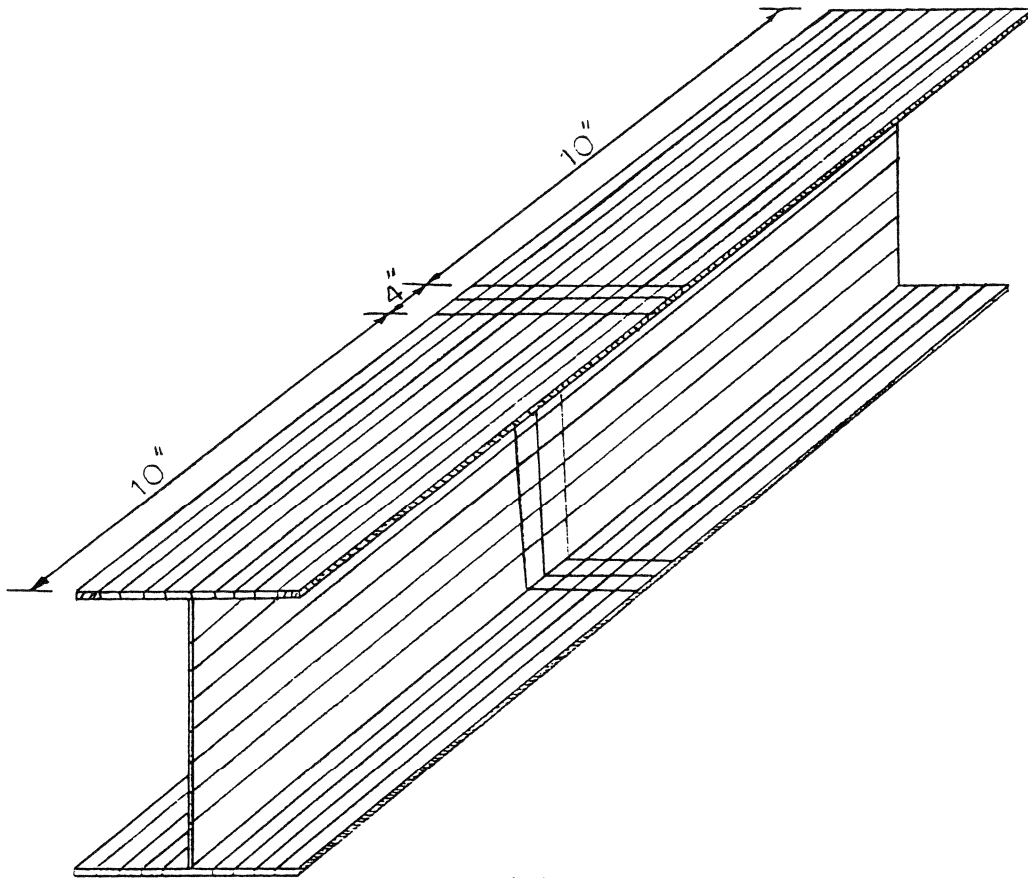


FIGURE 3-9 Model Material Property



(a)



(b)

FIGURE 3-10 Residual Stress Test

The method of "sectioning" [7] was used to obtain the measured residual strains and, consequently, residual stresses. A series of 10-inch gauge holes were laid out on the specimens and measured with a 1/10000 Whittemore strain gauge [8]. The difference in length before and after the sectioning is a measure of residual strains. Figure 3-10b shows the sectioning of the test samples. The 24-inch test sample cut out from the column sample was at a sufficient distance (12 inches) from the ends to offset any edge effect [9]. In addition, at several sections, electronic strain gauges were also used to check the Whittemore gauge readings. It was found that the results from the Whittemore strain gauge was very close to those of the electronic strain gauges.

Two segments were tested for residual strains and the results were very close to each other (Figure 3-11). The measured flange strain was about 0.12% at the center and 0.1% at the ends. For the web sections, the strain measured at both ends was around 0.14%, and diminished rapidly at sections positioned away from the welds to an average of 0.05%. Thus, it is clearly demonstrated that at the junction of flange and web, both flange and web were yielded because of the welding. But away from the weld, most of the member sections remained unyielded.

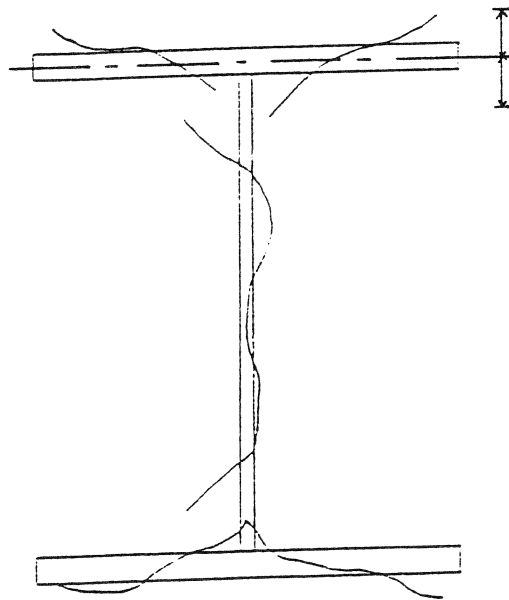
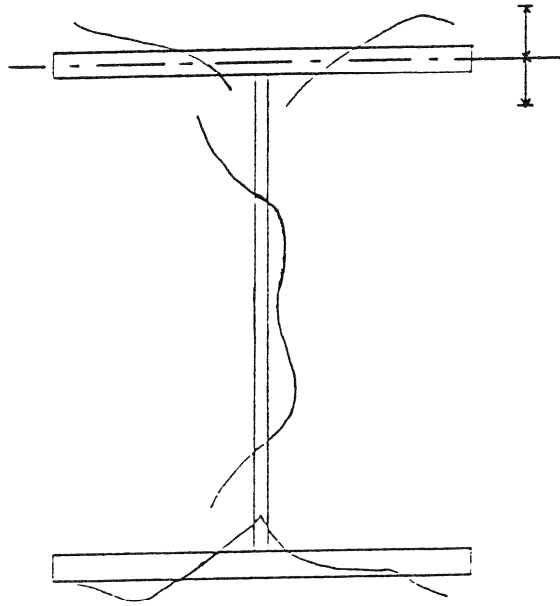


FIGURE 3-11 Residual Stress Distribution

SECTION 4 PROTOTYPE STRUCTURE TESTS

4.1 Test Program

The tests were carried out in six stages according to the test schedule:

1. Forced vibration tests of foundation plates alone;
2. Dynamic tests of the structure without concrete slabs;
3. Dynamic tests of the structure with concrete slabs;
4. Dynamic tests of the structure with different types of bracing systems;
5. Change the thickness of the foundation plate from 7.87 inches (20 cm) to 15.7 inches (40 cm), and repeat dynamic tests in stages 3 and 4;
6. Change the first floor into a box-shaped foundation and repeat test stages 3 and 4.

So far, test stages 1 through 4 have been completed, and the results are presented in this section.

4.2 Test Results

The dynamic characteristics of the prototype without floor plate were determined by four different test methods. They are the forced vibration, the ambient vibration, the free vibration, and the impact vibration tests. Each of these methods are described in the following subsections.

4.2.1 Prototype Structure Without Concrete Slabs

Forced Vibration Test: Forced vibration tests of the prototype structure without concrete slabs were conducted using a vibration generator located at the center of the foundation plate (Figure 4-1). X-X axis is in the direction of strong axis of the columns, while Y-Y is perpendicular to X-X. Excitation force was delivered by the generator in the X-X and Y-Y direction. The displacement transducers were placed at the center of the I-beam on every floor. Test results

showed that the natural frequencies were consistent among the frequency-response curves measured at different floors.

In the X-X direction, the first three natural frequencies of lateral vibration were 3.75 Hz, 12.64 Hz and 22.64 Hz, and the damping ratios were 1.2%, 0.9% and 1.0%. In the Y-Y direction, the first four natural frequencies of lateral vibration were 3.15 Hz, 9.86 Hz, 17.40 Hz and 21.50 Hz, and the damping ratios were 0.9%, 0.4%, 1.0% and 1.5%. The mode shapes are shown in Table 4-I. A comparison of the prototype frequencies between X-X and Y-Y direction is shown in Table 4-II. The displacement-response curve based on the roof measurement in the Y-Y direction is shown in Figure 4-2. In order to ensure the reliability of the damping ratios calculated, it was necessary to obtain more than five recording points within the half-power bandwidth. In forced vibration tests, the speed stability of the vibration generator must be within 0.01 to 0.005 Hz around the range of resonance peaks.

Ambient Vibration Tests: The natural frequencies of the first three lateral vibration modes in the X-X direction were 3.88 Hz, 12.75 Hz and 22.79 Hz. The damping ratios of the first two modes were 1.1% and 0.4%. In the Y-Y direction, the natural frequencies of the first four modes of lateral vibration were obtained. They were 3.19 Hz, 10.06 Hz, 16.84 Hz and 23.56 Hz. The damping ratios of the first three modes were 0.8%, 0.2% and 0.2%. A comparison of the prototype frequencies between the X-X and Y-Y directions is shown in Table 4-III. The mode shapes are shown in Table 4-IV. The first and second natural frequencies of the torsional vibration were obtained from the spectrum. They were 7.38 Hz and 14.88 Hz. For the first two mode shapes, the results obtained using forced and ambient vibration tests were found to have a satisfactory accuracy. For higher modes, the situation was not so satisfactory under the field testing condition. Sample spectra are presented in Figure 4-3 (X-X direction) and Figure 4-4 (Y-Y direction). A comparison of ambient and forced vibration tests (see Figure 4-5), shows that the correlation is very good in natural frequencies of the prototype structure. In a past study [10], the natural frequencies obtained from ambient vibration tests were found to be about 4% higher than those from forced vibration tests. In these tests, the measured first mode natural frequency shows that the difference is 2.9% (X-X direction) and 1.1% (Y-Y direction).

TABLE 4-I Prototype Mode Shape from Forced Vibration (without floor plate)

X - X			
Floor	1st Mode f=3.75	2nd Mode f=12.64	3rd Mode f=22.64
Roof	1.00	1.00	1.00
5th	0.92	0.13	0.62
4th	0.73	0.63	0.32
3rd	0.52	0.94	0.76
2nd	0.14	0.44	0.42

Y - Y			
Floor	1st Mode f=3.15	2nd Mode f=9.86	3rd Mode f=17.40
Roof	1.00	1.00	1.00
5th	0.85	0.17	0.56
4th	0.72	0.55	0.66
3rd	0.45	0.91	0.67
2nd	0.13	0.40	0.81

TABLE 4-II Translational Modes from Forced Vibration

Mode	X - X			Y - Y			
	1st	2nd	3rd	1st	2nd	3rd	4th
Frequency (Hz)	3.75	12.64	22.65	3.14	9.86	17.40	21.50
Damping ratio (%)	1.2	0.9	1.0	0.9	0.4	1.0	1.5

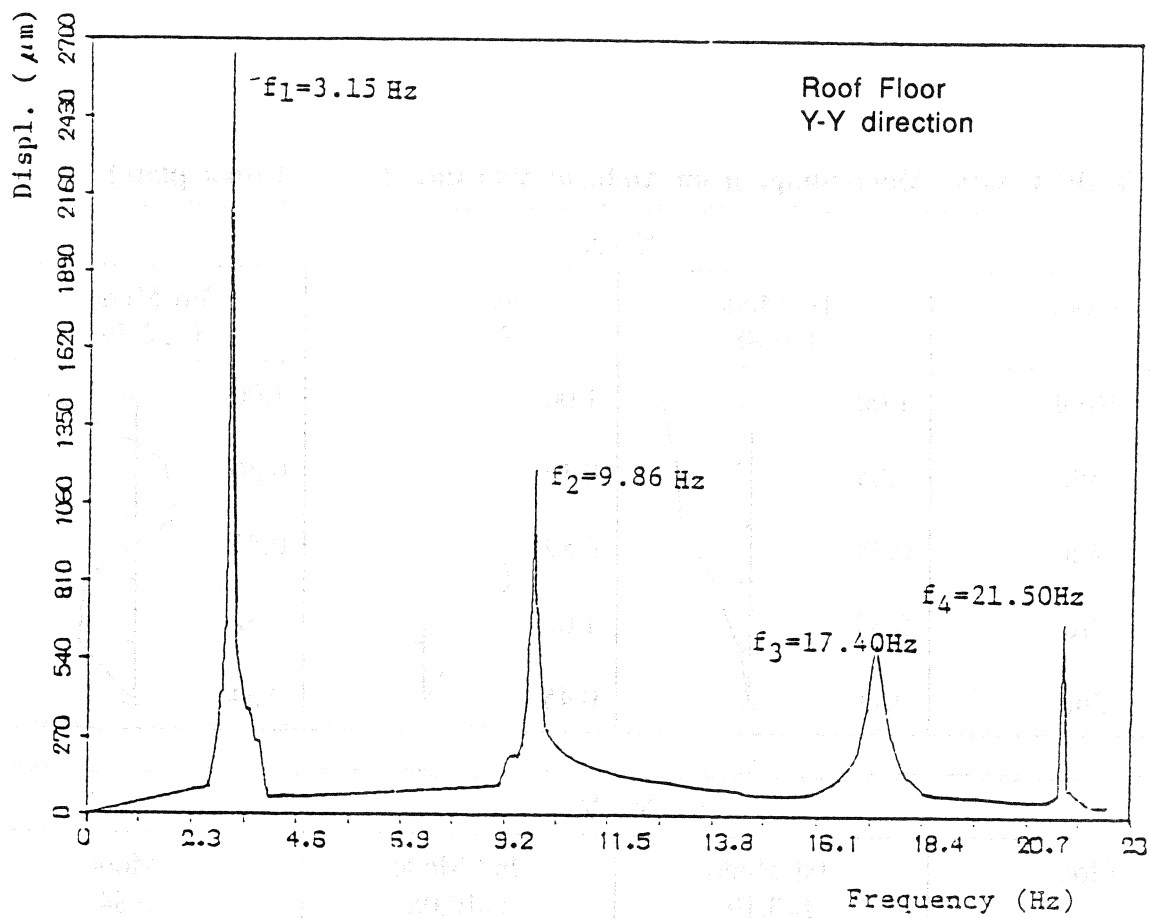





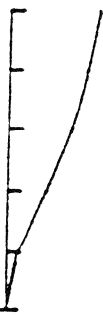
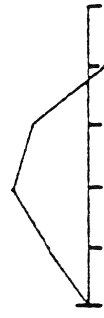

FIGURE 4-2 Force Vibration Displacement Response (without floor plate)

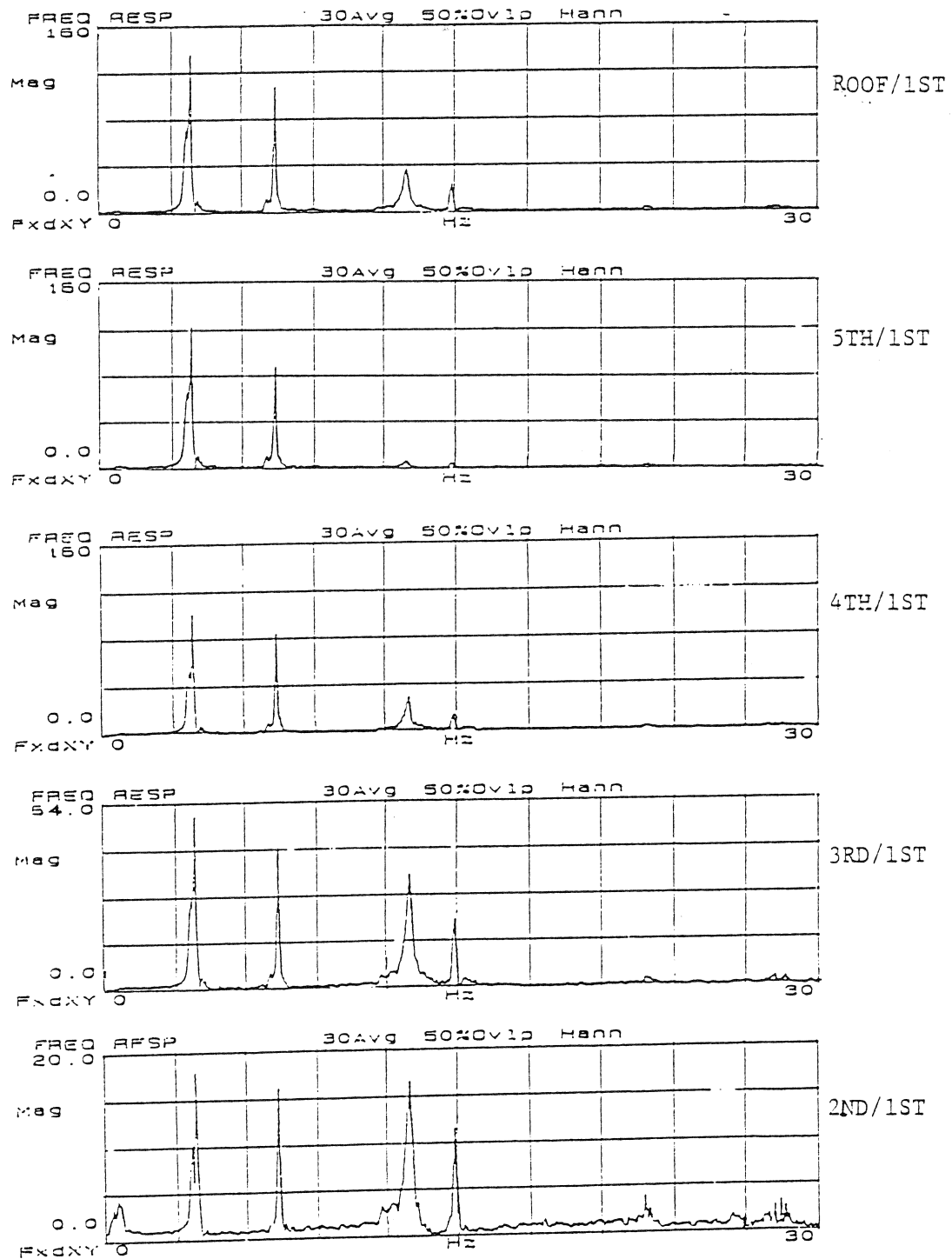
TABLE 4-III Translational Modes from Ambient Vibration

	X - X			Y - Y			
Mode	1st	2nd	3rd	1st	2nd	3rd	4th
Frequency (Hz)	3.88	12.75	22.79	3.19	10.06	16.84	23.56
Damping ratio (%)	1.1	0.4	-	0.8	0.2	0.2	-

TABLE 4-IV Mode Shape from Ambient Vibration (without floor plate)

X - X				
Floor	1st Mode f=3.88	2nd Mode f=12.75	3rd Mode f=22.79	
Roof	1.00	1.00	1.00	
5th	0.85	0.15	0.36	
4th	0.78	0.82	0.45	
3rd	0.39	1.06	0.52	
2nd	0.11	0.45	0.54	

Y - Y				
Floor	1st Mode f=3.19	2nd Mode f=10.06	3rd Mode f=16.84	
Roof	1.00	1.00	1.00	
5th	0.86	0.27	1.05	
4th	0.71	0.67	1.08	
3rd	0.40	0.98	1.66	
2nd	0.18	0.51	1.53	



**FIGURE 4-3 Transfer Function from Ambient Vibration at X-X Direction
(without floor plate)**

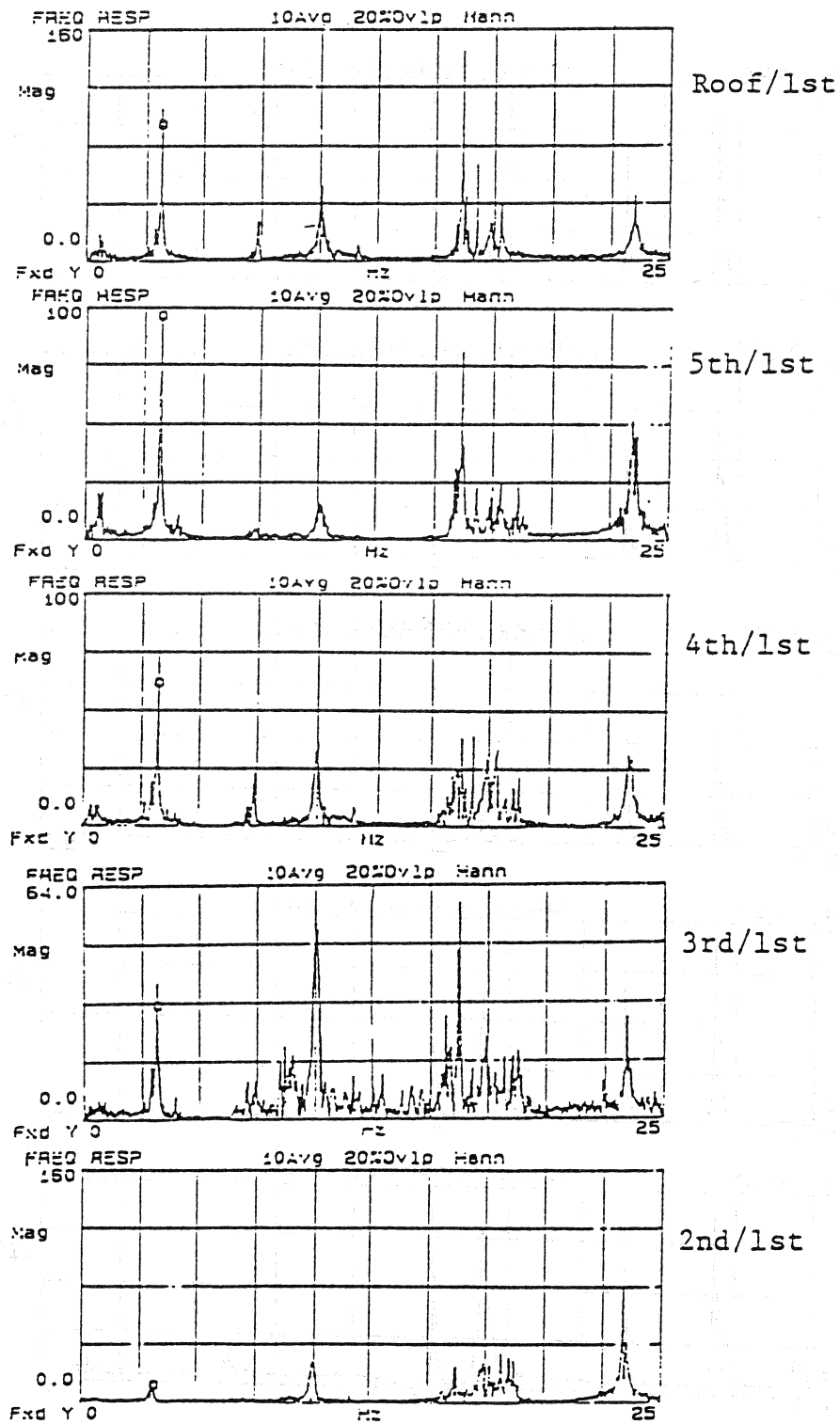


FIGURE 4-4 Transfer Function from Ambient Vibration at Y-Y Direction (without floor plate)

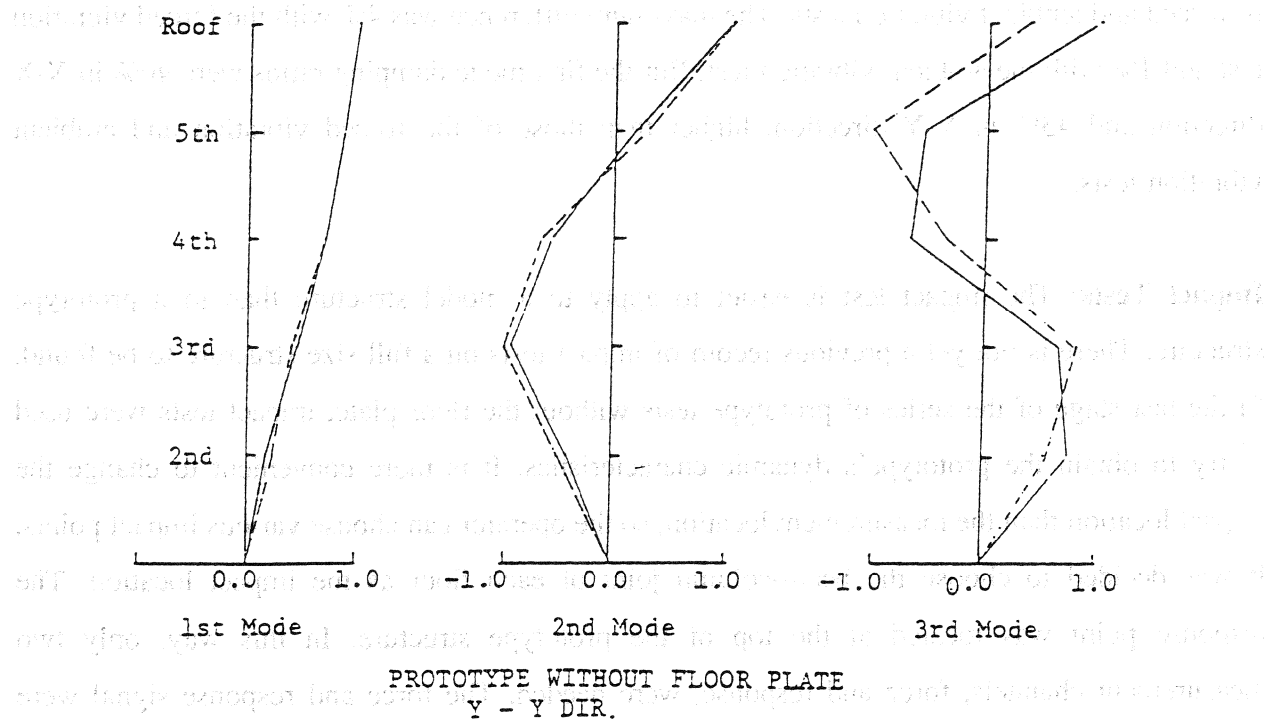
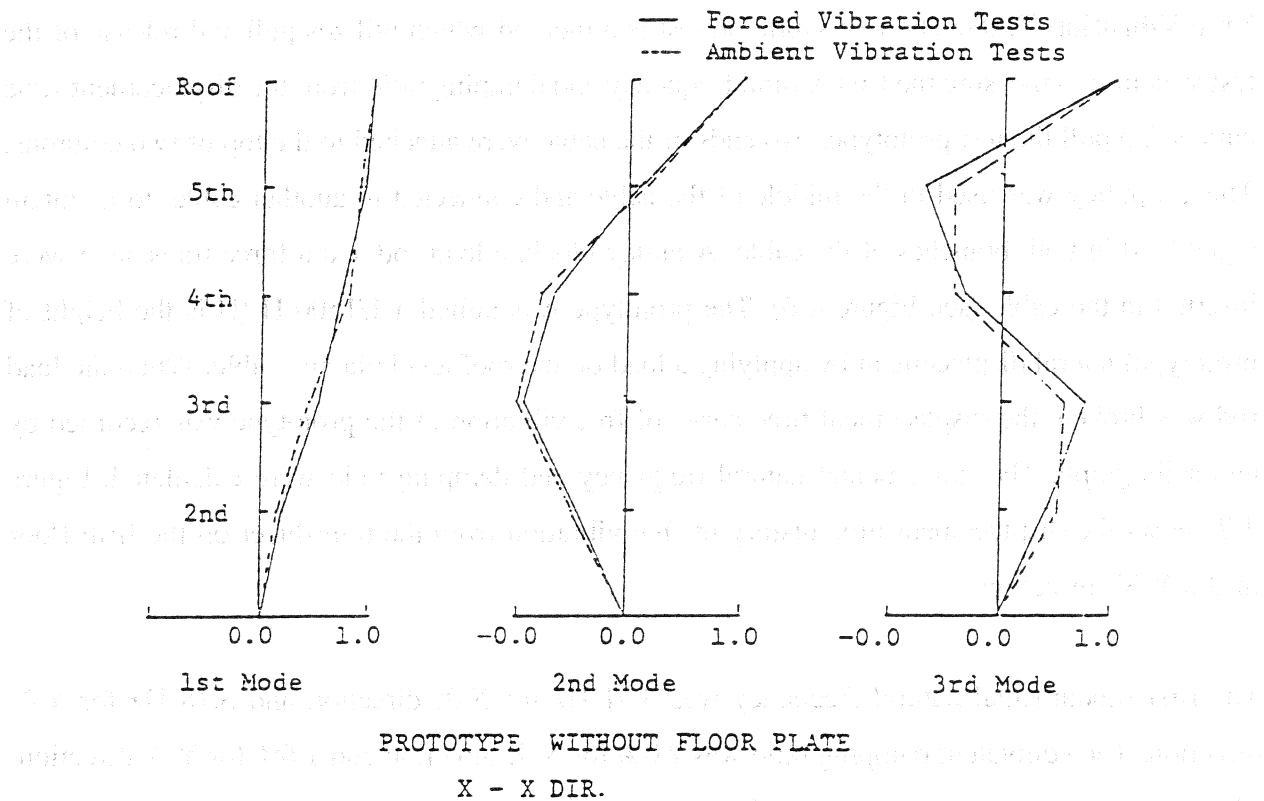


FIGURE 4-5 Mode Shape Comparison

Free Vibration Tests: The free vibration test is a method which utilizes pull and release of the test structure to measure the first natural frequency and damping ratio from the displacement-time curves. To pull the test prototype, two ends of the cable were attached to the top of two columns. Then, a pulley was used in the middle of the cable and connected to another cable, to maintain equal load in both branches of the cable. A pulley block, a load rod and a force transducer were inserted in the cable (see Figure 4-6). The prototype was pulled a $1/1500 H$ (H is the height of prototype) lateral displacement by applying a load on the roof level via one cable. When the load rod was broken, the displacement-time curve of free vibration of the prototype was recorded by an oscillograph. The fundamental natural frequency and damping ratio were calculated. Figure 4-7 shows the displacement-time history of free vibration from the transducer on the fifth floor in the Y-Y direction.

The first fundamental natural frequency was 3.91 Hz for X-X direction and 3.18 Hz for Y-Y direction. The equivalent damping ratio was 2.0% for X-X direction and 1.6% for Y-Y direction. The first natural frequencies obtained from the free vibration were in good agreement with that of forced and ambient vibration tests. The maximum difference was 4% with the forced vibration test and 1% with the ambient vibration test. But the first mode damping ratios were 40% in X-X direction and 43% in Y-Y direction, higher than those of the forced vibration and ambient vibration tests.

Impact Tests: The impact test is easier to apply to a model structure than to a prototype structure. There is not yet a previous record of impact tests on a full size structure to be found. In the last stage of the series of prototype tests without the floor plate, impact tests were used to try to obtain the prototype's dynamic characteristics. It is more convenient to change the impact location than the measurement location, so the operator can choose various impact points. It was decided to choose the beam-column joint of each floor as the impact location. The response point was located at the top of the prototype structure. In this way, only two measurement channels, force and response, were needed. The force and response signal were recorded by a tape recorder on the test field, so the modal parameters could be obtained from transfer functions by computer analysis. The block diagram of the measurement and analysis system are shown in Figure 4-8.

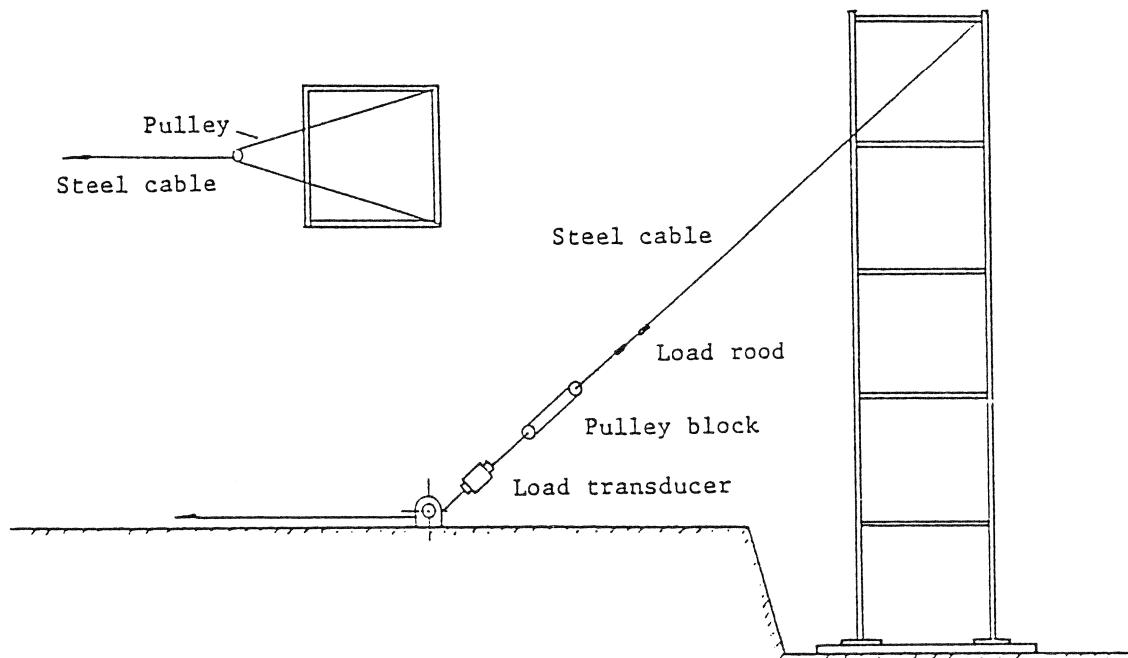


FIGURE 4-6 Test Setup of Free Vibration

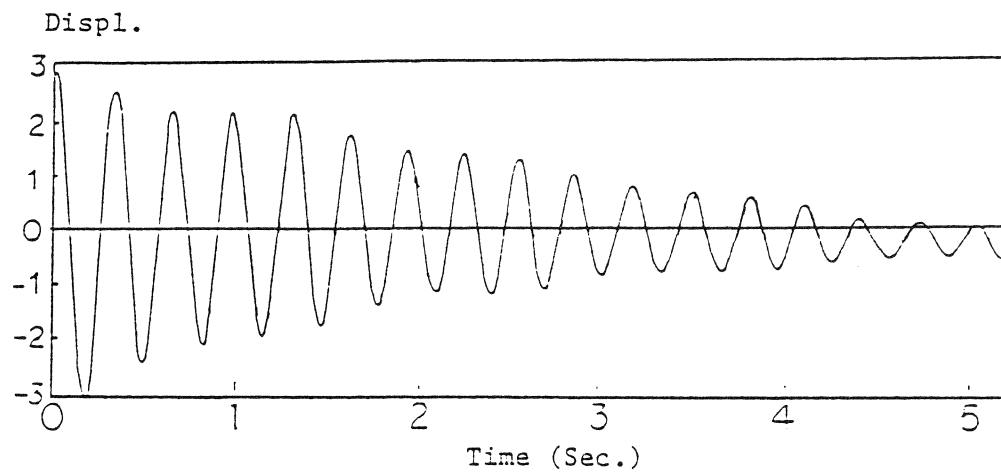


FIGURE 4-7 Time History of Free Vibration

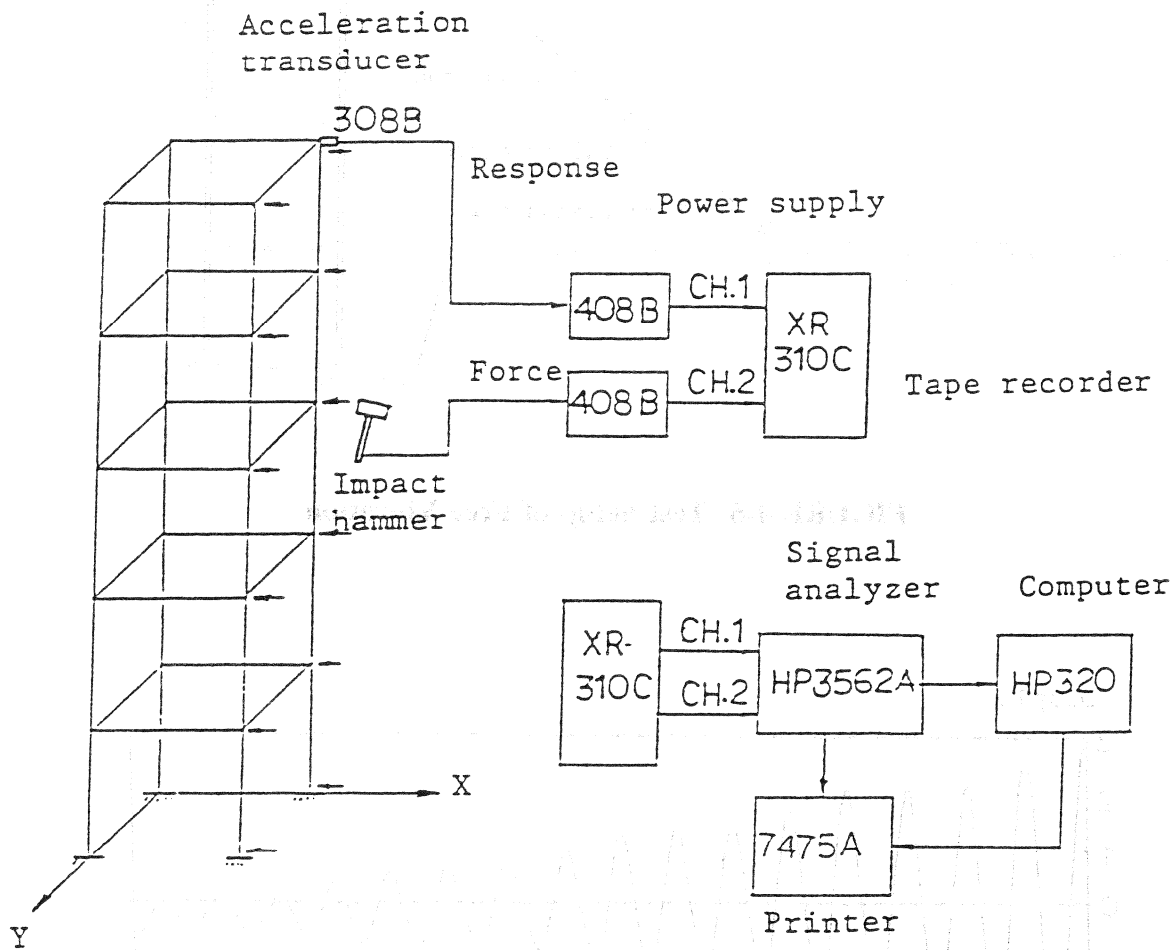


FIGURE 4-8 Block Diagram of Impact Vibration Tests

The natural frequencies and the first three mode shapes of lateral motion in X-X direction and the first two modes of torsional motion are shown in Figure 4-9. The first three natural frequencies were 3.75 Hz, 12.94 Hz and 22.80 Hz for the X-X direction, the second and third mode's equivalent damping ratios were 0.9% and 0.8%. In the Y-Y direction, the first four natural frequencies were 3.20 Hz, 10.05 Hz, 17.45 Hz and 23.60 Hz. (Table 4-V). The natural frequencies for the first two torsional modes were 7.38 Hz and 14.94 Hz, the damping ratios were 1.5% and 0.6% (Table 4-VI). The natural frequencies obtained from the impact vibration were close to those of forced, ambient, and free vibration tests. Specifically, it was in good agreement with ambient vibration tests. To compare the natural frequencies between the analytically predicted and the experimentally measured, the dynamic analysis were carried out using the computer program SAP-5 under the assumption of rigid foundation (see Table 4-VII).

4.2.2 Prototype Structure With Concrete Slabs

After the dynamic tests of the prototype without the floor plate were finished, the cast-in-place concrete floor, 3.15 inches (8.0 cm) thick, was poured on every floor. The testing load was 4.8 kip (2.18 ton) on every floor. The dynamic characteristics of the prototype with the floor plate was determined using forced and ambient vibration tests only.

Forced Vibration Tests: Forced vibration tests incorporated two methods in the first stage. First, the vibration generator was located at the center of the foundation plate of the prototype to excite the structure. Then the second vibration generator was moved to the neighboring foundation plate to generate vibration waves travelling through ground soil to excite the prototype.

1. **Vibration generator at the foundation plate under the prototype:** The first three natural frequencies in the X-X direction were 2.50 Hz, 8.47 Hz and 15.79 Hz and the modal equivalent damping ratios were 1.4%, 0.8% and 2.2%. Figure 4-10 is an example of how to determine damping ratio. The first three natural frequencies were 2.2 Hz, 6.78 Hz and 11.28 Hz for the Y-Y direction. The equivalent modal damping ratios were 0.9%, 1.4% and 0.6%. A comparison of the results between the two

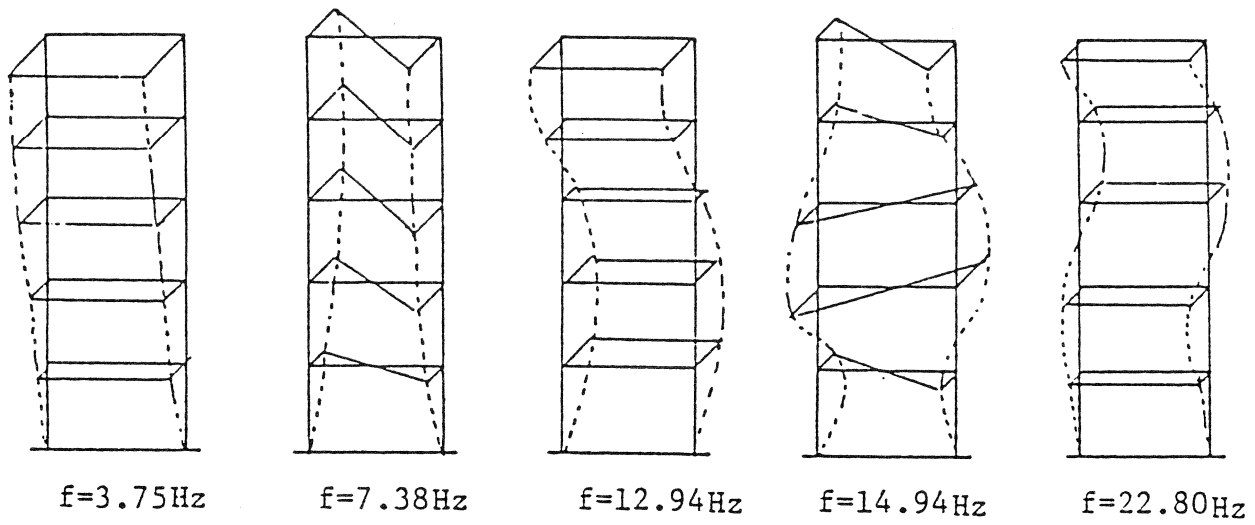


FIGURE 4-9 First Three Bending and First Two Torsional Modes of Prototype (without floor plate)

TABLE 4-V Results from Impact Test

	X - X			Y - Y			
Mode	1st	2nd	3rd	1st	2nd	3rd	4th
Frequency (hz)	3.75	12.94	22.80	3.20	10.05	17.45	23.60
Damping ratio (%)	-	0.9	0.8	-	-	-	-

TABLE 4-VI Torsional Modes

		Mode	
		1st	2nd
Ambient	Frequency (Hz)	7.38	14.88
	Damping ratio (%)	0.4	0.4
Impact	Frequency (Hz)	7.38	14.94
	Damping ratio (%)	1.5	0.6

TABLE 4-VII Comparison of Analytical and Experimental Results

	Natural frequency (Hz)						
	X - X			Y - Y			
	Mode			Mode			
	1st	2nd	3rd	1st	2nd	3rd	4th
Forced	3.75	12.64	22.65	3.14	9.86	17.40	21.50
Ambient	3.88	12.75	22.79	3.19	10.06	16.84	23.56
Free	3.91	-	-	3.18	-	-	-
Impact	3.75	12.94	22.80	3.20	10.05	17.45	23.0
Analysis (SAP5)	3.97	13.24	23.60	3.08	9.52	16.51	23.20

directions is shown in Table 4-VIII. The mode shapes are shown in Table 4-IX. After casting the concrete floor, the structural mass increased and the first three natural frequencies were reduced about 32% in the X-X and Y-Y directions. The first modal damping ratio increased about 14% in the X-X direction as well as the Y-Y direction. A comparison of the natural frequencies of the prototype without and with floor plate is shown in Table 4-X.

2. **Vibration generator on another foundation plate:** The excitation force was along the X-X direction only. The vibration wave passed through the soil and reached the foundation of the prototype. In this case, the dynamic characteristics of the prototype obtained from forced vibration tests should reflect the soil-structure interaction to a certain extent, in spite of the fact that only the top soil layer was involved. The first three natural frequencies were 2.52 Hz, 8.58 Hz and 16.10 Hz for the X-X direction. Damping for the second and third mode was 0.8% and 1.9%. The mode shapes are shown in Table 4-XI. The first three natural frequencies obtained from forced vibration in case (1) were 1.2% to 3.0% lower than those measured when the vibration generator was on the nearby foundation. A comparison of the test results from these two methods were shown in Table 4-XII.

Ambient Vibration Tests: In the ambient vibration tests, the displacement transducers were located at the center of each floor level. The first three natural frequencies were 2.52 Hz, 8.40 Hz and 15.60 Hz for X-X direction, and the first and second mode damping ratios were 0.6% and 0.9%. The first four natural frequencies were 2.19 Hz, 6.72 Hz, 11.10 Hz and 15.20 Hz for the Y-Y direction, and the first three modal damping ratios were 0.9%, 1.1% and 0.4%. (Table 4-XIII). The mode shapes are shown in Table 4-XIV. Sample spectra from ambient in the Y-Y direction are presented in Figure 4-11. A comparison of natural frequencies from ambient tests with the results from forced vibration tests show very good correlation. The difference in the first three natural frequencies was 0.7%, 0.8% and 1.2% in X-X direction and 0.4%, 0.8% and 1.6% in Y-Y direction. Figure 4-12 shows a comparison of mode shapes between forced and ambient vibration tests. The correlation of the first two mode shapes is good. The natural frequencies predicted analytically and measured experimentally are summarized in Table 4-XV.

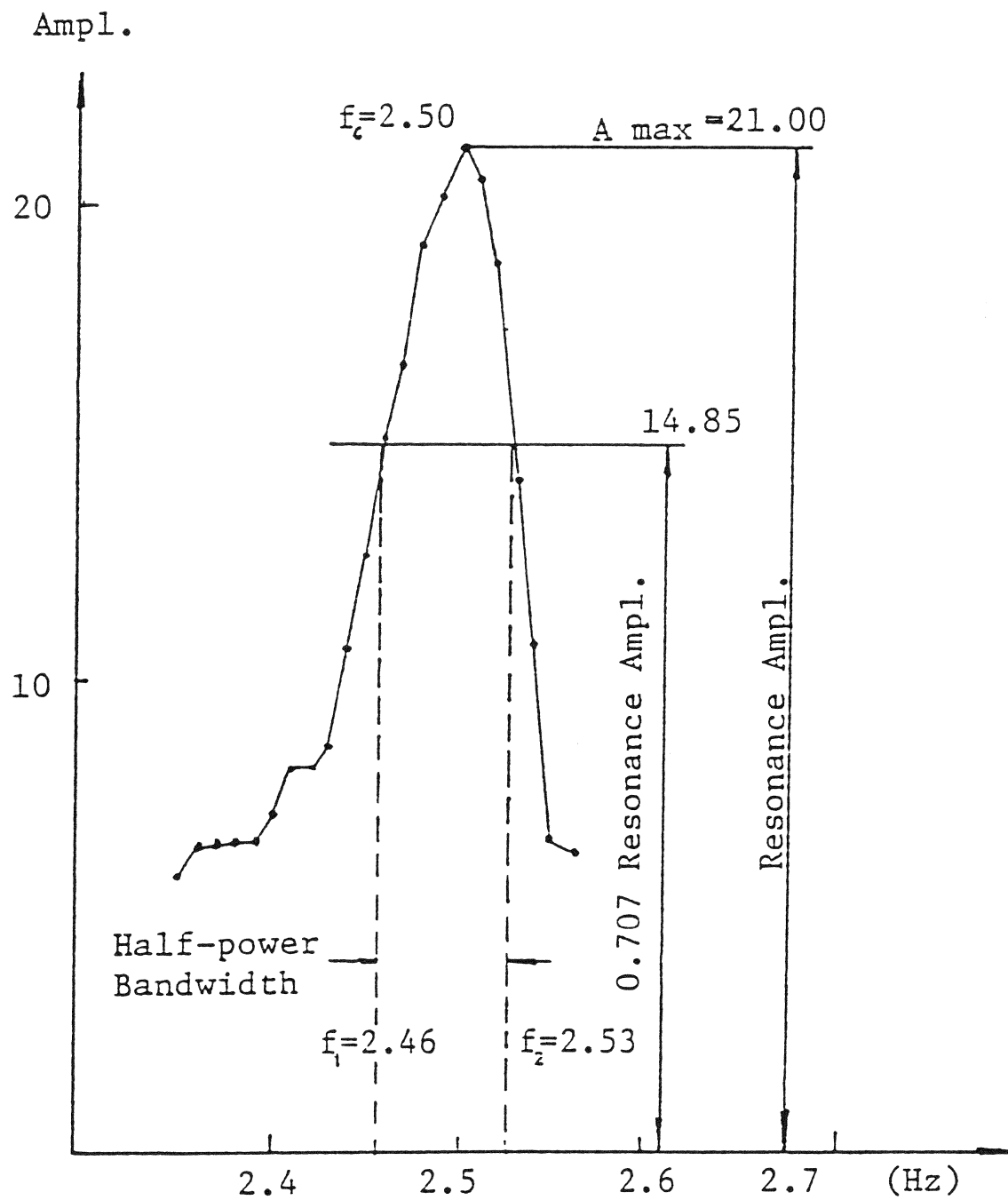
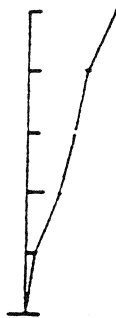
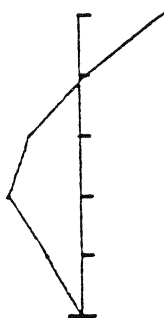
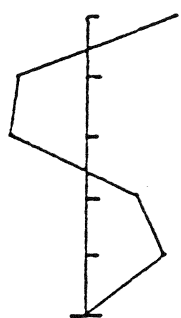


FIGURE 4-10 Force Vibration Test - Frequency Response Curve (1st Mode)
(with floor plate)

TABLE 4-VIII Results from Vibration Generator on the Foundation Under the Prototype

	X - X			Y - Y		
Mode	1st	2nd	3rd	1st	2nd	3rd
Frequency (Hz)	2.50	8.47	15.79	2.20	6.78	11.28
Damping ratio (%)	1.4	0.8	2.2	0.9	0.14	0.6

TABLE 4-IX Prototype Mode Shape from Forced Vibration Test (with floor plate)

X - X						
Floor	1st Mode f=2.50		2nd Mode f=8.47		3rd Mode f=15.79	
Roof	1.00		1.00		1.00	
5th	0.70		0.12		0.75	
4th	0.53		0.61		0.81	
3rd	0.36		0.87		0.63	
2nd	0.12		0.48		0.94	


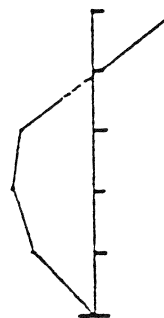
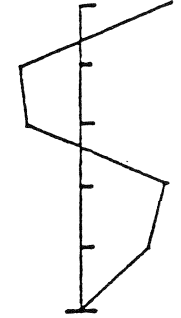
Y - Y						
Floor	1st Mode f=2.20		2nd Mode f=6.78		3rd Mode f=11.28	
Roof	1.00		1.00		1.00	
5th	0.77		0.17		0.98	
4th	0.65		0.89		0.89	
3rd	0.45		1.07		1.01	
2nd	0.15		0.83		0.88	

TABLE 4-X Natural Frequency Comparison

		Mode		
		1st	2nd	3rd
Prototype without floor plate	Frequency (Hz)	3.75	12.64	22.64
	Damping ratio (%)	1.2	0.9	1.0
Prototype with floor plate	Frequency (Hz)	2.50	8.47	15.79
	Damping ratio (%)	1.4	0.8	2.2

TABLE 4-XI Results from Vibration Generator on Another Foundation (with floor plate)


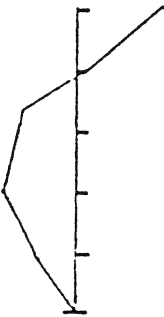
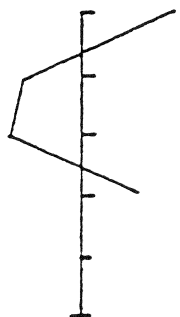
X - X Direction				
Floor	1st Mode f=2.52	2nd Mode f=8.58	3rd Mode f=16.10	
Roof	1.00 	1.00 	1.00 	
5th	0.72	0.14	0.70	
4th	0.55	0.64	0.86	
3rd	0.47	0.86	0.60	
2nd	0.13	0.52	-	

TABLE 4-XII Natural Frequency Comparison

	Direction	Mode		
		1st	2nd	3rd
Forced vibration *	X - X	2.50	8.47	15.79
Forced vibration **	X - X	2.52	8.58	16.10
Ambient vibration	X - X	2.52	8.40	15.60

* The vibration generator on the foundation of prototype

** The vibration generator on the other foundation

4.2.3 Dynamic Tests of Structures with Different Bracing Systems

Three different bracing systems: E, V and X, were installed on the structure in turn at this stage of the testing.

The force vibration method was adopted for these tests. The frequencies of different bracing systems are listed in Table 4-XVI together with their mode shape. The fundamental natural frequency was 3.88 Hz, 3.90 Hz, and 4.36 Hz for Eccentric, V, and X bracings, respectively. In comparison to the space frame without bracing, whose fundamental frequency was 2.2 Hz, it is obvious that the structural lateral stiffness increased due to the inclusion of different bracing systems. Also noted was that among the three bracing systems used in this study, X bracing created the largest increase while Eccentric bracing created the smallest increase.

4.3 Summary

In this section, dynamic tests on the prototype structure were reported. Several different methods of excitation were used to compare the system identification results. Both mode shape and frequency were very consistent among various identification procedures. Damping ratio was found to have a larger variation, which is quite common from past experience in the field test. This is caused partly by the theory of damping, which has not been rigidly defined, and partly by the small damping value inherent in the structure. In general, the test results are satisfactory.

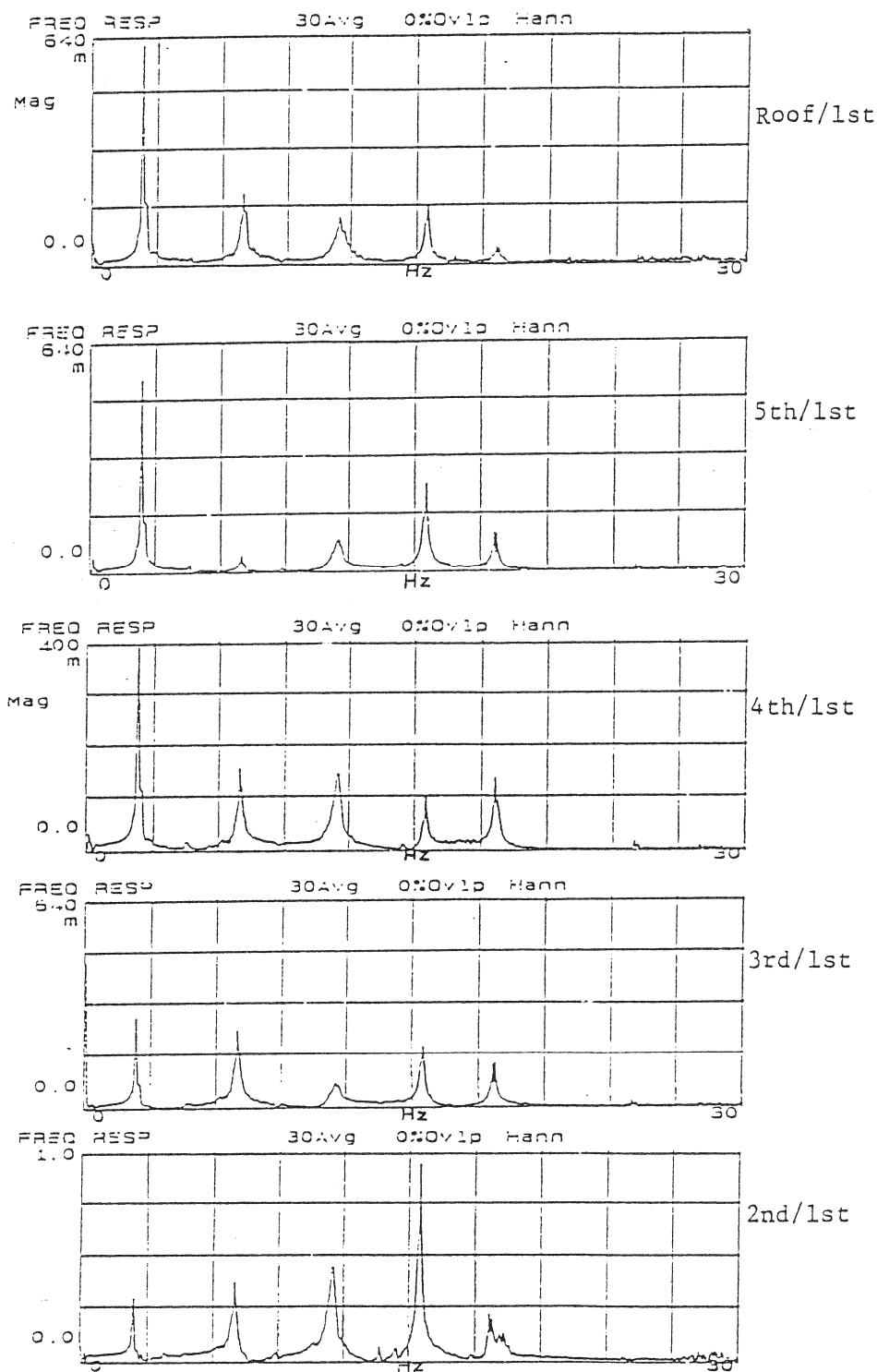
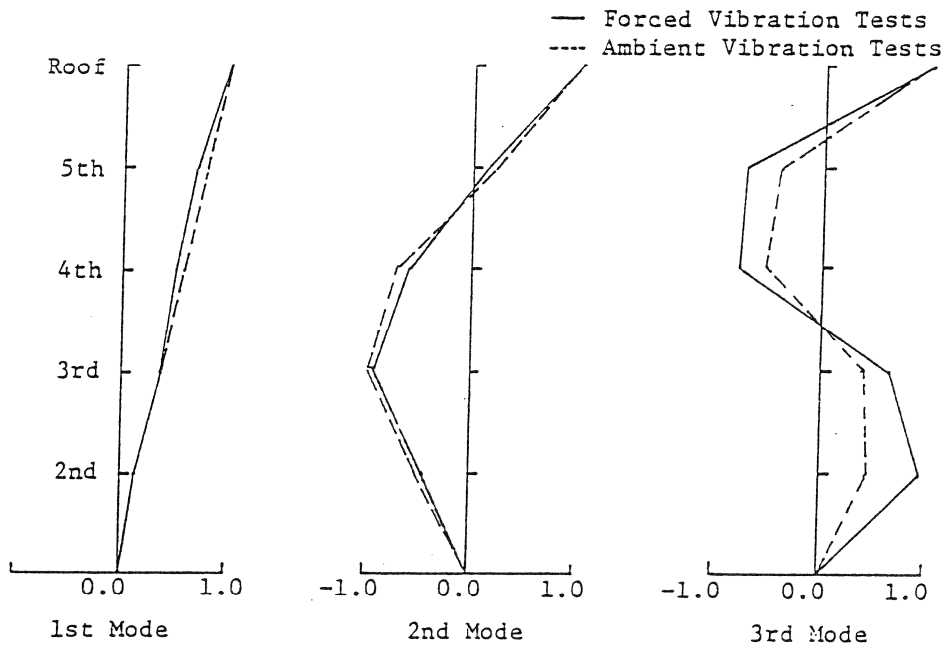
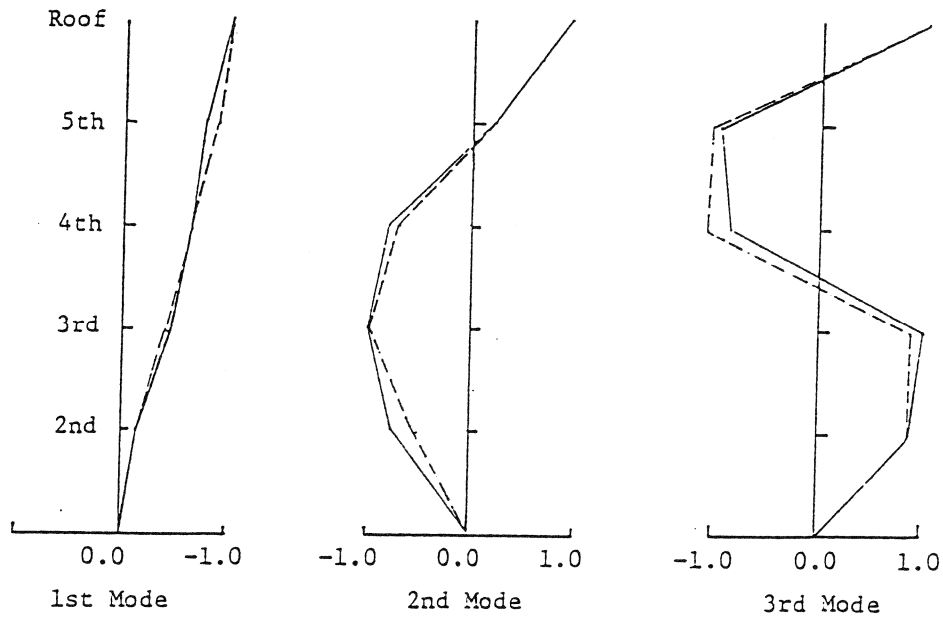


FIGURE 4-11 Transfer Function from Ambient Vibration Test in Y-Y Direction (with floor plate)



PROTOTYPE WITH FLOOR PLATE
X - X DIR.



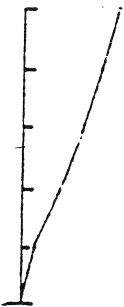
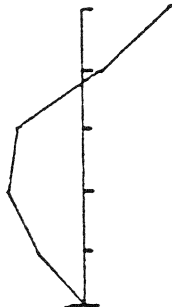

PROTOTYPE WITH FLOOR PLATE
Y - Y DIR.

FIGURE 4-12 Mode Shape Comparison

TABLE 4-XIII Results from Ambient Vibration

Direction	X - X			Y - Y			
Mode	1st	2nd	3rd	1st	2nd	3rd	4th
natural frequency (Hz)	2.52	8.40	15.60	2.19	6.72	11.10	15.20
damping ratio (%)	0.6	0.9	-	0.9	1.1	0.4	-

TABLE 4-XIV Mode Shapes from Ambient Vibration

X - X Dir						
Floor	1st Mode f=2.52		2nd Mode f=8.40		3rd Mode f=15.60	
Roof	1.00		1.00		1.00	
5th	0.85		0.21		0.36	
4th	0.62		0.77		0.38	
3rd	0.35		0.97		0.28	
2nd	0.12		0.52		0.36	


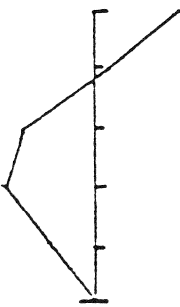
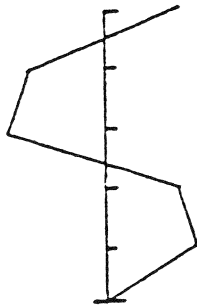
Y - Y Dir						
Floor	1st Mode f=2.19		2nd Mode f=6.72		3rd Mode f=11.10	
Roof	1.00		1.00		1.00	
5th	0.88		0.16		0.90	
4th	0.66		0.79		1.12	
3rd	0.40		1.06		0.85	
2nd	0.12		0.51		1.18	


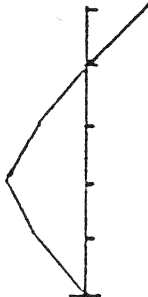
TABLE 4-XV Comparison of Analytical and Experimental Results


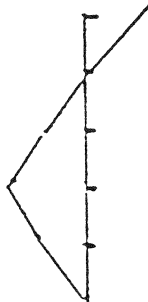
Test Method	Natural Frequency (Hz)						
	X - X Direction			Y - Y Direction			
	Mode			Mode			
	1st	2nd	3rd	1st	2nd	3rd	4th
Forced *	2.50	8.47	15.79	2.20	6.78	11.28	-
Forced **	2.52	8.58	16.10	-	-	-	-
Ambient	2.52	8.40	15.60	2.19	6.72	11.10	15.20
Analysis (sap-5)	3.16	10.11	18.58	2.25	6.78	11.37	15.36


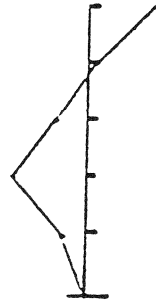
* The vibration generator on the foundation of prototype

** The vibration generator on the other foundation

TABLE 4-XVI Mode Shapes of Braced Frames

(E) Y - Y Direction				
	1st Mode f=3.88 (Hz)		2nd Mode f=13.22 (Hz)	
Roof	1.00		0.87	
5th	0.86		0.07	
4th	0.59		-0.61	
3rd	0.32		-1.00	
2nd	0.21		-0.66	

(V) Y - Y Direction				
	1st Mode f=3.90 (Hz)		2nd Mode f=14.60 (Hz)	
Roof	1.00		0.81	
5th	0.85		0.10	
4th	0.58		-0.52	
3rd	0.35		-1.00	
2nd	0.20		-0.69	

(X) Y - Y Direction				
	1st Mode f=4.36 (Hz)		2nd Mode f=15.10 (Hz)	
Roof	1.00		0.94	
5th	0.82		0.17	
4th	0.54		-0.43	
3rd	0.37		-1.00	
2nd	0.23		-0.36	

SECTION 5

MODEL TESTS

5.1 Introduction

The dynamic characteristics of the model were determined at the loading conditions, corresponding to that of the prototype with concrete slab. The objectives of the tests were as follows:

1. To correlate the dynamic behavior between model and prototype
2. To analyze the effect of increase in lateral stiffness.

5.2 Test Program and Instrumentation

Four structural types were tested: bare frame (F), eccentric (E), V, and X bracing. Because the bracings were designed to be bolted on the gusset plate, the structural integrity was not damaged after installation or removal of the different bracing types.

For every structural type, a two-minute white noise ground motion (see Figure 5-1) was used as the input from the foundation. A shaking table housed in the structural laboratory at the University at Buffalo provided the base excitation to the structure. Figure 5-1 shows that the input motion is uniform up to 40 Hz. However, components higher than 40 Hz displayed some increased magnitude which could not be corrected by the MTS control system after several off-line compensation iterations. However, this should not have affected the result of the transfer function. Therefore, it was accepted as the input ground motion.

Data taken from the experiment were accelerations at every floor and foundation as shown in Figure 5-2. ENDEVCO model 2262-25 low G piezoresistive accelerometers were used and were placed at the center of the beam span. Conditioners [11] to magnify signals had two different cut-

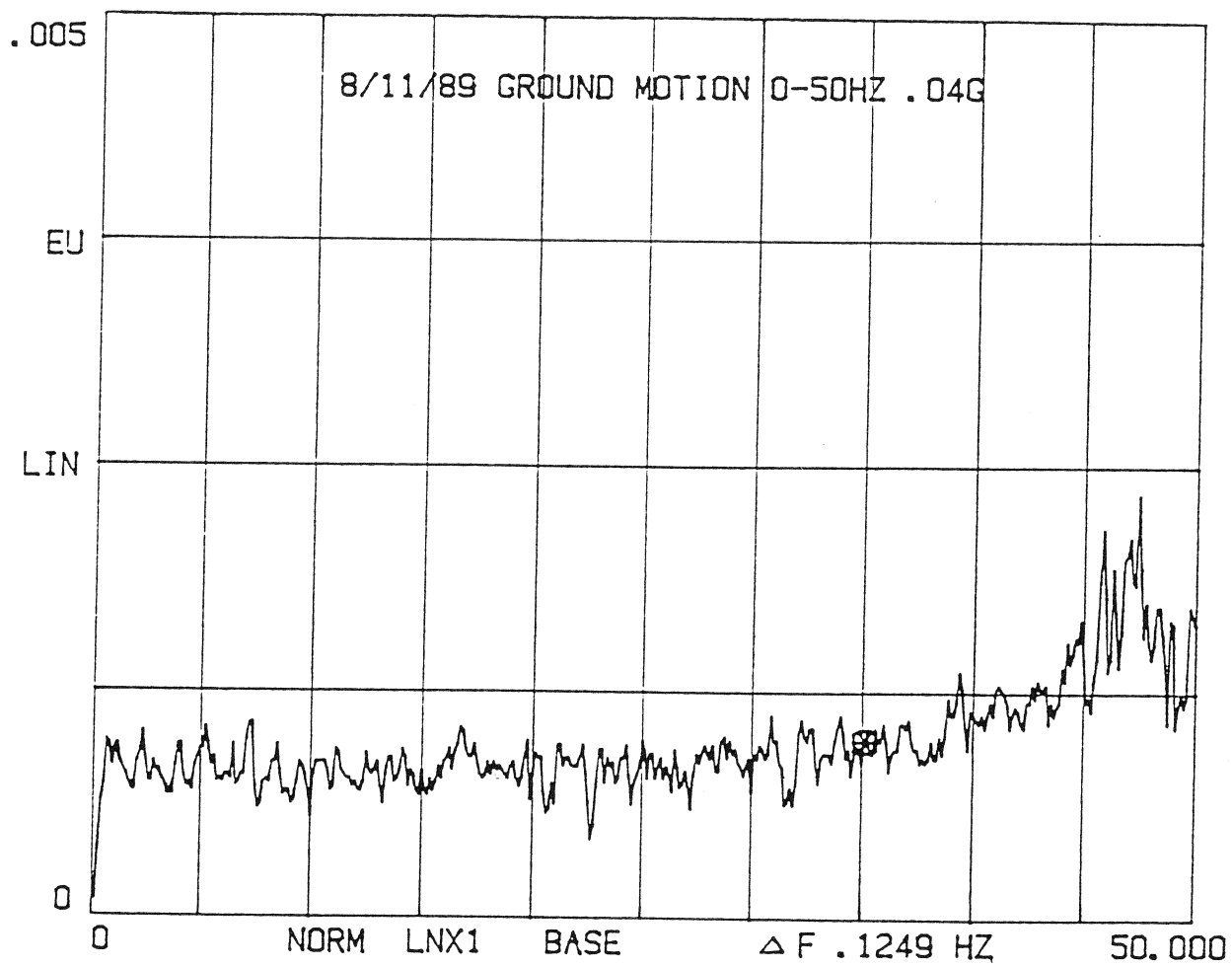


FIGURE 5-1 Spectrum of Input White Noise

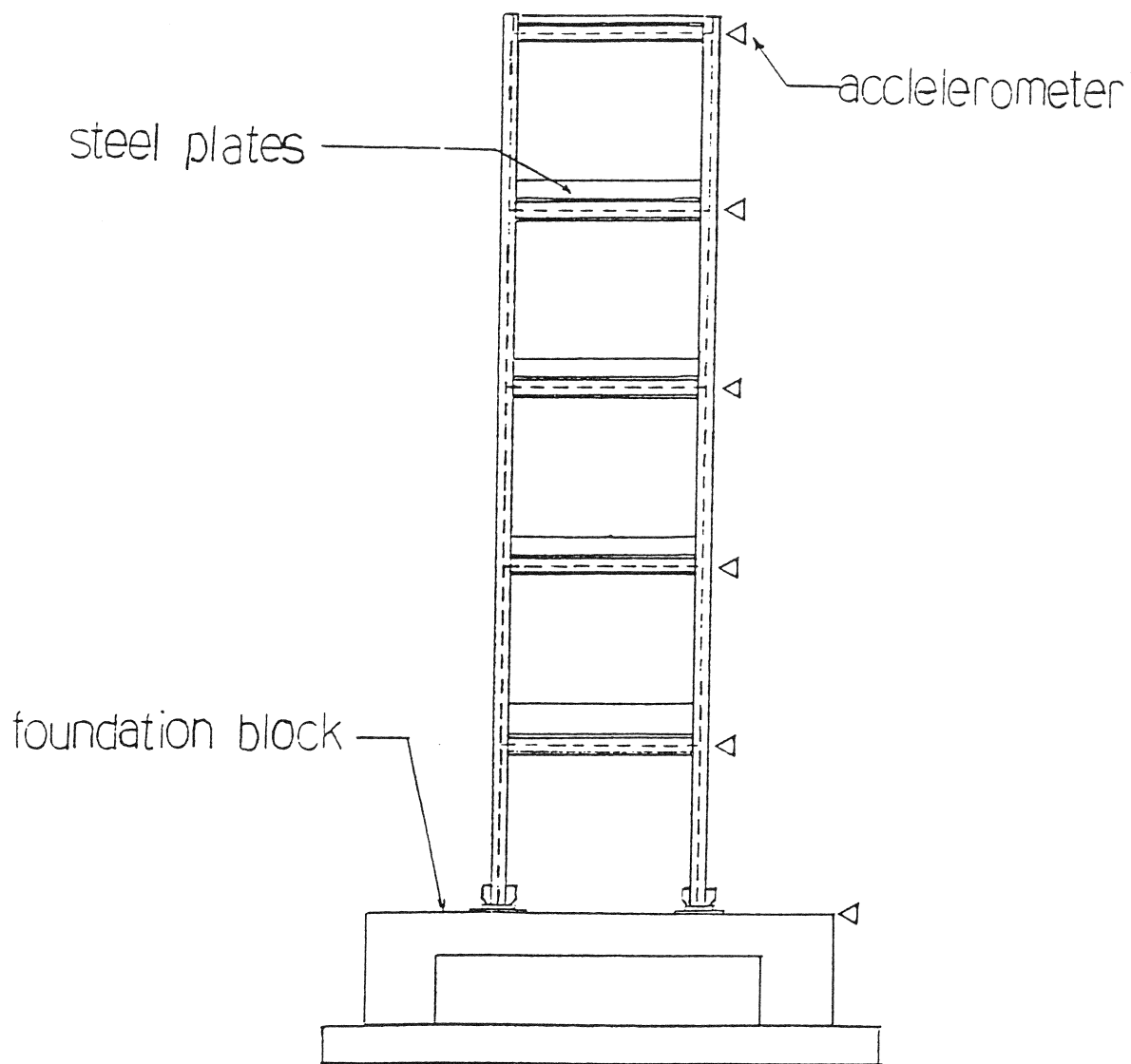


FIGURE 5-2 Instrumentation of Model Test

off frequency filters to choose from, one was 25 Hz and the other 50 Hz. The latter was chosen for the test.

As discussed by many dynamic textbooks, it is known that damping can also be obtained from the free vibration of the structure, using the theory of free vibration decay [16]. First mode damping can easily be obtained from the free vibration initiated from the quick release mechanism, which releases an initial deformation made by pulling a cable tied to the top of the structure. The free decay curve, as shown in Figure 5-3, can be used to find damping ratio, ξ , corresponding to the first mode by the following equation:

$$\xi = \frac{1}{2\pi n} \ln \left(\frac{u_P}{u_Q} \right) \quad (5.1)$$

where n is the number of cycles between P and Q, and u_P, u_Q are the peak magnitude of the decaying curve.

There are many approaches to obtain damping ratio in higher modes. Several techniques, such as Nyquist Circle Fit, Random Decrement [17], filtered impulse decay [18], etc., have been developed. In this experiment, a new approach was used to obtain higher mode damping.

Higher mode damping can be obtained by free vibration decay if no modal coupling exists. In general, it is quite difficult to produce a higher mode free vibration. The authors tried several strategies to produce such a phenomenon without success. Finally, it was tested quite successfully to produce the free vibration of the second and third mode. The approaches taken are described below.

First, the natural frequencies of the higher modes must be identified. Then, a programmed shaking table motion with sinusoidal excitation at the interested natural frequency was used to create the steady state response at the mode of interest. When the structure was in the steady state, the magnitude of the input motion was gradually reduced to zero in two seconds, while the

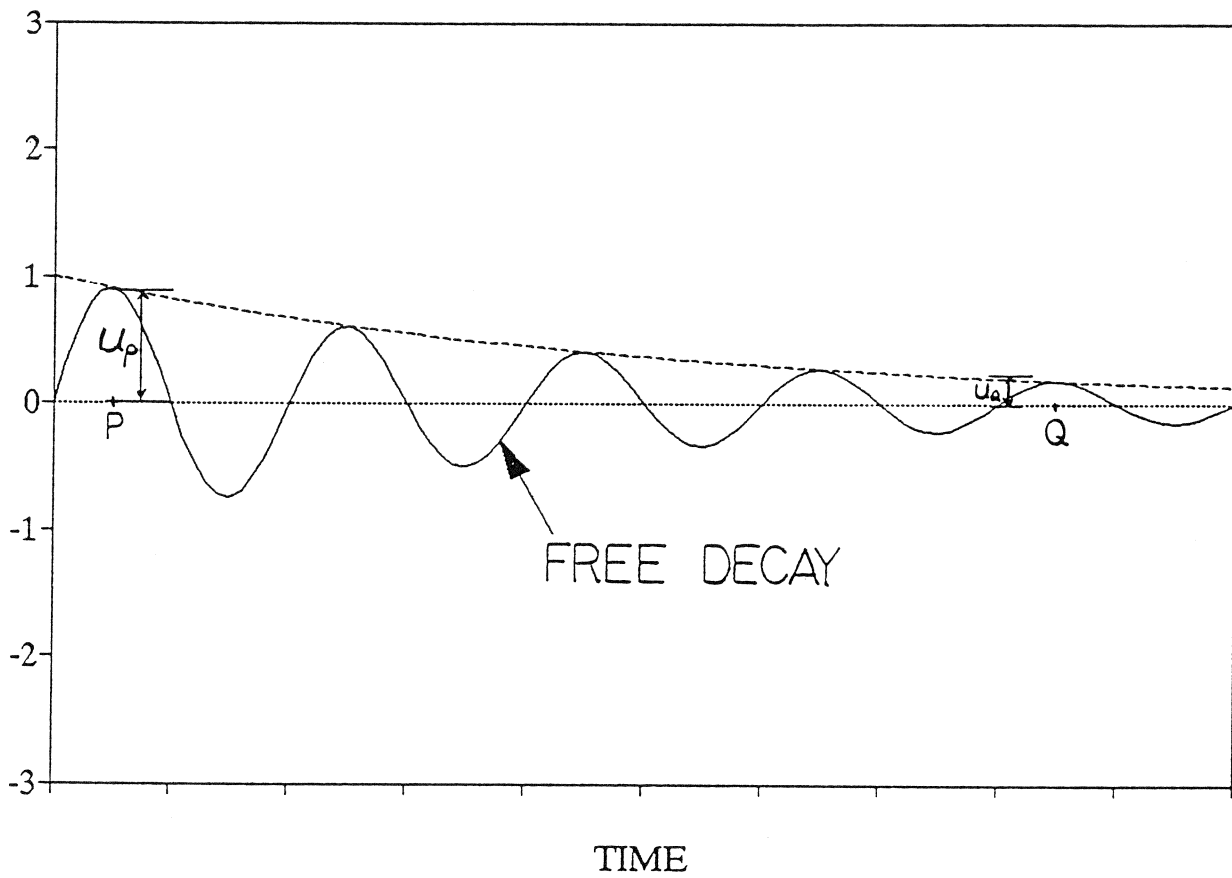


FIGURE 5-3 Free Decay Vibration

excitation frequency remained the same. After the table came to a stop, the structure was still vibrating at the rhythm of the excited higher mode and gradually decayed to background noise. In Figure 5-4a, it can be seen that the second mode free decay started behind line A-A. A Fourier Transform of time span between A-A and B-B is shown in Figure 5-4b. The vertical axis is in logarithmic scale and the second mode response is about one hundred times stronger than that of the first mode. Therefore, damping ratio for the higher mode can be obtained in the same manner as the first mode free decay. This approach was adopted for the evaluation of the second and third mode damping. A clearer response on the second mode than the third mode was observed in tests of different bracing systems.

5.3 Data Analysis

The data acquisition system [12] was set to have the sampling rate of 128 Hz throughout the test, thus the corresponding Nyquist frequency was 64 Hz, which was high enough to catch at least the first two modes. The total time sampled was 112 seconds, assuming that transient response will have minimum effect after 8 seconds. For the spectrum analysis, an 8-second interval was used to average results to minimize the noise. Hanning window was used to minimize the leakage problem.

The floor acceleration transfer functions with respect to the foundation acceleration were calculated by a spectrum analyzer [12]. Results for different structural types are shown in Figures 5-3 to 5-8. Symbols of F, E, V, and X correspond to Bare frame, Eccentric, V, and X bracing, and are used in the following text for convenience.

5.4 Test Results and Discussion

This section discusses the results from the model tests and their correlation with the prototype structure. Three subsections dealing with frequency, mode shape and damping ratio are presented in sequence.

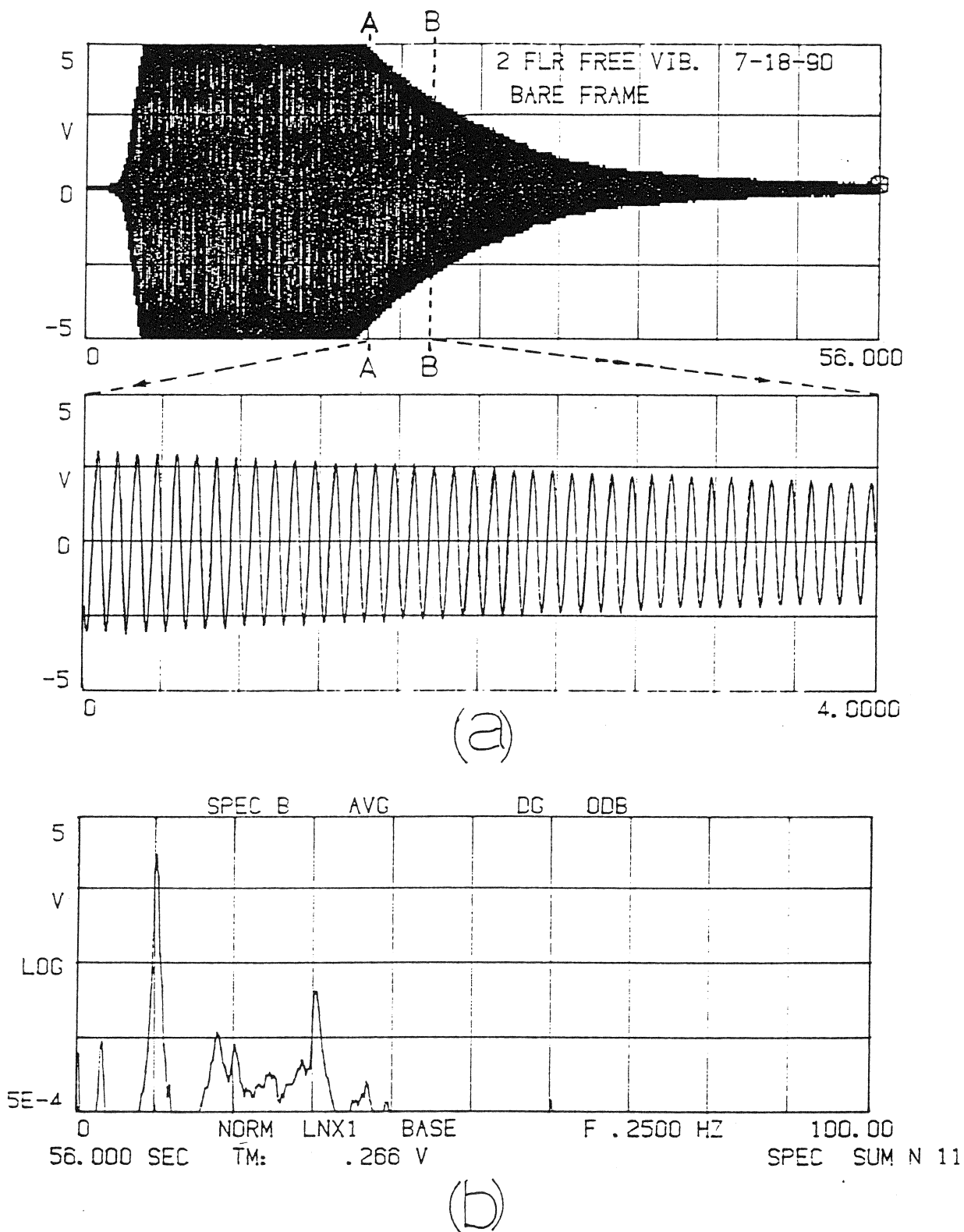


FIGURE 5-4 Higher Mode Free Vibration

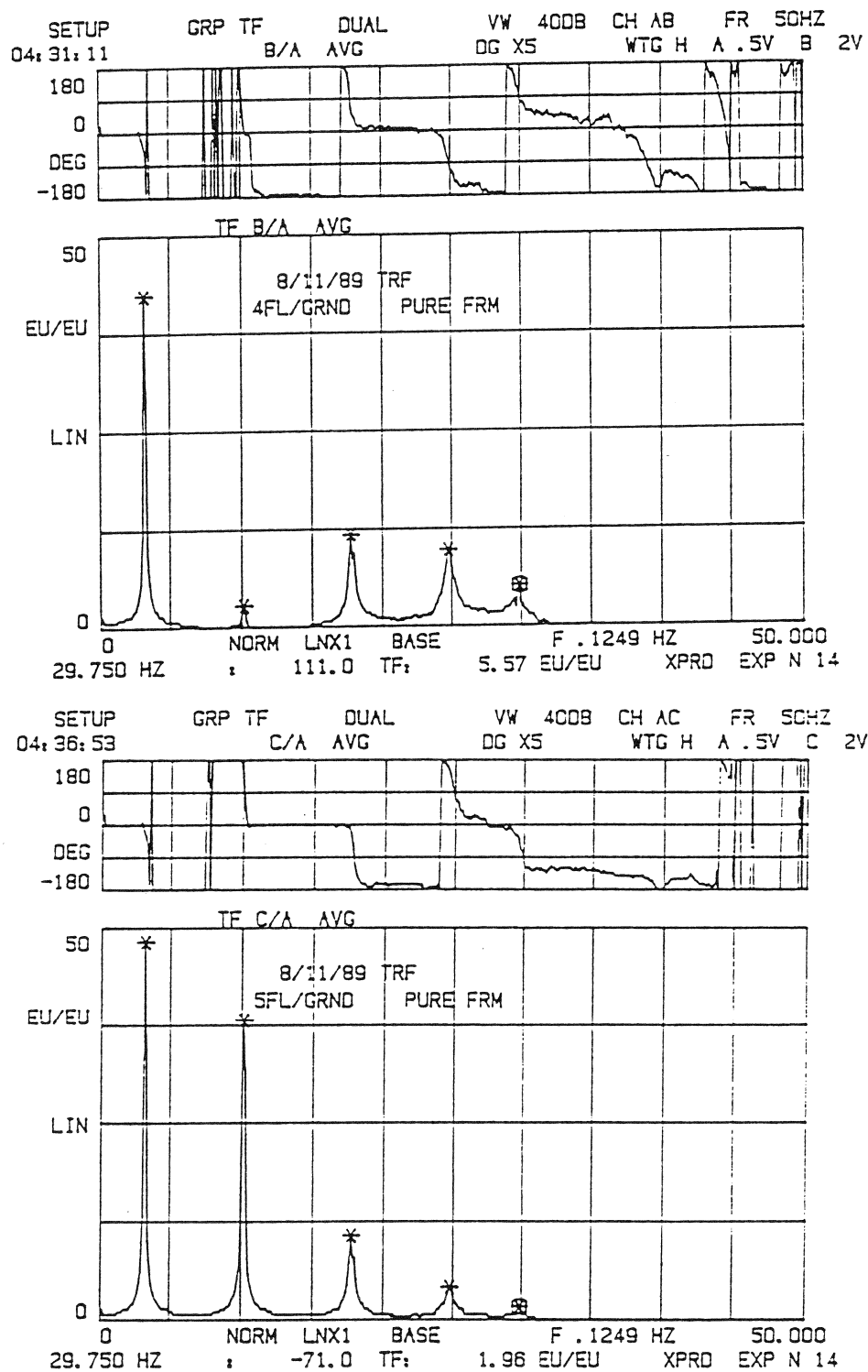


FIGURE 5-5 Transfer Function of "F"

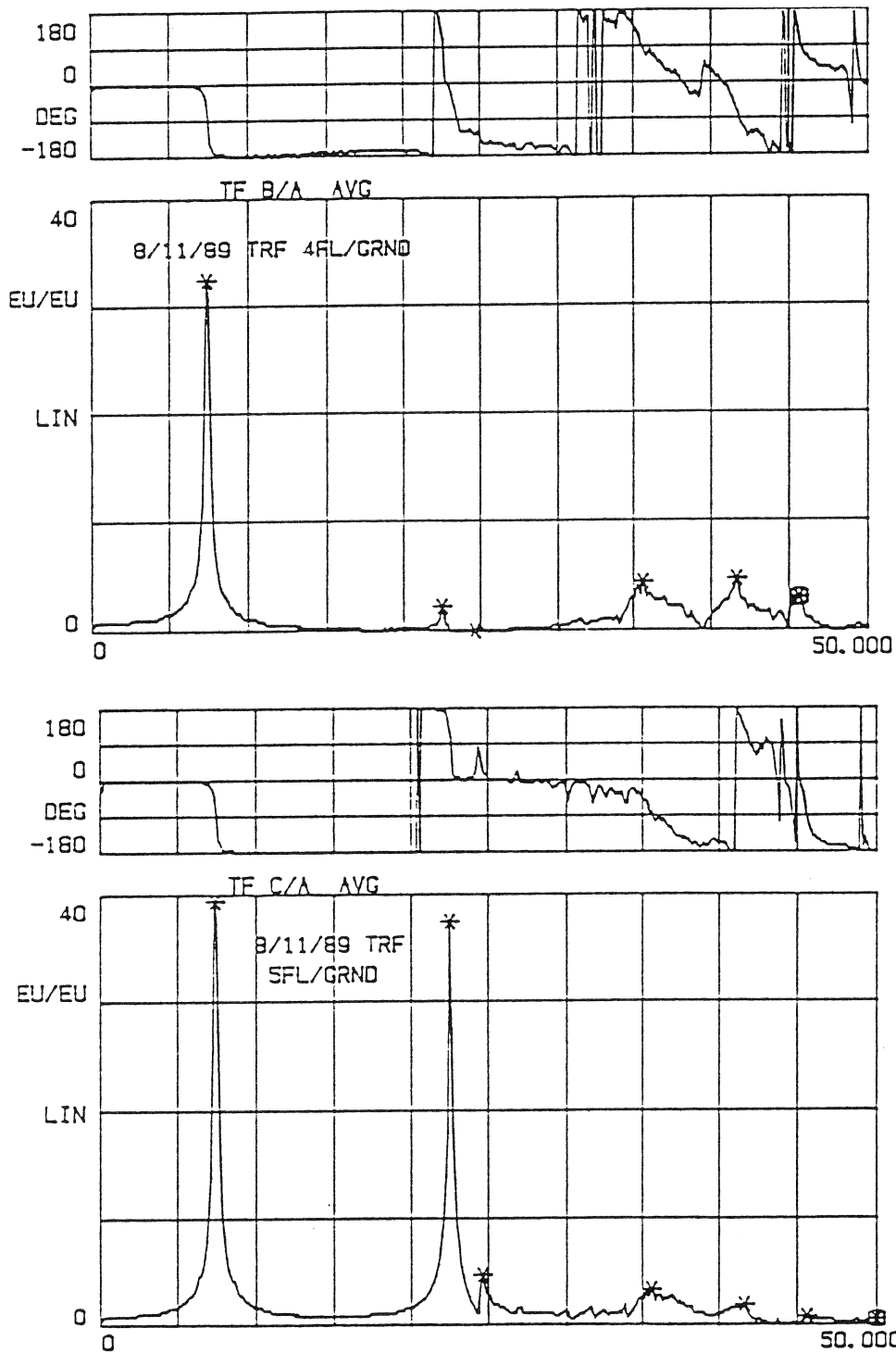


FIGURE 5-6 Transfer Function of "E"

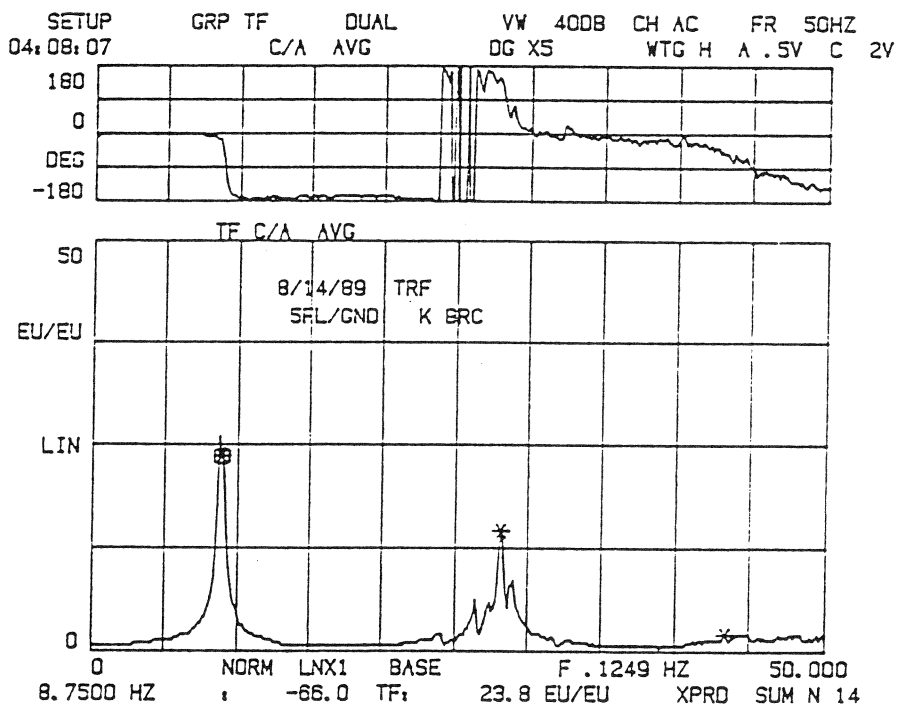
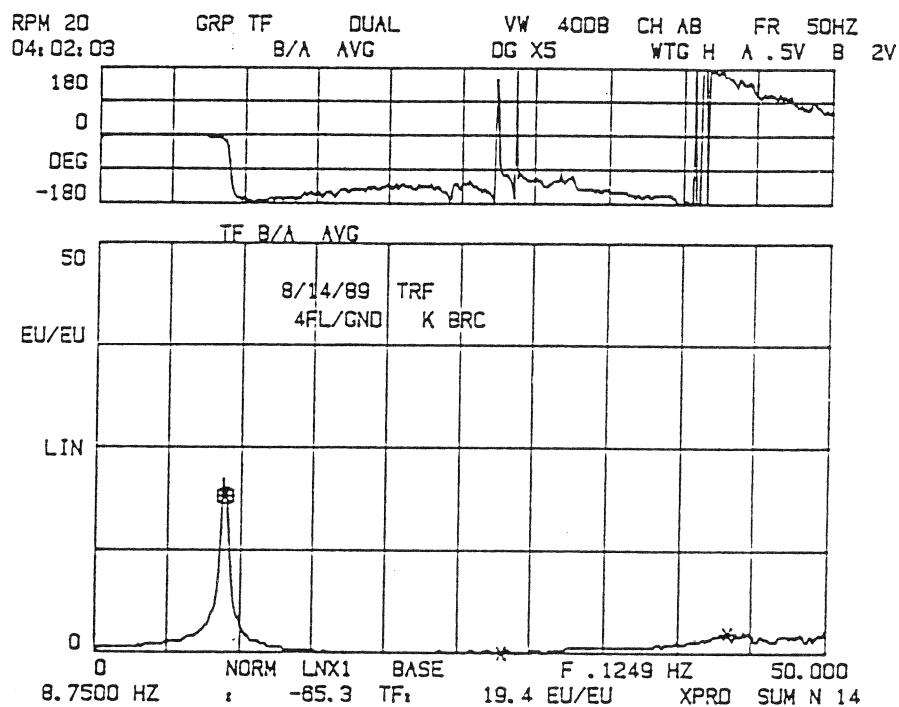


FIGURE 5-7 Transfer Function of "V"

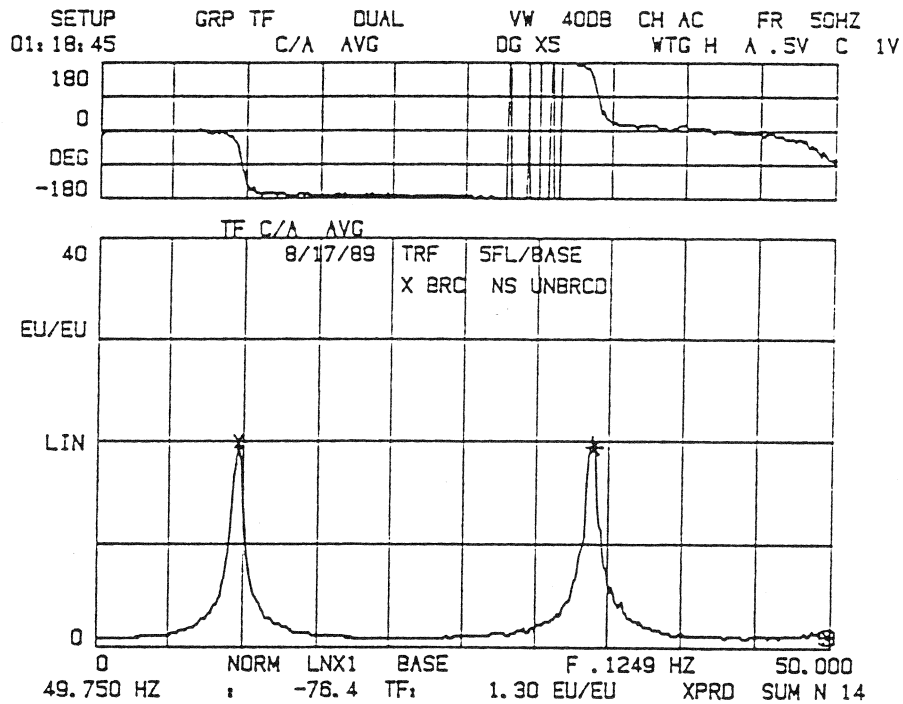
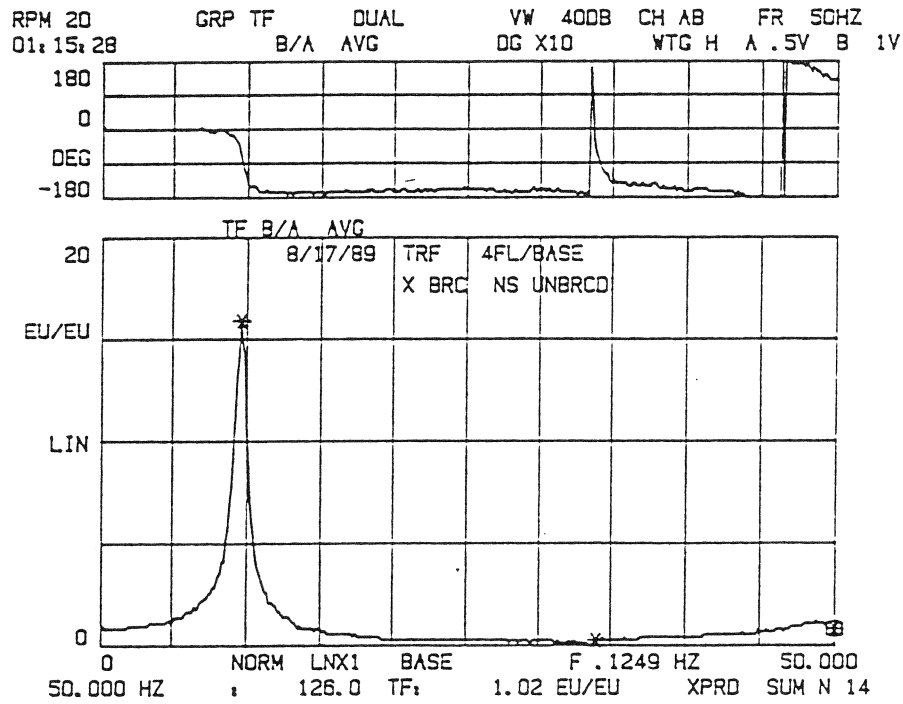


FIGURE 5-8 Transfer Function of "X"

5.4.1 Frequency

The natural frequencies of the model from the experiment are shown in Table 5-I. Also shown in the table are the analytical results calculated from a commercial package STAAD-III [13]. Several special features of the computer models are listed below:

1. Beam-column joints were modeled as rigid links on the beam, with the length on the model structure from the center of the joint to the face of the column.
2. Floor height and beam length was decided from the center to center distance as shown in Figure 3-1.
3. A plane frame model is used instead of a three dimensional model.
4. A six inch rigid link was imposed at the bottom of the columns to account for the wind plates, shown in Figure 3-4, connecting column to foundation.
5. Structural weight was lumped at beam-column connection.

Analyzing Table 5-I, it is found that the correlation between the computer model and experimental result was very good. The difference increases to 10% as structural stiffness becomes larger. This is due to the imperfection of computer modeling to account for the bracing stiffness. During the experiment, bracing members were recorded to have some out of plane vibration, which reduced the overall structure stiffness. In general, the analytical frequency is slightly higher than the experimental frequency. This is a reasonable result since analytical modeling assumes many boundary conditions that make it stiffer than the real structure.

Table 5-II shows the comparison between the model and prototype test. Listed below the model frequency is the Equivalent Prototype Frequency (EPF), in parenthesis, which is the equivalent frequency in prototype calculated by multiplying the scale factor, $\sqrt{0.4}$, by the experimental model frequency.

TABLE 5-I Frequency Comparison of Model Test Result

	AXIS METHOD	X - X (Hz)	Y - Y (Hz)			
			F	E	V	X
1ST MODE	EXPERIMENTAL	4.00	3.32	7.37	8.90	9.50
	ANALYTICAL	4.15	3.38	8.03	9.73	10.61
2ND MODE	EXPERIMENTAL	14.00	10.41	22.95	28.20	34.22
	ANALYTICAL	14.06	10.57	23.94	29.16	35.14
3RD MODE	EXPERIMENTAL	27.37	18.46	36.00	NA	NA
	ANALYTICAL	28.10	18.58	38.09	51.40	63.97

TABLE 5-II Mode Shape Comparison of Model and Prototype

	AXIS METHOD	X - X (Hz)	Y - Y (Hz)			
			F	E	V	X
1ST MODE	MODEL	4.00	3.32	7.37	8.90	9.50
	EPF	(2.5)	(2.1)	(4.7)	(5.6)	(6.0)
	PROTOTYPE	2.5	2.20	3.88	3.90	4.36
2ND MODE	MODEL	14.00	10.41	22.95	28.20	34.22
	EPF	(8.8)	(6.5)	(14.5)	(17.8)	(21.6)
	PROTOTYPE	8.47	6.78	13.22	14.60	15.10
3RD MODE	MODEL	27.37	18.46	36.00	NA	NA
	EPF	(17.3)	(11.7)	(22.8)	NA	NA
	PROTOTYPE	15.79	11.28	NA	NA	NA

Comparing EPF to prototype frequency, the accuracy of the scaled down model was determined. Examining Table 5-II, it can be seen that most of the EPF's are higher than the prototype frequency. This was expected by the authors since the prototype was built in the field, thus the assumption of fixed end column is not as rigidly defined as in the model. Also, soil-structure interaction was another factor contributing to the lower natural frequency of the prototype. Therefore, the result obtained is quite satisfactory except for the "F" frame in Y-Y direction.

The fundamental frequency change due to the inclusion of different bracing systems is obvious. The stiffness increase can be expressed in relation to the change of fundamental natural frequency if the structure is idealized as a one DOF structure system. The stiffness change from "F" to "E" can be calculated in the following form:

$$\frac{K_F}{K_E} = \left(\frac{f_E}{f_F} \right)^2 = \left(\frac{7.37}{3.32} \right)^2 = 4.92 \quad (5.2)$$

The increase of stiffness is apparent by adding different bracing. The change of stiffness is 4.92 for E bracing, 7.19 for V bracing, and 8.19 for X bracing.

Note that in the "F" case, the prototype has a natural frequency higher than the EPF. This is contrary to what is described above. Explanation of this phenomenon was sought and it was found that model construction was the cause of this discrepancy. It was described in Section 3.4, referring to Figure 3-8, that discrepancy between model and prototype does exist. The missing stiffener on the column would have contributed some extra stiffness to the structure. Had this stiffener been included in the model, the natural frequency of the model would be increased, since the column rigid zone in the model is lengthened by the combined action of the gusset plate and stiffener. This missing stiffener apparently is not as important in the braced structures, since bracing itself provides most of the stiffness to the structure. However, the bare frame structure relies entirely on the rigidity of its beams and column for stiffness.

5.4.2 Mode Shape

In this experiment, rigid floors are assumed so that the model structure is considered a five DOF dynamic model. Mode shapes are obtained from the ratio of transfer functions for a certain mode at different floors.

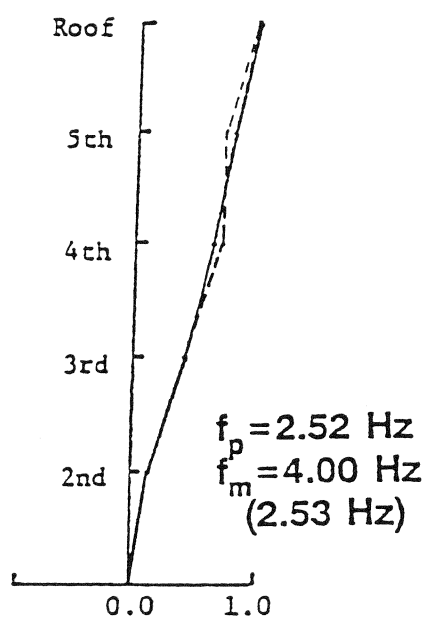
Since mode shape is a relative magnitude, the largest transfer function value is usually used as the base for normalization. For the first mode, the roof was used as the base, while for the second mode it was at the third floor.

The mode shape obtained from the model test are shown in Figure 5-9 and Figure 5-10 overlaid by the prototype mode shape. It is observed that there is less difference at the unbraced structure as in Figure 5-9 than the stiffer structure as in Figure 5-10. It is also observed that larger differences occurred at higher modes. In general, the results correspond to each other.

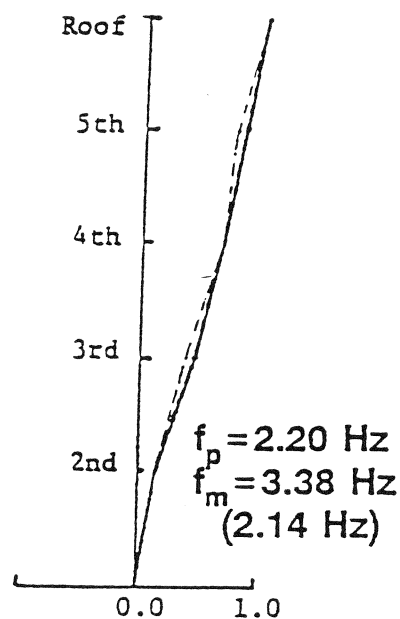
5.4.3 Damping

Damping is often obtained by the half power method. It is noteworthy that proportional damping theory is assumed in order to use the half power method. The zoom function [19] was widely used to calculate damping. In testing the F frame, the damping ratio calculated from the free decay vibration method matches quite well with that from the half power method. The zoom function doesn't work as well when the structural frequency increases. A smooth transfer function curve cannot be obtained at higher frequencies, thus a good estimate of higher mode damping was impossible.

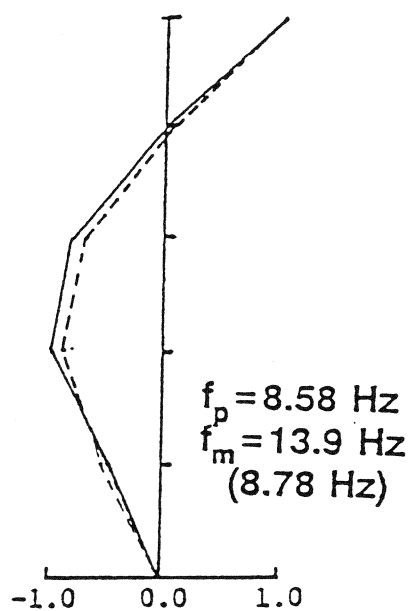
A new method to calculate higher mode damping through free vibration was used. Figure 5-11 illustrates a few examples of the result. Table 5-III shows the damping ratio comparison for the model and prototype. Since damping is structure dependent, there is no relationship between



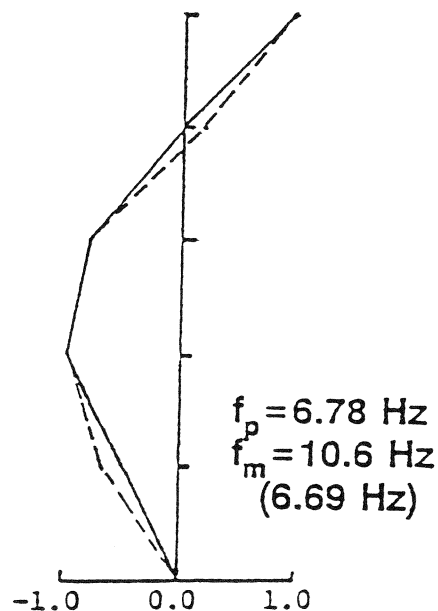
1st Mode
X-X Dir.



1st Mode
Y-Y Dir.



2nd Mode
X-X Dir.



2nd Mode
Y-Y Dir.

----- Prototype
 ——— Model

FIGURE 5-9 Comparison of Model and Prototype

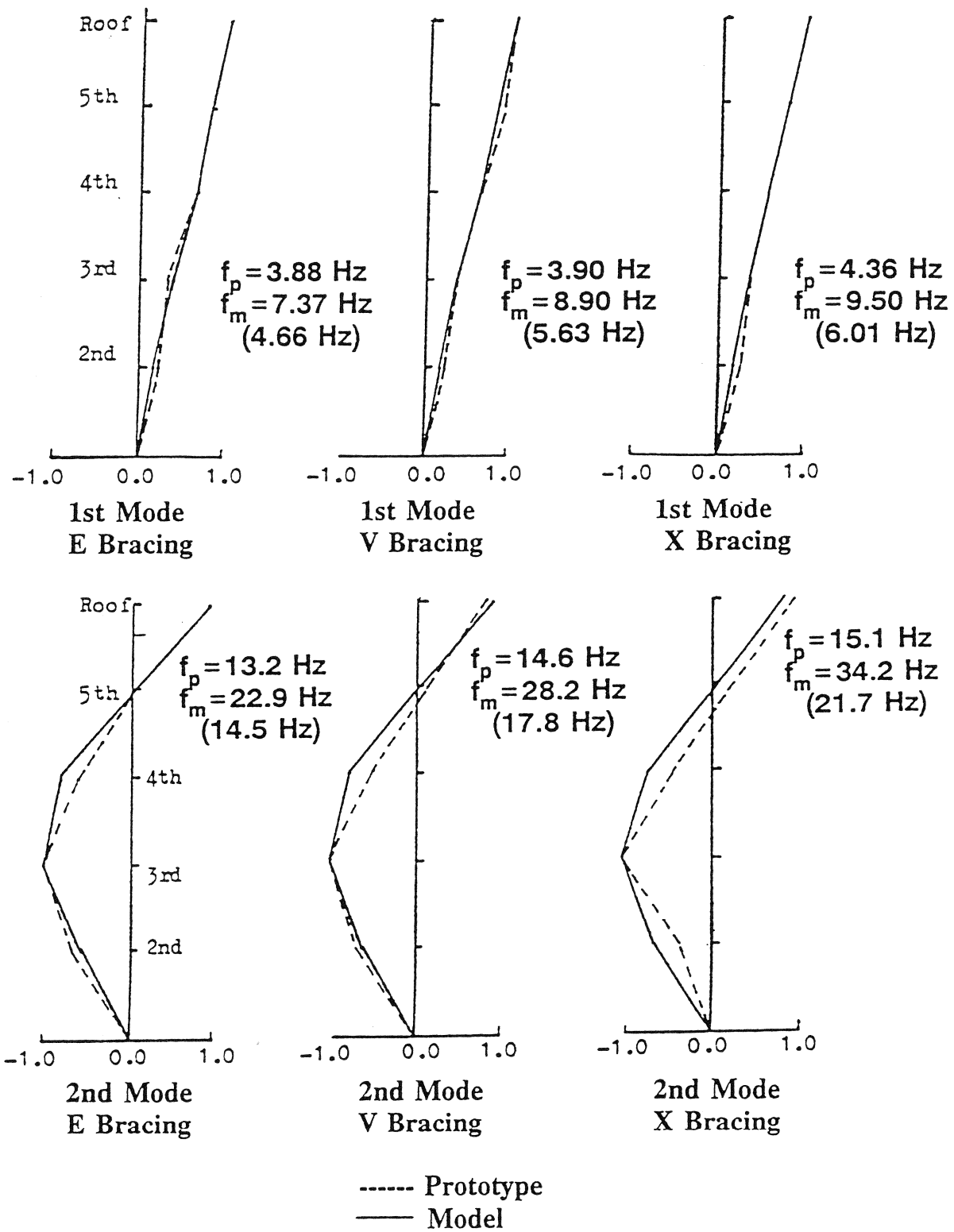


FIGURE 5-10 Comparison of Models and Prototype

prototype and model. From Table 5-III, it is known that the damping ratio in both structures is very small. A similar result can be found in several reports by other investigators [14,15].

Also noted is the gradual increase of the first mode damping in Y-Y direction as the lateral stiffness increases. It seems that the first mode damping ratio increases as the stiffness of the structure increases.

TABLE 5-III Damping Comparison of Model and Prototype

	AXIS STRUCTURE	X - X (%)	Y - Y (%)			
			F	E	V	X
1ST MODE	PROTOTYPE	1.4	0.9	1.40	1.70	2.20
	MODEL	0.2	0.15	0.20	0.24	0.30
2ND MODE	PROTOTYPE	0.8	1.4	NA	NA	3.80
	MODEL	NA	0.20	1.60	1.50	2.10
3RD MODE	PROTOTYPE	2.1	0.6	NA	NA	NA
	MODEL	NA	0.30	1.30	0.35	1.30

5.5 Summary

In this section, results from the laboratory test of the model structure, including bare frame and three braced frames, were reported. Correlation between the model and prototype were quite satisfactory. The incompleteness of the model has been explained.

A new method to estimate the higher mode damping is proposed. The experimental results from this method seem reasonable. More work to refine the technique would be useful in the future.

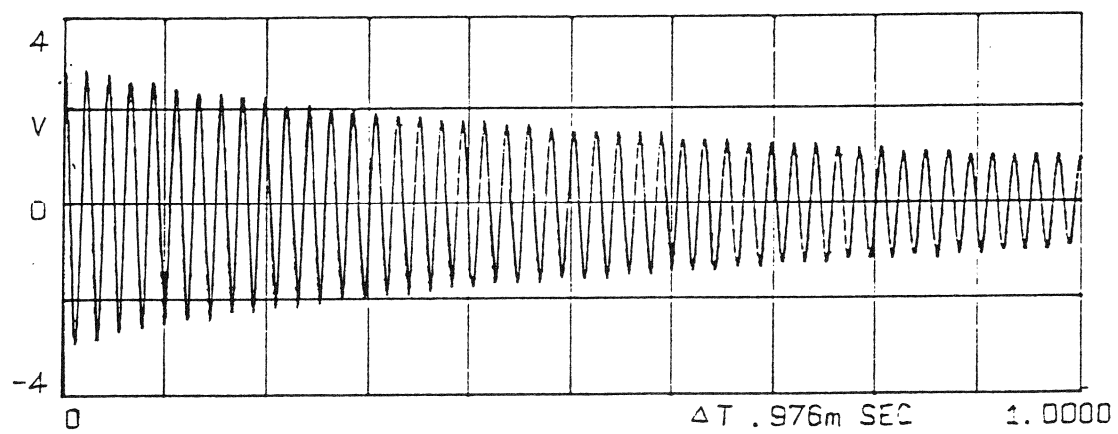
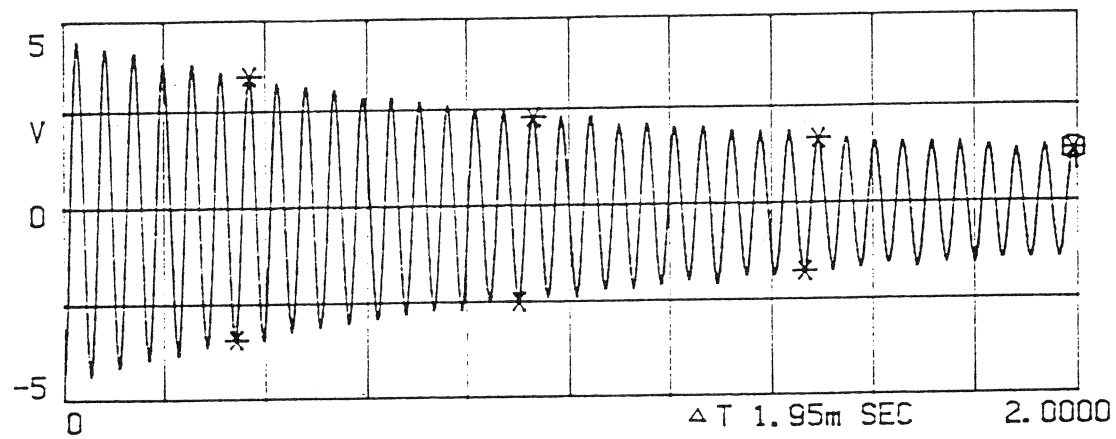


FIGURE 5-11 Higher Mode Free Vibration

SECTION 6 SUMMARY AND CONCLUSION

This report presents the first stage of test results from the US-China joint research project entitled **Cooperative Research for Dynamic Testing and Analysis**.

A full-sized five-story steel prototype structure was built in Beijing, China, and its scaled down model was built in the laboratory at the University at Buffalo. The prototype has the dimensions of 10.8 x 10.8 feet in plan and 48.9 feet in height. The model has a scale of 0.4 and was built with artificial mass to simulate the dynamic behavior of the prototype.

Experimental system identification tests were carried out in both locations to verify the relationship between the prototype and the model. Several new techniques were tried, with very good results, in identifying the basic structural properties. The prototype structure was tested with four different excitation methods. They were: force vibration with an eccentric vibrator, impact vibration with an impact hammer, ambient vibration, and free vibration from a pull-release technique.

The model structure was tested in the structural laboratory at UB. The frequencies, mode shapes and damping ratios were identified. Higher mode damping was measured by a new technique utilizing the MTS shaking table in the laboratory. The inclusion of bracings increased the lateral stiffness of the building. Three different bracing systems were tested and their strengthening effect was shown by the measured frequency increase.

It is concluded that the model structure is suitable to simulate the dynamic behavior of the prototype. Future research can benefit from this model because dynamic tests can be carried out in the laboratory before the final tests on the full-sized structure.

SECTION 7 REFERENCES

1. Blodget, O.W., **Design of Welded Structures**, The James F. Lincoln Arc Welding Foundation, 1982
2. Mills, R.S., H. Kirwinkler and J.M. Gere, **Model Tests on Earthquake Simulator Development and Implementation of Experimental Procedures**, Report No. 39, The John A. Blume Earthquake Engineering Center, Stanford University, June, 1979
3. Driscoll, G.C., L.S. Beedle, "Suggestions for Avoiding Beam-to-Column Web Connection Failure," *Engineering Journal*, AISC, 1st Qtr. 1982
4. Clough, R.W., D.T. Tang, **Earthquake Simulator Study of a Steel Frame Structure, Vol. 1: Experimental Results**, EERC 75-6, University of California, Berkeley, April 1975
5. Ketter, R.L., G.C. Lee, S.P. Prawel, **Structural Analysis and Design**, McGraw-Hill Book Company, New York, 1979
6. Cary, H.B., **Modern Welding Technology**, Prentice-Hall Inc., New Jersey, 1979
7. Huber, A.W., R.S. Beedle, "Residual Stresses and The Compressive Strength of Steel", *The Welding Journal*, Research Supplement, Vol. 33, December 1954
8. SOILTEST Inc., **Multi-Position Strain Gauge (Whittemore Type)**, Evanston, Illinois, March 1979
9. Beedle, L.C., L. Tall, "Basic Column Strength," *ASCE Proc. Paper 2555*, Vol. 86, ST 7, July 1960
10. Udawadia, F.E., and Trifunacs, M.D., "Ambient Vibration Tests of Full-Scale Structures," *Proc. of the Fifth World Conference on Earthquake Engineering*, Vol. 2, 1973
11. **2300 System Strain Gage Conditioning Amplifier Instruction Manual**, Measurements Group, Inc., North Carolina, 1985
12. **Operator's Manual SD 380Z Signal Analyzer**, Spectral Division, Scientific-Atlanta, San Diego, California, 1986
13. **STAAD-III, Integrated Structural Design System**, Revision 3.0, Research Engineers, Inc., NJ, 1989

14. Taoka, G.T., "Damping Measurements of Tall Structures", **Dynamic Response of Structures**, ASCE, 1981
15. Meyyappa, M., Palsson, H., Craig, J.I., "Modal Parameter Estimation For A Highrise Building Using Ambient Response Data Taken During Construction", **Dynamic Response of Structures**, ASCE, 1981
16. Craig, R.R. Jr., **Structural Dynamics - An Introduction to Computer Methods**, John Wiley and Sons, New York, 1984
17. Cole, H.A. Jr., "On-the-line Analysis of Random Vibrations," AIAA Paper No. 68-288
18. Rainer, J.H., "Dynamic Testing of Civil Engineering Structure," **Structural Dynamics and Earthquake Engineering**, 1979
19. Shaw, E., "Oral Presentation of Zoom Transform Technique," Computer Services of Canada, Ltd., Ottawa, Ont., Canada, 1970

**NATIONAL CENTER FOR EARTHQUAKE ENGINEERING RESEARCH
LIST OF TECHNICAL REPORTS**

The National Center for Earthquake Engineering Research (NCEER) publishes technical reports on a variety of subjects related to earthquake engineering written by authors funded through NCEER. These reports are available from both NCEER's Publications Department and the National Technical Information Service (NTIS). Requests for reports should be directed to the Publications Department, National Center for Earthquake Engineering Research, State University of New York at Buffalo, Red Jacket Quadrangle, Buffalo, New York 14261. Reports can also be requested through NTIS, 5285 Port Royal Road, Springfield, Virginia 22161. NTIS accession numbers are shown in parenthesis, if available.

- NCEER-87-0001 "First-Year Program in Research, Education and Technology Transfer," 3/5/87, (PB88-134275/AS).
- NCEER-87-0002 "Experimental Evaluation of Instantaneous Optimal Algorithms for Structural Control," by R.C. Lin, T.T. Soong and A.M. Reinhorn, 4/20/87, (PB88-134341/AS).
- NCEER-87-0003 "Experimentation Using the Earthquake Simulation Facilities at University at Buffalo," by A.M. Reinhorn and R.L. Ketter, to be published.
- NCEER-87-0004 "The System Characteristics and Performance of a Shaking Table," by J.S. Hwang, K.C. Chang and G.C. Lee, 6/1/87, (PB88-134259/AS). This report is available only through NTIS (see address given above).
- NCEER-87-0005 "A Finite Element Formulation for Nonlinear Viscoplastic Material Using a Q Model," by O. Gyebi and G. Dasgupta, 11/2/87, (PB88-213764/AS).
- NCEER-87-0006 "Symbolic Manipulation Program (SMP) - Algebraic Codes for Two and Three Dimensional Finite Element Formulations," by X. Lee and G. Dasgupta, 11/9/87, (PB88-219522/AS).
- NCEER-87-0007 "Instantaneous Optimal Control Laws for Tall Buildings Under Seismic Excitations," by J.N. Yang, A. Akbarpour and P. Ghaemmaghami, 6/10/87, (PB88-134333/AS).
- NCEER-87-0008 "IDARC: Inelastic Damage Analysis of Reinforced Concrete Frame - Shear-Wall Structures," by Y.J. Park, A.M. Reinhorn and S.K. Kunnath, 7/20/87, (PB88-134325/AS).
- NCEER-87-0009 "Liquefaction Potential for New York State: A Preliminary Report on Sites in Manhattan and Buffalo," by M. Budhu, V. Vijayakumar, R.F. Giese and L. Baumgras, 8/31/87, (PB88-163704/AS). This report is available only through NTIS (see address given above).
- NCEER-87-0010 "Vertical and Torsional Vibration of Foundations in Inhomogeneous Media," by A.S. Veletsos and K.W. Dotson, 6/1/87, (PB88-134291/AS).
- NCEER-87-0011 "Seismic Probabilistic Risk Assessment and Seismic Margins Studies for Nuclear Power Plants," by Howard H.M. Hwang, 6/15/87, (PB88-134267/AS).
- NCEER-87-0012 "Parametric Studies of Frequency Response of Secondary Systems Under Ground-Acceleration Excitations," by Y. Yong and Y.K. Lin, 6/10/87, (PB88-134309/AS).
- NCEER-87-0013 "Frequency Response of Secondary Systems Under Seismic Excitation," by J.A. HoLung, J. Cai and Y.K. Lin, 7/31/87, (PB88-134317/AS).
- NCEER-87-0014 "Modelling Earthquake Ground Motions in Seismically Active Regions Using Parametric Time Series Methods," by G.W. Ellis and A.S. Cakmak, 8/25/87, (PB88-134283/AS).
- NCEER-87-0015 "Detection and Assessment of Seismic Structural Damage," by E. DiPasquale and A.S. Cakmak, 8/25/87, (PB88-163712/AS).

- NCEER-87-0016 "Pipeline Experiment at Parkfield, California," by J. Isenberg and E. Richardson, 9/15/87, (PB88-163720/AS). This report is available only through NTIS (see address given above).
- NCEER-87-0017 "Digital Simulation of Seismic Ground Motion," by M. Shinozuka, G. Deodatis and T. Harada, 8/31/87, (PB88-155197/AS). This report is available only through NTIS (see address given above).
- NCEER-87-0018 "Practical Considerations for Structural Control: System Uncertainty, System Time Delay and Truncation of Small Control Forces," J.N. Yang and A. Akbarpour, 8/10/87, (PB88-163738/AS).
- NCEER-87-0019 "Modal Analysis of Nonclassically Damped Structural Systems Using Canonical Transformation," by J.N. Yang, S. Sarkani and F.X. Long, 9/27/87, (PB88-187851/AS).
- NCEER-87-0020 "A Nonstationary Solution in Random Vibration Theory," by J.R. Red-Horse and P.D. Spanos, 11/3/87, (PB88-163746/AS).
- NCEER-87-0021 "Horizontal Impedances for Radially Inhomogeneous Viscoelastic Soil Layers," by A.S. Veletsos and K.W. Dotson, 10/15/87, (PB88-150859/AS).
- NCEER-87-0022 "Seismic Damage Assessment of Reinforced Concrete Members," by Y.S. Chung, C. Meyer and M. Shinozuka, 10/9/87, (PB88-150867/AS). This report is available only through NTIS (see address given above).
- NCEER-87-0023 "Active Structural Control in Civil Engineering," by T.T. Soong, 11/11/87, (PB88-187778/AS).
- NCEER-87-0024 "Vertical and Torsional Impedances for Radially Inhomogeneous Viscoelastic Soil Layers," by K.W. Dotson and A.S. Veletsos, 12/87, (PB88-187786/AS).
- NCEER-87-0025 "Proceedings from the Symposium on Seismic Hazards, Ground Motions, Soil-Liquefaction and Engineering Practice in Eastern North America," October 20-22, 1987, edited by K.H. Jacob, 12/87, (PB88-188115/AS).
- NCEER-87-0026 "Report on the Whittier-Narrows, California, Earthquake of October 1, 1987," by J. Pantelic and A. Reinhorn, 11/87, (PB88-187752/AS). This report is available only through NTIS (see address given above).
- NCEER-87-0027 "Design of a Modular Program for Transient Nonlinear Analysis of Large 3-D Building Structures," by S. Srivastav and J.F. Abel, 12/30/87, (PB88-187950/AS).
- NCEER-87-0028 "Second-Year Program in Research, Education and Technology Transfer," 3/8/88, (PB88-219480/AS).
- NCEER-88-0001 "Workshop on Seismic Computer Analysis and Design of Buildings With Interactive Graphics," by W. McGuire, J.F. Abel and C.H. Conley, 1/18/88, (PB88-187760/AS).
- NCEER-88-0002 "Optimal Control of Nonlinear Flexible Structures," by J.N. Yang, F.X. Long and D. Wong, 1/22/88, (PB88-213772/AS).
- NCEER-88-0003 "Substructuring Techniques in the Time Domain for Primary-Secondary Structural Systems," by G.D. Manolis and G. Juhn, 2/10/88, (PB88-213780/AS).
- NCEER-88-0004 "Iterative Seismic Analysis of Primary-Secondary Systems," by A. Singhal, L.D. Lutes and P.D. Spanos, 2/23/88, (PB88-213798/AS).
- NCEER-88-0005 "Stochastic Finite Element Expansion for Random Media," by P.D. Spanos and R. Ghanem, 3/14/88, (PB88-213806/AS).

- NCEER-88-0006 "Combining Structural Optimization and Structural Control," by F.Y. Cheng and C.P. Pantelides, 1/10/88, (PB88-213814/AS).
- NCEER-88-0007 "Seismic Performance Assessment of Code-Designed Structures," by H.H-M. Hwang, J-W. Jaw and H-J. Shau, 3/20/88, (PB88-219423/AS).
- NCEER-88-0008 "Reliability Analysis of Code-Designed Structures Under Natural Hazards," by H.H-M. Hwang, H. Ushiba and M. Shinozuka, 2/29/88, (PB88-229471/AS).
- NCEER-88-0009 "Seismic Fragility Analysis of Shear Wall Structures," by J-W Jaw and H.H-M. Hwang, 4/30/88, (PB89-102867/AS).
- NCEER-88-0010 "Base Isolation of a Multi-Story Building Under a Harmonic Ground Motion - A Comparison of Performances of Various Systems," by F-G Fan, G. Ahmadi and I.G. Tadjbakhsh, 5/18/88, (PB89-122238/AS).
- NCEER-88-0011 "Seismic Floor Response Spectra for a Combined System by Green's Functions," by F.M. Lavelle, L.A. Bergman and P.D. Spanos, 5/1/88, (PB89-102875/AS).
- NCEER-88-0012 "A New Solution Technique for Randomly Excited Hysteretic Structures," by G.Q. Cai and Y.K. Lin, 5/16/88, (PB89-102883/AS).
- NCEER-88-0013 "A Study of Radiation Damping and Soil-Structure Interaction Effects in the Centrifuge," by K. Weissman, supervised by J.H. Prevost, 5/24/88, (PB89-144703/AS).
- NCEER-88-0014 "Parameter Identification and Implementation of a Kinematic Plasticity Model for Frictional Soils," by J.H. Prevost and D.V. Griffiths, to be published.
- NCEER-88-0015 "Two- and Three- Dimensional Dynamic Finite Element Analyses of the Long Valley Dam," by D.V. Griffiths and J.H. Prevost, 6/17/88, (PB89-144711/AS).
- NCEER-88-0016 "Damage Assessment of Reinforced Concrete Structures in Eastern United States," by A.M. Reinhorn, M.J. Seidel, S.K. Kunnath and Y.J. Park, 6/15/88, (PB89-122220/AS).
- NCEER-88-0017 "Dynamic Compliance of Vertically Loaded Strip Foundations in Multilayered Viscoelastic Soils," by S. Ahmad and A.S.M. Israil, 6/17/88, (PB89-102891/AS).
- NCEER-88-0018 "An Experimental Study of Seismic Structural Response With Added Viscoelastic Dampers," by R.C. Lin, Z. Liang, T.T. Soong and R.H. Zhang, 6/30/88, (PB89-122212/AS). This report is available only through NTIS (see address given above).
- NCEER-88-0019 "Experimental Investigation of Primary - Secondary System Interaction," by G.D. Manolis, G. Juhn and A.M. Reinhorn, 5/27/88, (PB89-122204/AS).
- NCEER-88-0020 "A Response Spectrum Approach For Analysis of Nonclassically Damped Structures," by J.N. Yang, S. Sarkani and F.X. Long, 4/22/88, (PB89-102909/AS).
- NCEER-88-0021 "Seismic Interaction of Structures and Soils: Stochastic Approach," by A.S. Veletsos and A.M. Prasad, 7/21/88, (PB89-122196/AS).
- NCEER-88-0022 "Identification of the Serviceability Limit State and Detection of Seismic Structural Damage," by E. DiPasquale and A.S. Cakmak, 6/15/88, (PB89-122188/AS). This report is available only through NTIS (see address given above).
- NCEER-88-0023 "Multi-Hazard Risk Analysis: Case of a Simple Offshore Structure," by B.K. Bhartia and E.H. Vanmarcke, 7/21/88, (PB89-145213/AS).

- NCEER-88-0024 "Automated Seismic Design of Reinforced Concrete Buildings," by Y.S. Chung, C. Meyer and M. Shinozuka, 7/5/88, (PB89-122170/AS). This report is available only through NTIS (see address given above).
- NCEER-88-0025 "Experimental Study of Active Control of MDOF Structures Under Seismic Excitations," by L.L. Chung, R.C. Lin, T.T. Soong and A.M. Reinhorn, 7/10/88, (PB89-122600/AS).
- NCEER-88-0026 "Earthquake Simulation Tests of a Low-Rise Metal Structure," by J.S. Hwang, K.C. Chang, G.C. Lee and R.L. Ketter, 8/1/88, (PB89-102917/AS).
- NCEER-88-0027 "Systems Study of Urban Response and Reconstruction Due to Catastrophic Earthquakes," by F. Kozin and H.K. Zhou, 9/22/88, (PB90-162348/AS).
- NCEER-88-0028 "Seismic Fragility Analysis of Plane Frame Structures," by H.H.-M. Hwang and Y.K. Low, 7/31/88, (PB89-131445/AS).
- NCEER-88-0029 "Response Analysis of Stochastic Structures," by A. Kardara, C. Bucher and M. Shinozuka, 9/22/88, (PB89-174429/AS).
- NCEER-88-0030 "Nonnormal Accelerations Due to Yielding in a Primary Structure," by D.C.K. Chen and L.D. Lutes, 9/19/88, (PB89-131437/AS).
- NCEER-88-0031 "Design Approaches for Soil-Structure Interaction," by A.S. Veletsos, A.M. Prasad and Y. Tang, 12/30/88, (PB89-174437/AS). This report is available only through NTIS (see address given above).
- NCEER-88-0032 "A Re-evaluation of Design Spectra for Seismic Damage Control," by C.J. Turkstra and A.G. Tallin, 11/7/88, (PB89-145221/AS).
- NCEER-88-0033 "The Behavior and Design of Noncontact Lap Splices Subjected to Repeated Inelastic Tensile Loading," by V.E. Sagan, P. Gergely and R.N. White, 12/8/88, (PB89-163737/AS).
- NCEER-88-0034 "Seismic Response of Pile Foundations," by S.M. Mamoon, P.K. Banerjee and S. Ahmad, 11/1/88, (PB89-145239/AS).
- NCEER-88-0035 "Modeling of R/C Building Structures With Flexible Floor Diaphragms (IDARC2)," by A.M. Reinhorn, S.K. Kunnath and N. Panahshahi, 9/7/88, (PB89-207153/AS).
- NCEER-88-0036 "Solution of the Dam-Reservoir Interaction Problem Using a Combination of FEM, BEM with Particular Integrals, Modal Analysis, and Substructuring," by C-S. Tsai, G.C. Lee and R.L. Ketter, 12/31/88, (PB89-207146/AS).
- NCEER-88-0037 "Optimal Placement of Actuators for Structural Control," by F.Y. Cheng and C.P. Pantelides, 8/15/88, (PB89-162846/AS).
- NCEER-88-0038 "Teflon Bearings in Aseismic Base Isolation: Experimental Studies and Mathematical Modeling," by A. Mokha, M.C. Constantinou and A.M. Reinhorn, 12/5/88, (PB89-218457/AS). This report is available only through NTIS (see address given above).
- NCEER-88-0039 "Seismic Behavior of Flat Slab High-Rise Buildings in the New York City Area," by P. Weidlinger and M. Ettouney, 10/15/88, (PB90-145681/AS).
- NCEER-88-0040 "Evaluation of the Earthquake Resistance of Existing Buildings in New York City," by P. Weidlinger and M. Ettouney, 10/15/88, to be published.
- NCEER-88-0041 "Small-Scale Modeling Techniques for Reinforced Concrete Structures Subjected to Seismic Loads," by W. Kim, A. El-Attar and R.N. White, 11/22/88, (PB89-189625/AS).

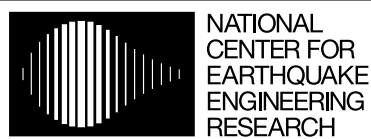
- NCEER-88-0042 "Modeling Strong Ground Motion from Multiple Event Earthquakes," by G.W. Ellis and A.S. Cakmak, 10/15/88, (PB89-174445/AS).
- NCEER-88-0043 "Nonstationary Models of Seismic Ground Acceleration," by M. Grigoriu, S.E. Ruiz and E. Rosenblueth, 7/15/88, (PB89-189617/AS).
- NCEER-88-0044 "SARCF User's Guide: Seismic Analysis of Reinforced Concrete Frames," by Y.S. Chung, C. Meyer and M. Shinozuka, 11/9/88, (PB89-174452/AS).
- NCEER-88-0045 "First Expert Panel Meeting on Disaster Research and Planning," edited by J. Pantelic and J. Stoyke, 9/15/88, (PB89-174460/AS).
- NCEER-88-0046 "Preliminary Studies of the Effect of Degrading Infill Walls on the Nonlinear Seismic Response of Steel Frames," by C.Z. Chrysostomou, P. Gergely and J.F. Abel, 12/19/88, (PB89-208383/AS).
- NCEER-88-0047 "Reinforced Concrete Frame Component Testing Facility - Design, Construction, Instrumentation and Operation," by S.P. Pessiki, C. Conley, T. Bond, P. Gergely and R.N. White, 12/16/88, (PB89-174478/AS).
- NCEER-89-0001 "Effects of Protective Cushion and Soil Compliancy on the Response of Equipment Within a Seismically Excited Building," by J.A. HoLung, 2/16/89, (PB89-207179/AS).
- NCEER-89-0002 "Statistical Evaluation of Response Modification Factors for Reinforced Concrete Structures," by H.H-M. Hwang and J-W. Jaw, 2/17/89, (PB89-207187/AS).
- NCEER-89-0003 "Hysteretic Columns Under Random Excitation," by G-Q. Cai and Y.K. Lin, 1/9/89, (PB89-196513/AS).
- NCEER-89-0004 "Experimental Study of 'Elephant Foot Bulge' Instability of Thin-Walled Metal Tanks," by Z-H. Jia and R.L. Ketter, 2/22/89, (PB89-207195/AS).
- NCEER-89-0005 "Experiment on Performance of Buried Pipelines Across San Andreas Fault," by J. Isenberg, E. Richardson and T.D. O'Rourke, 3/10/89, (PB89-218440/AS).
- NCEER-89-0006 "A Knowledge-Based Approach to Structural Design of Earthquake-Resistant Buildings," by M. Subramani, P. Gergely, C.H. Conley, J.F. Abel and A.H. Zaghaw, 1/15/89, (PB89-218465/AS).
- NCEER-89-0007 "Liquefaction Hazards and Their Effects on Buried Pipelines," by T.D. O'Rourke and P.A. Lane, 2/1/89, (PB89-218481).
- NCEER-89-0008 "Fundamentals of System Identification in Structural Dynamics," by H. Imai, C-B. Yun, O. Maruyama and M. Shinozuka, 1/26/89, (PB89-207211/AS).
- NCEER-89-0009 "Effects of the 1985 Michoacan Earthquake on Water Systems and Other Buried Lifelines in Mexico," by A.G. Ayala and M.J. O'Rourke, 3/8/89, (PB89-207229/AS).
- NCEER-89-R010 "NCEER Bibliography of Earthquake Education Materials," by K.E.K. Ross, Second Revision, 9/1/89, (PB90-125352/AS).
- NCEER-89-0011 "Inelastic Three-Dimensional Response Analysis of Reinforced Concrete Building Structures (IDARC-3D), Part I - Modeling," by S.K. Kunnath and A.M. Reinhorn, 4/17/89, (PB90-114612/AS).
- NCEER-89-0012 "Recommended Modifications to ATC-14," by C.D. Poland and J.O. Malley, 4/12/89, (PB90-108648/AS).
- NCEER-89-0013 "Repair and Strengthening of Beam-to-Column Connections Subjected to Earthquake Loading," by M. Corazao and A.J. Durrani, 2/28/89, (PB90-109885/AS).

- NCEER-89-0014 "Program EXKAL2 for Identification of Structural Dynamic Systems," by O. Maruyama, C-B. Yun, M. Hoshiya and M. Shinozuka, 5/19/89, (PB90-109877/AS).
- NCEER-89-0015 "Response of Frames With Bolted Semi-Rigid Connections, Part I - Experimental Study and Analytical Predictions," by P.J. DiCorso, A.M. Reinhorn, J.R. Dickerson, J.B. Radzinski and W.L. Harper, 6/1/89, to be published.
- NCEER-89-0016 "ARMA Monte Carlo Simulation in Probabilistic Structural Analysis," by P.D. Spanos and M.P. Mignolet, 7/10/89, (PB90-109893/AS).
- NCEER-89-P017 "Preliminary Proceedings from the Conference on Disaster Preparedness - The Place of Earthquake Education in Our Schools," Edited by K.E.K. Ross, 6/23/89.
- NCEER-89-0017 "Proceedings from the Conference on Disaster Preparedness - The Place of Earthquake Education in Our Schools," Edited by K.E.K. Ross, 12/31/89, (PB90-207895). This report is available only through NTIS (see address given above).
- NCEER-89-0018 "Multidimensional Models of Hysteretic Material Behavior for Vibration Analysis of Shape Memory Energy Absorbing Devices, by E.J. Graesser and F.A. Cozzarelli, 6/7/89, (PB90-164146/AS).
- NCEER-89-0019 "Nonlinear Dynamic Analysis of Three-Dimensional Base Isolated Structures (3D-BASIS)," by S. Nagarajaiah, A.M. Reinhorn and M.C. Constantinou, 8/3/89, (PB90-161936/AS). This report is available only through NTIS (see address given above).
- NCEER-89-0020 "Structural Control Considering Time-Rate of Control Forces and Control Rate Constraints," by F.Y. Cheng and C.P. Pantelides, 8/3/89, (PB90-120445/AS).
- NCEER-89-0021 "Subsurface Conditions of Memphis and Shelby County," by K.W. Ng, T-S. Chang and H-H.M. Hwang, 7/26/89, (PB90-120437/AS).
- NCEER-89-0022 "Seismic Wave Propagation Effects on Straight Jointed Buried Pipelines," by K. Elhmadi and M.J. O'Rourke, 8/24/89, (PB90-162322/AS).
- NCEER-89-0023 "Workshop on Serviceability Analysis of Water Delivery Systems," edited by M. Grigoriu, 3/6/89, (PB90-127424/AS).
- NCEER-89-0024 "Shaking Table Study of a 1/5 Scale Steel Frame Composed of Tapered Members," by K.C. Chang, J.S. Hwang and G.C. Lee, 9/18/89, (PB90-160169/AS).
- NCEER-89-0025 "DYNA1D: A Computer Program for Nonlinear Seismic Site Response Analysis - Technical Documentation," by Jean H. Prevost, 9/14/89, (PB90-161944/AS). This report is available only through NTIS (see address given above).
- NCEER-89-0026 "1:4 Scale Model Studies of Active Tendon Systems and Active Mass Dampers for Aseismic Protection," by A.M. Reinhorn, T.T. Soong, R.C. Lin, Y.P. Yang, Y. Fukao, H. Abe and M. Nakai, 9/15/89, (PB90-173246/AS).
- NCEER-89-0027 "Scattering of Waves by Inclusions in a Nonhomogeneous Elastic Half Space Solved by Boundary Element Methods," by P.K. Hadley, A. Askar and A.S. Cakmak, 6/15/89, (PB90-145699/AS).
- NCEER-89-0028 "Statistical Evaluation of Deflection Amplification Factors for Reinforced Concrete Structures," by H.H.M. Hwang, J-W. Jaw and A.L. Ch'ng, 8/31/89, (PB90-164633/AS).
- NCEER-89-0029 "Bedrock Accelerations in Memphis Area Due to Large New Madrid Earthquakes," by H.H.M. Hwang, C.H.S. Chen and G. Yu, 11/7/89, (PB90-162330/AS).

- NCEER-89-0030 "Seismic Behavior and Response Sensitivity of Secondary Structural Systems," by Y.Q. Chen and T.T. Soong, 10/23/89, (PB90-164658/AS).
- NCEER-89-0031 "Random Vibration and Reliability Analysis of Primary-Secondary Structural Systems," by Y. Ibrahim, M. Grigoriu and T.T. Soong, 11/10/89, (PB90-161951/AS).
- NCEER-89-0032 "Proceedings from the Second U.S. - Japan Workshop on Liquefaction, Large Ground Deformation and Their Effects on Lifelines, September 26-29, 1989," Edited by T.D. O'Rourke and M. Hamada, 12/1/89, (PB90-209388/AS).
- NCEER-89-0033 "Deterministic Model for Seismic Damage Evaluation of Reinforced Concrete Structures," by J.M. Bracci, A.M. Reinhorn, J.B. Mander and S.K. Kunnath, 9/27/89.
- NCEER-89-0034 "On the Relation Between Local and Global Damage Indices," by E. DiPasquale and A.S. Cakmak, 8/15/89, (PB90-173865).
- NCEER-89-0035 "Cyclic Undrained Behavior of Nonplastic and Low Plasticity Silts," by A.J. Walker and H.E. Stewart, 7/26/89, (PB90-183518/AS).
- NCEER-89-0036 "Liquefaction Potential of Surficial Deposits in the City of Buffalo, New York," by M. Budhu, R. Giese and L. Baumgrass, 1/17/89, (PB90-208455/AS).
- NCEER-89-0037 "A Deterministic Assessment of Effects of Ground Motion Incoherence," by A.S. Veletsos and Y. Tang, 7/15/89, (PB90-164294/AS).
- NCEER-89-0038 "Workshop on Ground Motion Parameters for Seismic Hazard Mapping," July 17-18, 1989, edited by R.V. Whitman, 12/1/89, (PB90-173923/AS).
- NCEER-89-0039 "Seismic Effects on Elevated Transit Lines of the New York City Transit Authority," by C.J. Costantino, C.A. Miller and E. Heymsfield, 12/26/89, (PB90-207887/AS).
- NCEER-89-0040 "Centrifugal Modeling of Dynamic Soil-Structure Interaction," by K. Weissman, Supervised by J.H. Prevost, 5/10/89, (PB90-207879/AS).
- NCEER-89-0041 "Linearized Identification of Buildings With Cores for Seismic Vulnerability Assessment," by I-K. Ho and A.E. Aktan, 11/1/89, (PB90-251943/AS).
- NCEER-90-0001 "Geotechnical and Lifeline Aspects of the October 17, 1989 Loma Prieta Earthquake in San Francisco," by T.D. O'Rourke, H.E. Stewart, F.T. Blackburn and T.S. Dickerman, 1/90, (PB90-208596/AS).
- NCEER-90-0002 "Nonnormal Secondary Response Due to Yielding in a Primary Structure," by D.C.K. Chen and L.D. Lutes, 2/28/90, (PB90-251976/AS).
- NCEER-90-0003 "Earthquake Education Materials for Grades K-12," by K.E.K. Ross, 4/16/90, (PB91-113415/AS).
- NCEER-90-0004 "Catalog of Strong Motion Stations in Eastern North America," by R.W. Busby, 4/3/90, (PB90-251984)/AS.
- NCEER-90-0005 "NCEER Strong-Motion Data Base: A User Manual for the GeoBase Release (Version 1.0 for the Sun3)," by P. Friberg and K. Jacob, 3/31/90 (PB90-258062/AS).
- NCEER-90-0006 "Seismic Hazard Along a Crude Oil Pipeline in the Event of an 1811-1812 Type New Madrid Earthquake," by H.H.M. Hwang and C-H.S. Chen, 4/16/90(PB90-258054).
- NCEER-90-0007 "Site-Specific Response Spectra for Memphis Sheahan Pumping Station," by H.H.M. Hwang and C.S. Lee, 5/15/90, (PB91-108811/AS).

- NCEER-90-0008 "Pilot Study on Seismic Vulnerability of Crude Oil Transmission Systems," by T. Ariman, R. Dobry, M. Grigoriu, F. Kozin, M. O'Rourke, T. O'Rourke and M. Shinozuka, 5/25/90, (PB91-108837/AS).
- NCEER-90-0009 "A Program to Generate Site Dependent Time Histories: EQGEN," by G.W. Ellis, M. Srinivasan and A.S. Cakmak, 1/30/90, (PB91-108829/AS).
- NCEER-90-0010 "Active Isolation for Seismic Protection of Operating Rooms," by M.E. Talbott, Supervised by M. Shinozuka, 6/8/9, (PB91-110205/AS).
- NCEER-90-0011 "Program LINEARID for Identification of Linear Structural Dynamic Systems," by C-B. Yun and M. Shinozuka, 6/25/90, (PB91-110312/AS).
- NCEER-90-0012 "Two-Dimensional Two-Phase Elasto-Plastic Seismic Response of Earth Dams," by A.N. Yiagos, Supervised by J.H. Prevost, 6/20/90, (PB91-110197/AS).
- NCEER-90-0013 "Secondary Systems in Base-Isolated Structures: Experimental Investigation, Stochastic Response and Stochastic Sensitivity," by G.D. Manolis, G. Juhn, M.C. Constantinou and A.M. Reinhorn, 7/1/90, (PB91-110320/AS).
- NCEER-90-0014 "Seismic Behavior of Lightly-Reinforced Concrete Column and Beam-Column Joint Details," by S.P. Pessiki, C.H. Conley, P. Gergely and R.N. White, 8/22/90, (PB91-108795/AS).
- NCEER-90-0015 "Two Hybrid Control Systems for Building Structures Under Strong Earthquakes," by J.N. Yang and A. Danielians, 6/29/90, (PB91-125393/AS).
- NCEER-90-0016 "Instantaneous Optimal Control with Acceleration and Velocity Feedback," by J.N. Yang and Z. Li, 6/29/90, (PB91-125401/AS).
- NCEER-90-0017 "Reconnaissance Report on the Northern Iran Earthquake of June 21, 1990," by M. Mehraein, 10/4/90, (PB91-125377/AS).
- NCEER-90-0018 "Evaluation of Liquefaction Potential in Memphis and Shelby County," by T.S. Chang, P.S. Tang, C.S. Lee and H. Hwang, 8/10/90, (PB91-125427/AS).
- NCEER-90-0019 "Experimental and Analytical Study of a Combined Sliding Disc Bearing and Helical Steel Spring Isolation System," by M.C. Constantinou, A.S. Mokha and A.M. Reinhorn, 10/4/90, (PB91-125385/AS).
- NCEER-90-0020 "Experimental Study and Analytical Prediction of Earthquake Response of a Sliding Isolation System with a Spherical Surface," by A.S. Mokha, M.C. Constantinou and A.M. Reinhorn, 10/11/90, (PB91-125419/AS).
- NCEER-90-0021 "Dynamic Interaction Factors for Floating Pile Groups," by G. Gazetas, K. Fan, A. Kaynia and E. Kausel, 9/10/90, (PB91-170381/AS).
- NCEER-90-0022 "Evaluation of Seismic Damage Indices for Reinforced Concrete Structures," by S. Rodriguez-Gomez and A.S. Cakmak, 9/30/90, PB91-171322/AS).
- NCEER-90-0023 "Study of Site Response at a Selected Memphis Site," by H. Desai, S. Ahmad, E.S. Gazetas and M.R. Oh, 10/11/90, (PB91-196857/AS).
- NCEER-90-0024 "A User's Guide to Strongmo: Version 1.0 of NCEER's Strong-Motion Data Access Tool for PCs and Terminals," by P.A. Friberg and C.A.T. Susch, 11/15/90, (PB91-171272/AS).
- NCEER-90-0025 "A Three-Dimensional Analytical Study of Spatial Variability of Seismic Ground Motions," by L-L. Hong and A.H.-S. Ang, 10/30/90, (PB91-170399/AS).

- NCEER-90-0026 "MUMOID User's Guide - A Program for the Identification of Modal Parameters," by S. Rodriguez-Gomez and E. DiPasquale, 9/30/90, (PB91-171298/AS).
- NCEER-90-0027 "SARCF-II User's Guide - Seismic Analysis of Reinforced Concrete Frames," by S. Rodriguez-Gomez, Y.S. Chung and C. Meyer, 9/30/90, (PB91-171280/AS).
- NCEER-90-0028 "Viscous Dampers: Testing, Modeling and Application in Vibration and Seismic Isolation," by N. Makris and M.C. Constantinou, 12/20/90 (PB91-190561/AS).
- NCEER-90-0029 "Soil Effects on Earthquake Ground Motions in the Memphis Area," by H. Hwang, C.S. Lee, K.W. Ng and T.S. Chang, 8/2/90, (PB91-190751/AS).
- NCEER-91-0001 "Proceedings from the Third Japan-U.S. Workshop on Earthquake Resistant Design of Lifeline Facilities and Countermeasures for Soil Liquefaction, December 17-19, 1990," edited by T.D. O'Rourke and M. Hamada, 2/1/91, (PB91-179259/AS).
- NCEER-91-0002 "Physical Space Solutions of Non-Proportionally Damped Systems," by M. Tong, Z. Liang and G.C. Lee, 1/15/91, (PB91-179242/AS).
- NCEER-91-0003 "Seismic Response of Single Piles and Pile Groups," by K. Fan and G. Gazetas, 1/10/91, (PB92-174994/AS).
- NCEER-91-0004 "Damping of Structures: Part 1 - Theory of Complex Damping," by Z. Liang and G. Lee, 10/10/91, (PB92-197235/AS).
- NCEER-91-0005 "3D-BASIS - Nonlinear Dynamic Analysis of Three Dimensional Base Isolated Structures: Part II," by S. Nagarajaiah, A.M. Reinhorn and M.C. Constantinou, 2/28/91, (PB91-190553/AS).
- NCEER-91-0006 "A Multidimensional Hysteretic Model for Plasticity Deforming Metals in Energy Absorbing Devices," by E.J. Graesser and F.A. Cozzarelli, 4/9/91.
- NCEER-91-0007 "A Framework for Customizable Knowledge-Based Expert Systems with an Application to a KBES for Evaluating the Seismic Resistance of Existing Buildings," by E.G. Ibarra-Anaya and S.J. Fenves, 4/9/91, (PB91-210930/AS).
- NCEER-91-0008 "Nonlinear Analysis of Steel Frames with Semi-Rigid Connections Using the Capacity Spectrum Method," by G.G. Deierlein, S-H. Hsieh, Y-J. Shen and J.F. Abel, 7/2/91, (PB92-113828/AS).
- NCEER-91-0009 "Earthquake Education Materials for Grades K-12," by K.E.K. Ross, 4/30/91, (PB91-212142/AS).
- NCEER-91-0010 "Phase Wave Velocities and Displacement Phase Differences in a Harmonically Oscillating Pile," by N. Makris and G. Gazetas, 7/8/91, (PB92-108356/AS).
- NCEER-91-0011 "Dynamic Characteristics of a Full-Size Five-Story Steel Structure and a 2/5 Scale Model," by K.C. Chang, G.C. Yao, G.C. Lee, D.S. Hao and Y.C. Yeh," 7/2/91.



Headquartered at the State University of New York at Buffalo

State University of New York at Buffalo
Red Jacket Quadrangle
Buffalo, New York 14261
Telephone: 716/645-3391
FAX: 716/645-3399

ISSN 1088-3800